Coral Calcification and Ocean Acidification

2

Paul L. Jokiel, Christopher P. Jury, and Ilsa B. Kuffner

Abstract

Over 60 years ago, the discovery that light increased calcification in the coral plant-animal symbiosis triggered interest in explaining the phenomenon and understanding the mechanisms involved. Major findings along the way include the observation that carbon fixed by photosynthesis in the zooxanthellae is translocated to animal cells throughout the colony and that corals can therefore live as autotrophs in many situations. Recent research has focused on explaining the observed reduction in calcification rate with increasing ocean acidification (OA). Experiments have shown a direct correlation between declining ocean pH, declining aragonite saturation state (Ω_{arag}), declining [CO_3^{2-}] and coral calcification. Nearly all previous reports on OA identify Ω_{arag} or its surrogate [CO_3^{2-}] as the factor driving coral calcification. However, the alternate "Proton Flux Hypothesis" stated that coral calcification is controlled by diffusion limitation of net H^+ transport through the boundary layer in relation to availability of dissolved inorganic carbon (DIC). The "Two Compartment Proton Flux Model" expanded this explanation and synthesized diverse observations into a universal model that explains many paradoxes of coral metabolism, morphology and plasticity of growth form in addition to observed coral skeletal growth response to OA. It is now clear that irradiance is the main driver of net photosynthesis (P_{net}), which in turn drives net calcification (G_{net}), and alters pH in the bulk water surrounding the coral. P_{net} controls [CO_3^{2-}] and thus Ω_{arag} of the bulk water over the diel cycle. Changes in Ω_{arag} and pH lag behind G_{net} throughout the daily cycle by two or more hours. The flux rate P_{net}, rather than concentration-based parameters (e.g., Ω_{arag}, [CO_3^{2-}], pH and [DIC]:[H^+] ratio) is the primary driver of G_{net}. Daytime coral metabolism rapidly removes DIC from the bulk seawater. Photosynthesis increases the bulk seawater pH while providing the energy that drives calcification and increases in G_{net}. These relationships result in a correlation between G_{net} and Ω_{arag}, with both parameters being variables dependent on P_{net}. Consequently the correlation between G_{net} and Ω_{arag} varies widely between different locations and times depending on the relative metabolic contributions of various calcifying and photosynthesizing organisms and local rates of carbonate dissolution. High rates of H^+ efflux continue for several hours following the mid-day G_{net} peak suggesting that corals have difficulty in shedding waste protons as described by the Proton Flux Model. DIC flux (uptake) tracks P_{net} and G_{net} and drops off rapidly after the photosynthesis-calcification maxima, indicating that corals can cope more effectively with the problem of limited DIC supply compared to the problem of eliminating

P.L. Jokiel (✉) • C.P. Jury
Hawaii Institute of Marine Biology, University of Hawaii,
1346Kaneohe, HI 96744, USA
e-mail: jokiel@hawaii.edu

I.B. Kuffner
U.S. Geological Survey, St. Petersburg Coastal and Marine Science
Center, 600 4th Street South, St. Petersburg, FL 33701, USA

D.K. Hubbard et al. (eds.), *Coral Reefs at the Crossroads*,
Coral Reefs of the World 6, DOI 10.1007/978-94-017-7567-0_2

H^+. Predictive models of future global changes in coral and coral reef growth based on oceanic Ω_{arag} must include the influence of future changes in localized P_{net} on G_{net} as well as changes in rates of reef carbonate dissolution. The correlation between Ω_{arag} and G_{net} over the diel cycle is simply the result of increasing pH due to photosynthesis that shifts the CO_2-carbonate system equilibria to increase [CO_3^{2-}] relative to the other DIC components of [HCO_3^-] and [CO_2]. Therefore Ω_{arag} closely tracks pH as an effect of P_{net}, which also drives changes in G_{net}. Measurements of DIC flux and H^+ flux are far more useful than concentrations in describing coral metabolism dynamics. Coral reefs are systems that exist in constant disequilibrium with the water column.

Keywords

Calcification • Corals • Ocean acidification • Seawater CO_2-carbonate system • Aragonite saturation state • Boundary layers • Phase lag

2.1 Introduction

Reviews have recently been published on coral calcification (Allemand et al. 2011), on the effects of ocean acidification on coral calcification (Erez et al. 2011) and on the geological record of ocean acidification (Hönisch et al. 2012). These documents provide a wealth of background information. This chapter provides an updated synthesis including new insights on coral physiology and calcification relevant to the geology and paleo-ecology of coral reefs.

2.1.1 Basic Coral Anatomy and Physiology

Reef corals are coelenterates formed by an outer body wall and a basal body wall that enclose a space called the coelenteron. Terminology used here follows that of Galloway et al. (2007). The outer body wall in contact with sea water consists of two tissue layers – an outer epidermis and an inner gastrodermis separated by a jelly-like substance called mesoglea (Fig. 2.1a). Likewise, the basal body wall is a mirror image that consists of the calicodermis and a gastrodermis separated by mesoglea. The space between the two body walls is a cavity called the coelenteron, which interconnects the polyps of the colony and opens to the external seawater through the polyp mouths. The intracellular symbiotic zooxanthellae reside mainly within the cells of the gastrodermis of the surface body wall. The zooxanthellae are photosynthetic and are capable of providing all of the energy needed for basic metabolism of the coral (Muscatine et al. 1984). However, heterotrophic food inputs are still important. Well-fed corals exhibit higher growth rates and greater stress tolerance compared to less-fed colonies (Ferrier-Pagès et al. 2003; Grottoli et al. 2006; Edmunds 2011; Connolly et al. 2012). Calcification occurs in the calcifying fluid located between the calicodermis and the skeleton. A presumed proton transfer process increases the pH and saturation state of the fluid to a point where $CaCO_3$ crystallizes onto the skeleton as aragonite (Furla et al. 2000a, 2000b; Cohen and McConnaughey 2003; Allemand et al. 2004; Cohen and Holcomb 2009; Venn et al. 2011). Energy is needed to drive this process with up to 30 % of the coral's energy budget devoted to calcification (Allemand et al. 2011).

The contemporary four cell-layer structure with metabolic pathways as proposed by Furla et al. (2000a, 2000b) and Allemand et al. (2004) is shown in Fig. 2.1a. This model requires neutralization of the H^+ produced by calcification using OH^- produced by photosynthesis. However, there is a contradiction. The distal areas of the corallum that are growing most rapidly lack gastrodermal cells and their contained zooxanthellae (Gladfelter 1982; Brown et al. 1983; Gladfelter 1983; Tambutté et al. 2007). Jokiel (2011a) hypothesized that H^+ is released directly into the water column in rapidly calcifying areas of the coral (Fig. 2.1b). An alternative explanation is that OH^- is transported from areas of the coral undergoing rapid photosynthesis to areas of the coral undergoing rapid calcification. McConnaughey and Whelan (1997) proposed that calcification at branch tips could discharge protons into seawater within the coelenteron. This water could be transported by ciliary currents to the abundant photosynthetic zooxanthellae in the lateral polyps.

Most studies involve incubation of corals in static containers under controlled conditions with extrapolation of the changes measured in the carbonate-CO_2 chemistry of bulk seawater to precipitation of $CaCO_3$ in the calcifying fluid adjacent to the coral skeleton. These results must be viewed with caution because there is an organism located between the calcifying space and the bulk water being measured as well as a boundary layer (BL) between the organism and the water column. Calcification is under biological control and mediated by organic tissue that separates the calcifying surface from overlying seawater. Therefore calcification occurs in a medium (i.e. the

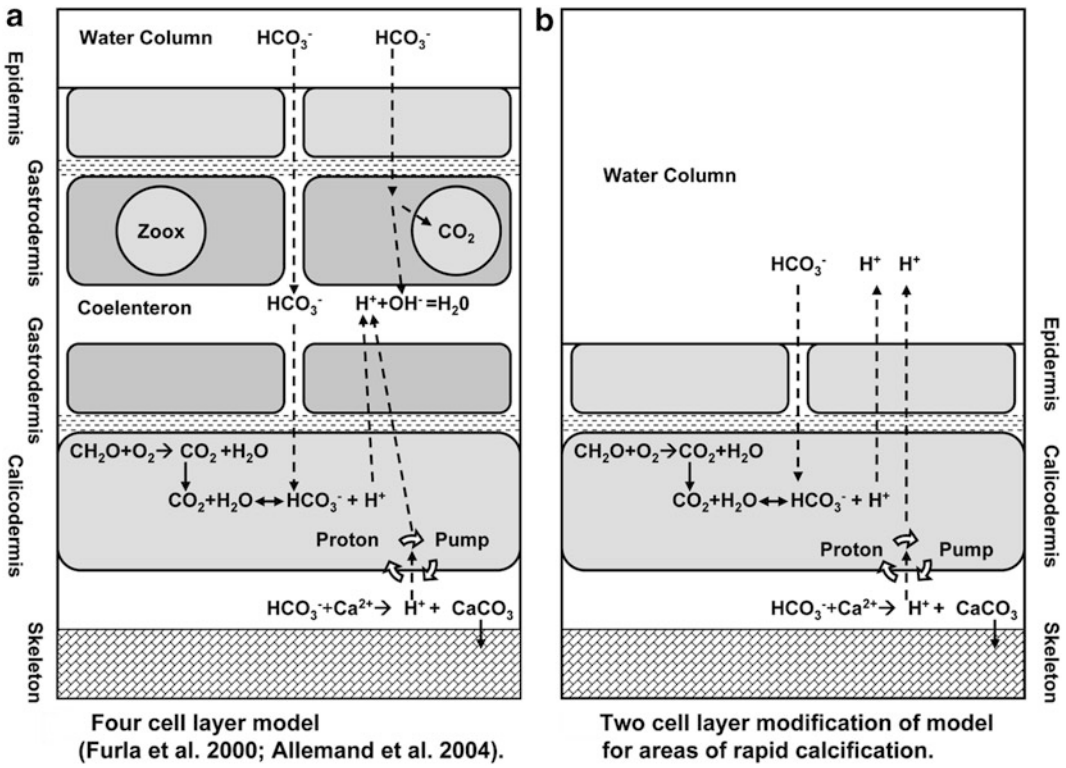

Fig. 2.1 Classic four cell-layer model of calcification (**a**) compared to two cell layer structure of rapidly calcifying areas of the corallum (**b**) as described by Tambutté et al. (2007). Note that protons generated by calcification in (**b**) are shown being released directly into the water column rather than being neutralized by photosynthesis as proposed by Furla et al. 2000a, 2000b; and Allemand et al. 2004 (Figure from Jokiel (2011b) used with permission from the Journal of Experimental Marine Biology and Ecology)

calcifying fluid) that has different carbonate-CO_2 chemistry than the bulk seawater as materials are exchanged through the BL. Additional information on processes occurring within the coral tissues and the BL has been provided through use of microprobes (Kühl et al. 1995; Al-Horani et al. 2003a, 2005a), isotope chemistry (Goreau 1977; Allison et al. 1996; Al-Horani et al. 2005a) and direct measurement of pH within coral tissues (Venn et al. 2009, 2011, 2013). Most of the models have focused on rates of biological processes that occur at the interface between the calicodermis and the coral skeleton (Fig. 2.1a). More recently, Jokiel (2011a, 2011b) has developed a model based on physical control of material flux through the BL and into the water column (Fig. 2.1b).

2.1.2 Coral Morphology

The growth forms of reef corals (Fig. 2.2) are extremely varied (Veron 2000), which has confounded understanding of basic metabolic processes and patterns of calcification. How can a simple organism consisting of only two tissue layers with a total of four cell layers produce so many intricate growth forms? The key to understanding lies in the observation (Fig. 2.3) that all coral growth forms can be reduced to the topological equivalent of a hemisphere containing the photosynthetic polyps and/or tissues containing dense concentrations of zooxanthellae (zone of rapid photosynthesis or ZP) surrounded by a hemisphere dominated by calcification polyps and/or tissues devoid of zooxanthellae (zone of rapid calcification or ZC). Cells and polyps located in the distal portions of a colony (ZC) have few or no zooxanthellae, giving these areas a white appearance (Figs. 2.2 and 2.3).

2.1.3 Models of Light Enhanced Calcification (LEC)

The discovery that calcification in reef corals is accelerated in the light (Kawaguti and Sakumoto 1948) led to the conclusion that photosynthesis by zooxanthellae must somehow be involved in the biochemical pathways of calcification. Experimental evidence was eventually developed by Vandermeulen et al. (1972) who showed that blocking photosynthesis results in a marked reduction in calcification. A number of LEC models have been presented (reviewed by Gattuso et al. 1999; Cohen and Holcomb 2009; Allemand et al. 2011). Goreau (1959) proposed that calcification is

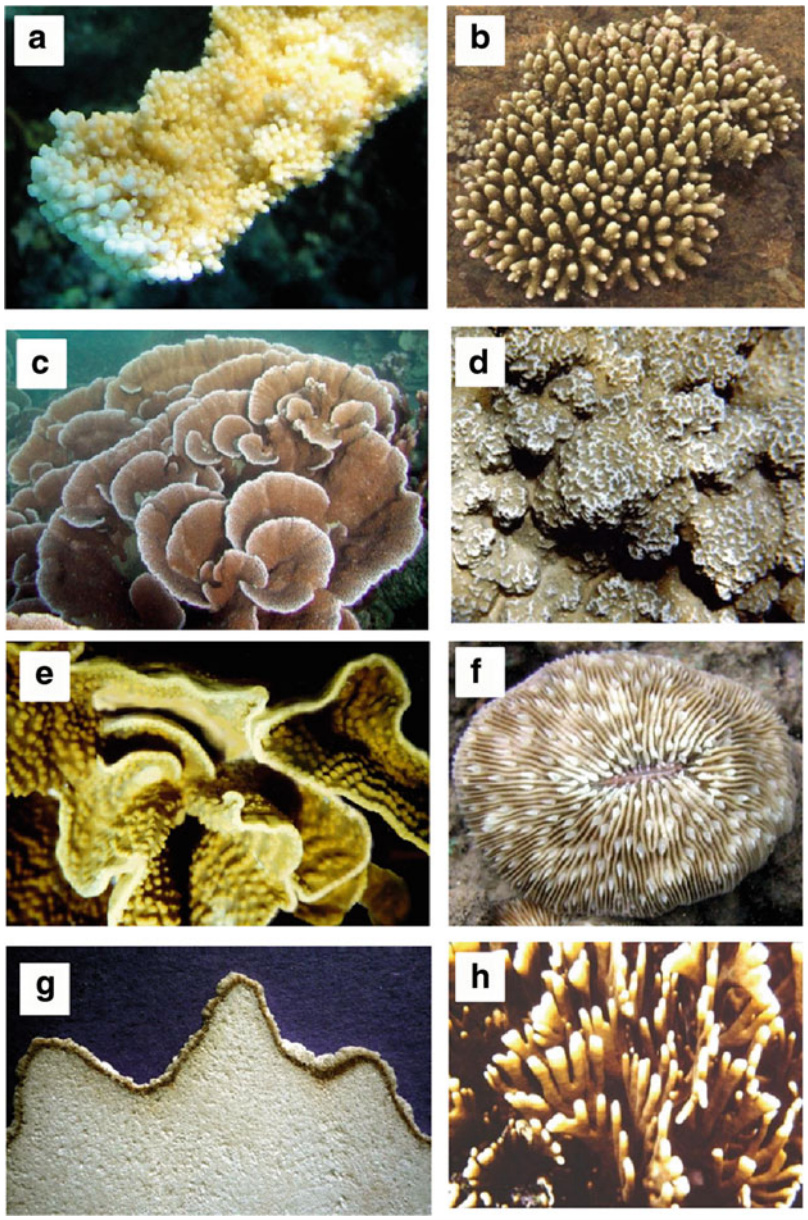

Fig. 2.2 Variation in coral morphology (**a**) branch tip of *Acropora palmata*, (**b**) colony of branching *Acropora humilis* (**c**) plate-like colony of *Montipora capitata* (**d**) encrusting *Porites rus* (**e**) foliose *Turbinaria* sp. (**f**) solitary coral *Fungia scutaria* (**g**) cross-section skeleton of a massive *Porites* sp. (**h**) branched, non-scleractinian hydrocoral *Millepora tenera*. Note that all growth forms lack zooxanthellae on the rapidly growing distal branch tips, distal plate margins, and distal edges of septae and trabeculae as shown in Fig. 2.3

accelerated in light due to removal of CO_2 from calcification sites by photosynthetic zooxanthellae. This model requires the zooxanthellae to be located at or near the calcification site, but actually they are located far from the site of calcification (Fig. 2.1). Further, the proposed chemical reactions have not been supported by experimental data. Simkiss (1964) advanced a model based on the removal of phosphate "crystal poisons" from calcification sites by photosynthetic zooxanthellae, but this model also suffers from the requirement that zooxanthellae must be located close to calcification sites. A similar explanation for LEC is that the zooxanthellae act as kidneys to remove the metabolic wastes in the coral animal that can inhibit calcification (Yonge 1968; Crossland and Barnes 1974). Muscatine (1990) suggested that perhaps photosynthesis and calcification are not connected through carbonate chemistry, but rather show a linkage simply because photosynthesis provides energy for calcification. This view was supported by the work of Colombo-Pallotta et al. (2010) who report that calcification in symbiotic corals is not strictly a "light-enhanced" or "dark-repressed" process, but rather, the products of photosynthesis have a critical role in calcification, which should be viewed as a "photosynthesis-driven" process.

Several recent models of coral calcification involve the zooxanthellae in the removal or neutralization of excess protons produced by calcification. McConnaughey and Whelan (1997) proposed that calcification in corals enhances photosynthesis by providing a source of protons that convert seawater HCO_3^- to CO_2 and H_2O, thereby supplying some of the CO_2 used in photosynthesis. Furla et al. (2000a)

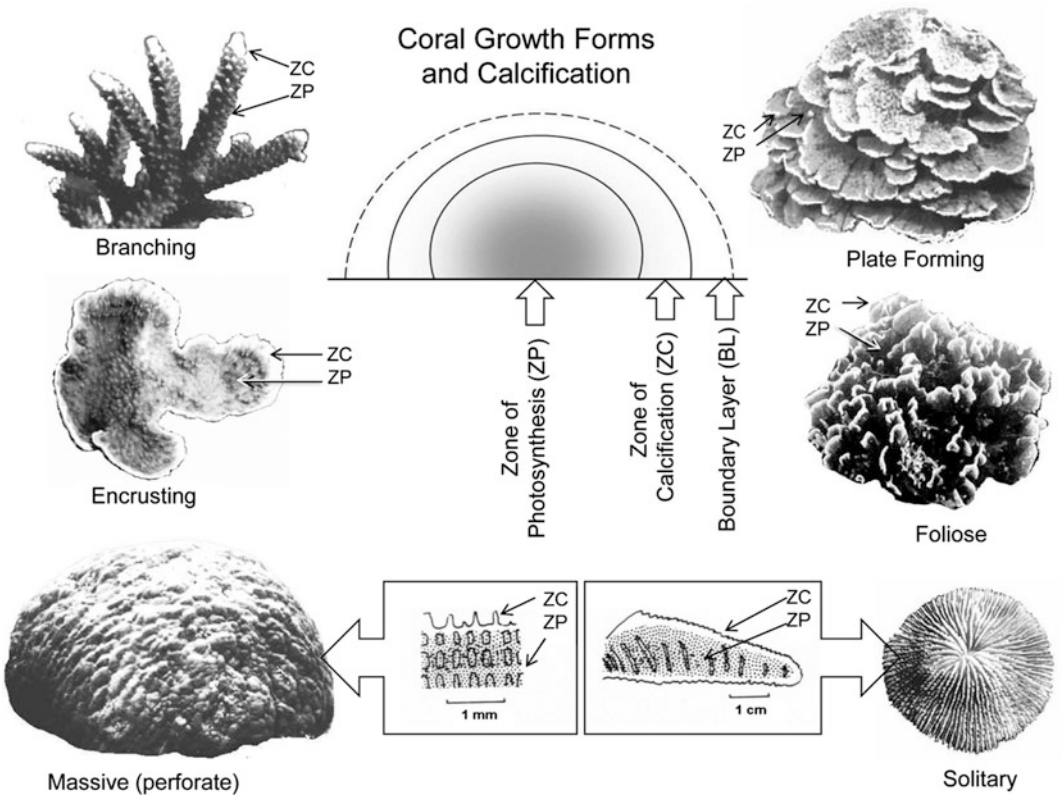

Fig. 2.3 Coral growth forms showing areas of rapid calcification (*ZC*) in relation to areas of photosynthesis (*ZP*) relative to the boundary layer (*BL*). In every case, the ZC is located between the ZP and the BL

determined that the major source of total dissolved inorganic carbon (DIC) used in calcification is from respiration (70–75 % of total $CaCO_3$ deposition), while only 25–30 % originates from the external seawater. The models of Furla et al. (2000a, 2000b) and Allemand et al. (1998) involve various pathways for buffering the H^+ produced during calcification using OH^- produced by photosynthesis (Fig. 2.1a). In contrast, a more recent model (Jokiel 2011a, 2011b, 2013; Jokiel et al. 2014a; Jokiel 2015) is focused on factors controlling dissipation of protons into the water column and uptake of DIC.

During daylight hours the high tissue oxygen tension resulting from photosynthesis will stimulate respiration (Mass et al. 2010). Colombo-Pallotta et al. (2010) found that under normal physiological conditions, a 42 % increase in seawater oxygen concentration promotes a twofold increase in dark-calcification rates relative to controls. Apparently hyperoxia is necessary to maintain a high respiration rate in areas where extremely high calcification is occurring. Colombo-Pallotta et al. (2010) presented a model in which the oxygen and glycerol produced by photosynthesis are translocated to the calicodermal cells, where these materials are used by the mitochondria to generate ATP, which in turn is used to drive calcification. Corals, like other marine animals, are believed to maintain a very low intracellular calcium level when compared to seawater. This implies highly active Ca^{2+}-ATPase with energy supplied from respiration (Al-Horani et al. 2003b). They also contend that Ca^{2+}-ATPase has a dual function: (1). the transport of Ca^{2+} to the site of calcification and (2). the removal of H^+ that increases the aragonite saturation state in the calcifying fluid and facilitates the reaction toward $CaCO_3$ formation. This model does not account for the disposal of the waste product H^+, which ultimately must diffuse into the surrounding bulk water.

2.1.4 Other Models of Coral Calcification

Muscatine (1973) proposed that calcification in corals may be limited by synthesis of skeletal organic matrix produced by the zooxanthellae. Synthesis of organic matrix does appear to be a critical prerequisite for coral calcification, and especially for crystal nucleation, though it is unclear to what extent organic matrix synthesis is likely to limit coral calcification under most circumstances (reviewed by Allemand et al. 2011). The "inhibitory enzyme model" based on the observation that surface seawater is supersaturated with respect to aragonite was developed by Chave (1984). According to this model enzymes prevent

mineralization at some locations while allowing mineralization at other specific locations to occur passively by precipitation of aragonite.

2.1.5 Chemistry of Ocean Acidification, Photosynthesis and Calcification

Presentations on ocean acidification inevitably involve three equations (e.g., Royal Society 2005; Kleypas et al. 2006). The first equation describes how increased atmospheric CO_2 caused by anthropogenic burning of fossil fuels dissolves in the oceanic surface waters to form carbonic acid which dissociates into a bicarbonate ion and a proton:

$$CO_2 + H_2O \Leftrightarrow HCO_3^- + H^+ \qquad (2.1)$$

The second equation describes the dissociation of a carbonate ion to a bicarbonate ion and another proton:

$$HCO_3^- \Leftrightarrow CO_3^{2-} + H^+ \qquad (2.2)$$

The third equation shows the carbonate ion combining with a calcium ion to form calcium carbonate:

$$CO_3^{2-} + Ca^{2+} \Leftrightarrow CaCO_3 \qquad (2.3)$$

Changes in seawater pH shift the equilibria among the various forms of dissolved inorganic carbon (DIC) so the distribution of CO_2, HCO_3^- and CO_3^{2-} shifts with pH (Fig. 2.4).

Concentrations of the various forms of inorganic carbon shift with changing pH as follows:

$$CO_2 + H_2O \Leftrightarrow H^+ + HCO_3^- \Leftrightarrow 2H^+ + CO_3^{2-} \qquad (2.4)$$

Calcification rate in coral incubation experiments is often determined by measuring change in total alkalinity (A_T) which is defined as the capacity of water to neutralize H^+. Coral calcification lowers A_T through release of protons (Eqs. 2.5, 2.6 and 2.7). In theory, calcification inevitably produces an excess of H^+ and thus reduces total alkalinity (A_T) by two moles for every mole of $CaCO_3$ precipitated (Kinsey 1978; Smith and Kinsey 1978). This relationship has now been verified directly by comparing A_T flux to Ca^{2+} flux in a coral reef flume system (Murillo et al. 2014). Therefore, Eq. 2.3 is misleading if taken out of context. Calcification equations must include two protons on the product side. The correct equations for calcification are as follows:

$$Ca^{2+} + (CO_2 + H_2O) \Leftrightarrow CaCO_3 + 2H^+ \qquad (2.5)$$

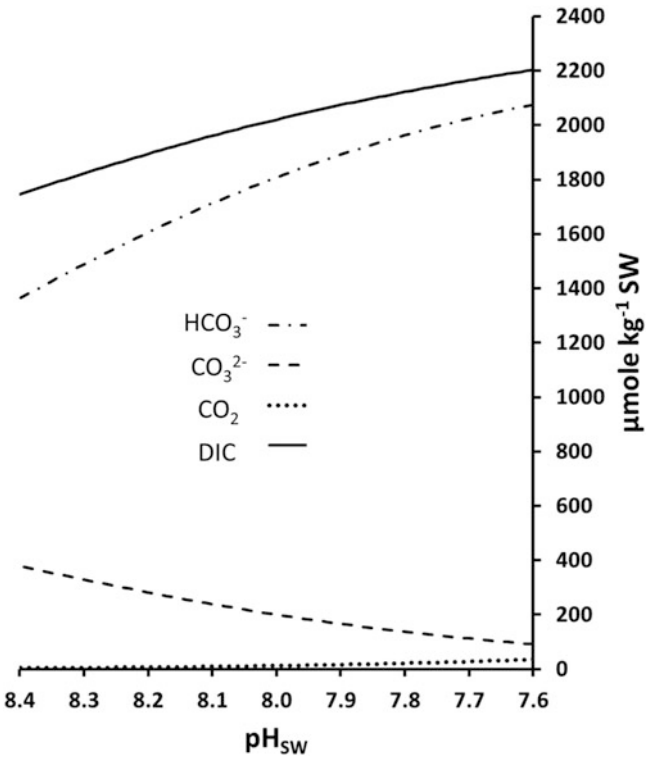

Fig. 2.4 Change in distribution of CO_2, HCO_3^-, CO_3^{2-} and DIC with changes in pH that occur due to coral metabolism and/or increasing ocean acidification (OA). Calculations were performed using CO2SYS (Pierrot et al. 2006) at T = 25 °C, S = 35 ppt, A_T =2300 µmol/kg SW

$$\updownarrow$$

$$Ca^{2+} + \left(H^+ + HCO_3^-\right) \Leftrightarrow CaCO_3 + 2H^+ \qquad (2.6)$$

$$\updownarrow$$

$$Ca^{2+} + \left(2H^+ + CO_3^{2-}\right) \Leftrightarrow CaCO_3 + 2H^+ \qquad (2.7)$$

Equations 2.5, 2.6 and 2.7 are written in two dimensions with a red arrow showing the relationship among the carbonate species (in parentheses) that shift with the changes in $[H^+]$ described as Eq. 2.4. Dissolution is the reverse of the calcification reaction. Net calcification (G_{net}) is the sum of calcification (positive flux) and dissolution (negative flux). When the equations are written correctly in this manner the importance of protons becomes apparent with two moles of H^+ produced for every mole of $CaCO_3$ precipitated regardless of which form of dissolved inorganic carbon (DIC) is involved.

The following equations describe photosynthetic carbohydrate formation from the various available CO_2 species:

$$(CO_2 + H_2O) \Leftrightarrow CH_2O + O_2 \quad (2.8)$$

$$\updownarrow$$

$$\left(H^+ + HCO_3^-\right) \Leftrightarrow CH_2O + O_2 \quad (2.9)$$

$$\updownarrow$$

$$\left(2H^+ + CO_3^{2-}\right) \Leftrightarrow CH_2O + O_2 \quad (2.10)$$

The photosynthesis equations are also written in two dimensions with the red arrows showing changes in distribution of species that occurs (Eq. 2.4) with shifts in pH. Note that photosynthesis increases pH (lowers $[H^+]$) while the reverse reaction of respiration decreases pH (increases $[H^+]$). Net photosynthesis (P_{net}) is the sum of photosynthesis (positive flux) and respiration (negative flux). Photosynthesis has a balanced charge (Eqs. 2.8, 2.9 and 2.10), so does not change A_T (Smith and Key 1975).

In sum, photosynthesis and calcification both lower the seawater DIC, while respiration and $CaCO_3$ dissolution raise DIC. Only the precipitation or dissolution of $CaCO_3$ significantly alters A_T. Consequently, changes in A_T can be used to calculate G_{net} and are widely used in this regard. Photosynthesis and respiration can radically alter $[H^+]$ and therefore relative concentration of CO_3^{2-}, HCO_3^- and CO_2. Coral calcification is a biological process that is heavily influenced by the associated processes of photosynthesis and respiration (e.g., changing P_{net}) that modify pH. Protons can be considered a waste product of calcification (Eqs. 2.5, 2.6 and 2.7) and O_2 a waste product of photosynthesis (Eqs. 2.8 and 2.9).

2.1.6 Conceptual Stumbling Blocks

The Calcification Equations The widespread use of Eqs. 2.1, 2.2 and 2.3, with emphasis on Eq. 2.3, fails to communicate the importance of H^+ as a waste product as shown by Eqs. 2.5, 2.6 and 2.7. The importance of Eqs. 2.5, 2.6 and 2.7 cannot be overemphasized – calcification will always result in the production of two moles of H^+ for every mole of $CaCO_3$ precipitated (Kinsey 1978; Smith and Kinsey 1978).

Coral calcification occurs in the space between the innermost tissue layer of the coral (calicodermis) and the skeleton (Fig. 2.1). However, the real physiological questions do not concern the Ω_{arag} at the site of calcification, which is under significant control by the coral animal. Rather, we need to know if the protons produced by calcification in the coral are dissipating out of the organism at a rate sufficient to avoid acidosis of tissues. Measurements of the changes in CO_2-carbonate chemistry of the bulk water do not necessarily relate directly to chemistry of the calcification fluid. Furthermore, measurements made using changes in the chemistry of the bulk water during coral incubations cannot distinguish between whether the supply side or product side of Eqs. 2.5, 2.6 and 2.7 is responsible for the change in G_{net}. The stoichiometry and measured changes in seawater chemistry will be the same for both cases.

The pH Concept An additional conceptual problem traces its roots to the fact that $[H^+]$ is often reported as pH where:

$$pH = -\log[H^+] \quad (2.11)$$

The problem here is that pH represents a double non-linear transformation of $[H^+]$ (i.e. the log of a reciprocal) that disguises the magnitude of change in $[H^+]$. The widespread use of pH rather than $[H^+]$ results from the fact that pH is easily measured with a pH electrode. However, the pH electrode measures activity of H^+ rather than $[H^+]$. Nevertheless, pH has a long history of use and is universally reported in research papers. Physiological systems generally respond to activity of H^+ (rather than concentration), so use of pH is a convenient index of acid-base conditions. Physical processes outside of the organism (such as diffusion through a boundary layer) respond to concentration. The use of pH (-log $[H^+]$) rather than $[H^+]$ clouds the fact that immense changes in $[H^+]$ occur across diffusion barriers that form outside of the tissues. The strength of these gradients increases with increasing OA (Jokiel 2011a).

Until recently the focus on limiting factors for coral calcification rate has been on the reactants (left side of Eqs. 2.5, 2.6 and 2.7), with an emphasis on uptake of specific forms of DIC. Failure to dissipate H^+ from the site of calcification, through the tissues and out through the seawater boundary layer (right side of Eqs. 2.5, 2.6 and 2.7), will cause acidosis and disruption of normal biological processes. An excellent analogy is furnished by the companion process of photosynthesis in reef corals. Photosynthesis produces fixed carbon as a product while calcification produces calcium carbonate as a product. Photosynthesis produces the "waste product" O_2 while calcification produces the "waste product" H^+. Boundary layer thickness can control primary production by limiting efflux of O_2 from the coral. Increased water motion decreases boundary layer thickness, increases O_2 flux rate and increases primary production (Mass et al. 2010). By analogy, boundary layer thickness presumably can control proton efflux and thereby control calcification rate. Corals have evolved a very sophisticated morphology that results in a highly effective means of dealing with the waste products of O_2 and H^+ (Jokiel 2011a, 2011b).

The importance of HCO_3^- uptake to coral metabolism is shown by the abundance of the enzyme carbonic anhydrase (CA) in reef corals. The reaction described in Eq. 2.1 is accelerated by CA which has a reaction rate that is among of the fastest of all enzymes. Coral tissues and zooxanthellae contain large amounts of CA (Graham and Smillie 1976; Weis et al. 1989) which play a major role in controlling transport of CO_2 throughout the coral colony. Al-Horani et al. (2003a) identified CA bound to the membranes of the epidermal cells of the surface body wall. Moya et al. (2008) identified CA in the calicodermis, which controls the precipitation of skeletal material. Wherever the conversion between CO_2 and HCO_3^- is very fast (i.e. such as occurs in the presence of CA) in comparison to the rate of diffusion, a difference in HCO_3^- concentration corresponding to the CO_2 tension difference will be established (Enns 1967).

2.1.7 The Concept of Aragonite Saturation State (Ω_{arag}) in Relation to Ocean Acidification (OA)

Burning of fossil fuels continues to increase the concentration of CO_2 in the atmosphere. When the anthropogenic CO_2 is absorbed by seawater, chemical reactions occur that reduce seawater pH, increase bicarbonate ion (HCO_3^-) and decrease carbonate ion (CO_3^{2-}) concentration (Fig. 2.4) in a process commonly referred to as ocean acidification (OA). These reactions are described in a review by Feely et al. (2009). A doubling of pre-industrial levels of oceanic pCO_2 is predicted to occur at some point within this century (IPCC 2001, 2007), unless we radically limit our burning of fossil fuels. Increased pCO_2 in sea water leads to a decreased aragonite saturation state (Ω_{arag}). Aragonite is the primary mineral form of $CaCO_3$ that is laid down by corals, so the question arose as to how the declining Ω_{arag} would impact living coral populations. Smith and Buddemeier (1992) stated that increased CO_2 would lead to reduced coral calcification rates. Their conclusion was subsequently confirmed by laboratory studies showing that calcification rates of reef-building corals could decline by 20–40 % under twice present day pCO_2 conditions (Gattuso et al. 1999; Langdon et al. 2000; Marubini et al. 2001, 2003; Langdon and Atkinson 2005). These early observations led to a growing concern about the impact of OA on corals and coral reefs (Kleypas et al. 1999a, 1999b; Orr et al. 2005; Hoegh-Guldberg et al. 2007; Carpenter et al. 2008; Veron 2008).

The saturation state concept is widely used by physical chemists in describing seawater carbonate chemistry. The saturation state of aragonite (Ω_{arag}), which is the mineral form of $CaCO_3$ precipitated by reef corals, is of particular interest. The term is defined by the equation:

$$\Omega_{arag} = \frac{[Ca^{2+}][CO_3^{2-}]}{K_{sp}} \quad (2.12)$$

where K_{sp} is the solubility product of aragonite. The $[Ca^{2+}]$ in normal present-day oceanic seawater is essentially constant at 10.3 mmol kg^{-1} SW, normalized to salinity. Likewise, K_{sp} is a constant (at a given temperature, pressure, and salinity), so in shallow oceanic waters Ω_{arag} is directly proportional to $[CO_3^{2-}]$. Intensive work over the past 25 years (reviewed by Feely et al. 2009) has led to a much greater understanding of how combustion of fossil fuels is leading to lower (Ω_{arag}) in the surface waters of the ocean.

2.1.8 Relationship Between Ω_{arag}, the [DIC]:[H^+] Ratio and Coral Calcification (G_{net})

The concept of the [DIC]:[H^+] ratio introduced by Jokiel (2011a) provides a new insight into the controls on coral calcification that has now been supported by observations in other organisms such as coccolithophores (Cyronak et al. 2015) and marine bivalves (Thomsen et al. 2015). A major difficulty with the Ω_{arag} model is failure to explain why G_{net} decreases with increasing OA in the face of increasing [DIC] and increasing $[HCO_3^-]$ (Fig. 2.4). G_{net} increases under higher $[HCO_3^-]$ (Herfort et al. 2008; Marubini et al. 2008; Jury et al. 2010), so G_{net} should increase with increasing OA. Jokiel (2011a) estimated that the increase in G_{net} due to increased $[HCO_3^-]$ caused by a doubling of pCO_2 from pre-industrial levels will only be 3.8 % compared to the predicted decrease in G_{net} of 32 % due to increased $[H^+]$ for a net decrease of 28.2 %. Thus any benefit to skeletal growth caused by higher $[HCO_3^-]$ will be overwhelmed by an order of magnitude greater negative impact due to increased $[H^+]$.

We can demonstrate the relationship between G_{net} and the seawater CO_2-carbonate system parameters of A_T, Ω_{arag}, CO_3^{2-}, HCO_3^-, $CO_{2(aq)}$, H^+ and the [DIC]:[H^+] ratio from a biological perspective. Rather than following the physical chemistry approach of using saturation state we can employ a physiological organism-centered approach based on documented metabolic processes. The major focus must be that any protons generated by the calcification reaction must dissipate out of the coral. Also, there must be uptake of DIC if the coral is to calcify.

The chemistry of the CO_2 -carbonate system is complex, but only two parameters are needed to calculate the distribution of DIC species and Ω_{arag} in seawater at known salinity (S), temperature (T), and pressure (P). The relationship between the major parameters of the system can be

demonstrated simply by varying pCO_2 at constant A_T, S, T and P. As pCO_2 increases, pH decreases (i.e. $[H^+]$ increases), [DIC] increases, $[CO_3^{2-}]$ decreases, and Ω_{arag} decreases. The opposite is true for decreasing pCO_2. In other words, $[H^+]$ varies directly with [DIC] under increasing OA and inversely with $[CO_3^{2-}]$. The rules of proportionality (Tourniaire and Pulos 1985) allow us to state this relationship mathematically using proportionality constant (k_1) as follows:

$$[H^+] = \frac{[DIC]}{[CO_3^{2-}]} k_1 \tag{2.13}$$

These terms can be rearranged as follows:

$$[CO_3^{2-}] = \frac{[DIC]}{[H^+]} k_1 \tag{2.14}$$

In oceanic surface water, Ω_{arag} is proportional to $[CO_3^{2-}]$, so we can rewrite the equation with a different proportionality constant (k_2) as:

$$\Omega_{arag} = \frac{[DIC]}{[H^+]} k_2 \tag{2.15}$$

There is a large body of data showing that G_{net} is proportional to Ω_{arag}. Therefore we can rewrite Eq. 2.15 as:

$$G_{net} = \frac{[DIC]}{[H^+]} k_3 \tag{2.16}$$

Equation 2.16 could also be derived from the observation of Schneider and Erez (2006) that G_{net} is directly proportional to [DIC] and inversely proportional to $[H^+]$. The plot of G_{net} versus Ω_{arag} (or G_{net} versus $[CO_3^{2-}]$) should be similar to the plot of G_{net} versus the [DIC]:$[H^+]$ ratio times the appropriate proportionality constant. In other words we need not resort to the Ω_{arag} concept of physical chemistry, but can describe coral calcification based on physiologically relevant parameters.

Bach (2015) used a physical chemistry approach to further investigate these relationships. He rearranged the seawater carbonate system equations to demonstrate the proportional relationship between $[CO_3^{2-}]$ and the $[HCO_3^-]$:$[H^+]$ ratio where $[HCO_3^-]$ is the inorganic carbon substrate and $[H^+]$ functions as a calcification inhibitor as previously defined by Jokiel (2011a). Due to this proportionality rule, he points out that calcification rates will always correlate well with the ratio of $[HCO_3^-]$:$[H^+]$ and equally well to [DIC]: $[H^+]$, $[CO_3^{2-}]$ or Ω_{arag} when T, S, and P are constant. Thus, the correlations between calcification and $[CO_3^{2-}]$ or Ω_{arag} that have previously been reported can be attributed to the combined influence of $[HCO_3^-]$ and $[H^+]$, which provide a more meaningful physiological parameter than Ω_{arag}.

The [DIC]:$[H^+]$ ratio concept is an alternate way of viewing net calcification that can be tested. A high quality data set is available from Langdon et al. (2000), who conducted long term static tests in highly modified sea water chemistries. This work was carried out over a number of years in the 2650 m^3 "ocean" coral reef mesocosm of Biosphere-2 located near Tucson, Arizona. Effects of sea water carbonate chemistry on G_{net} were determined under various sea water chemistries in an assembled community of coral reef organisms consisting of corals, calcifying algae, and other typical reef biota. The investigators manipulated the saturation state of the water by adding various amounts of $NaHCO_3$, Na_2CO_3 and $CaCl_2$. They found that G_{net} was a function of the product of $[Ca^{2+}]$ and $[CO_3^{2-}]$, leading to their conclusion that "saturation state (and not pH, pCO_2, or HCO_3^-) affects coral reef calcification". Data reported for A_T, Ca^{2+}, CO_3^{2-}, HCO_3^-, Ω_{arag}, pH and G_{net} during each of the experimental trials (Appendix Table 2.1) was used to calculate [DIC], $[H^+]$ and the [DIC]:$[H^+]$ ratio. Analysis of these data shows a non-significant relationship between G_{net} and $[Ca^{2+}]$ (Fig. 2.5a), reflecting the superabundance of Ca^{2+} ($\approx$10 mmole kg^{-1}) in relation to CO_3^{2-}($\approx$0.2 mmol kg^{-1}) or DIC ($\approx$2 mmol kg^{-1}). The lack of a relationship between G_{net} and Ca^{2+} supports the observations of Gagnon et al. (2012) that describe exchange of Ca^{2+} and other cations between seawater and the calcifying fluid over the course of a few hours. The mechanism for this type of transport appears to be a voltage-dependent Ca^{2+} channel that accelerates the trans-epithelial transport of Ca^{2+} used for coral calcification (Zoccola et al. 1999), but it has not been shown to transport anions such as CO_3^{2-}. Presumably then, the small differences in $[Ca^{2+}]$ that occur over geologically short timescales are not a major driver of calcification (Fig. 2.5a). In contrast, G_{net} shows a significant correlation with the DIC:H^+ ratio (Fig. 2.5b). In retrospect, the significant relationship between G_{net} and $[CO_3^{2-}]$ or its surrogate Ω_{arag} is due to correlation of Ω_{arag} with the DIC:H^+ ratio (Fig. 2.5c).

2.1.9 Boundary Layers (BL) and Material Exchange Between the Water Column and the Coral

The role of the boundary layer (BL) in controlling material flux in corals and other organisms is one of the keys to understanding calcification in corals. Corals create frictional drag which slows water velocity. Three sub-component layers of the BL have previously been defined and measured (Shashar et al. 1996).

The Diffusion Boundary Layer (DBL) is a quiescent layer of water adjacent to the coral tissue and is important in relation to diffusion-limited processes such as respiration and photosynthesis. Much of the work on boundary layer limitation of material exchange has been focused on this innermost layer. Shapiro et al. (2014) present direct

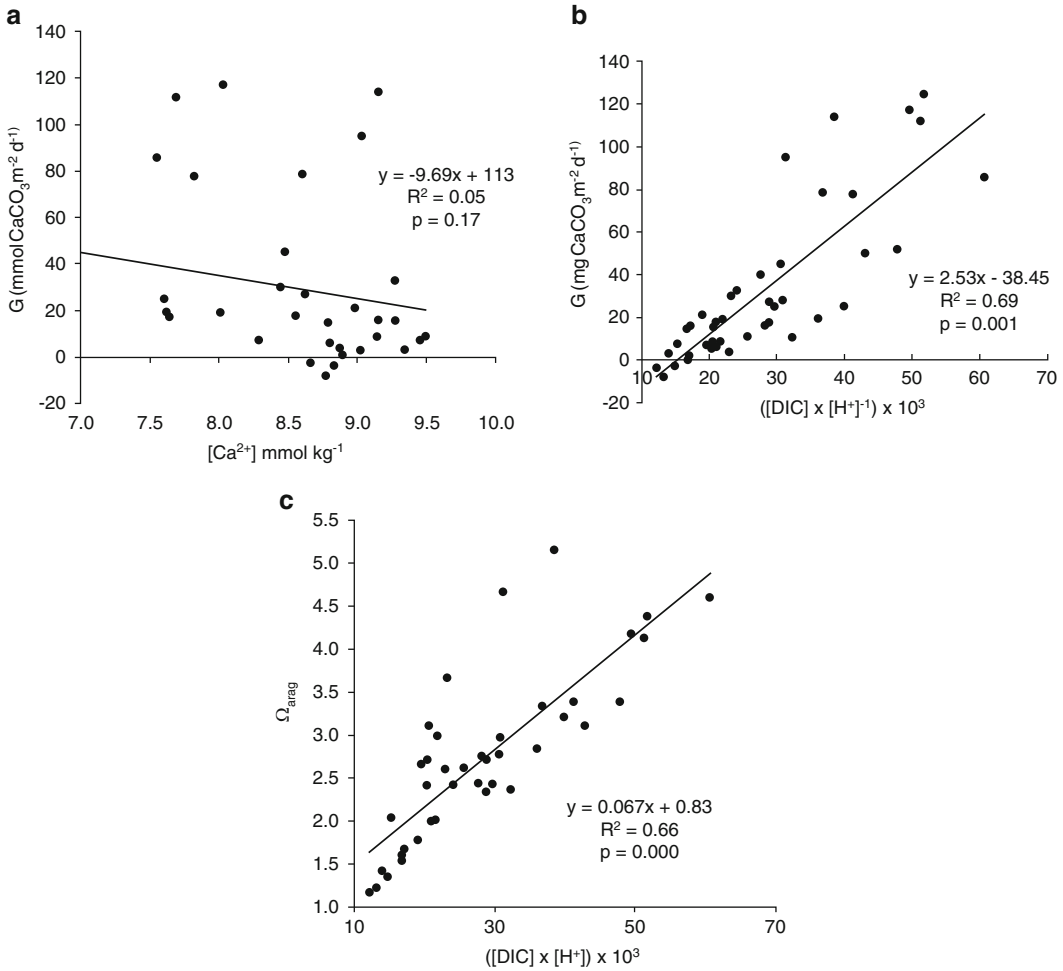

Fig. 2.5 Biosphere-2 data from Langdon et al. (2000) showing: (a.) G_{net} as a function of Ca^{2+}, (b.) G_{net} as a function of the [DIC]:[H^+] ratio and (c.) Ω_{arag} vs. [DIC]:[H^+] ratio (Data are presented in Appendix Table 2.1)

microscopic evidence that corals can at least partially overcome limitation by molecular diffusion in the DBL by developing strong vortical flows driven by motile epidermal cilia covering their entire tissue surface. Ciliary beating produces quasi-steady arrays of counter-rotating vortices that vigorously stir a layer of water extending up to 2 mm from the coral surface, but requires expenditure of energy. Under low ambient flow velocities, these vortices can control the exchange of nutrients and oxygen between the coral and its environment, enhancing mass transfer rates by up to 400 %.

The Momentum Boundary Layer (MBL) controls water movement near the colony and is thicker by an order of magnitude than the DBL. The Benthic Boundary Layer (BBL) incorporates the DBL and MBL to describe the frictional drag of the complex benthic structures on flow near the bottom and controls the exchange of water between the reef and the overlying water column. The BBL studied by Shashar et al. (1996) was more than 1 m thick with a roughness height of 31 cm and a shear velocity of 0.42 cm s^{-1}.

The present discussion of the BL will be focused on the DBL, which produces a thin layer of stagnant seawater adjacent to the coral tissue. This quiescent layer influences the flux of material between the corallum and the water column. The transport of Ca^{2+}, CO_2, CO_3^{2-}, HCO_3^-, O_2, nutrients and H^+ through the BL is limited by the physical processes of diffusion and advection (e.g., Jokiel 1978; Shashar et al. 1993; Lesser et al 1994; Shashar et al. 1996; Kaandorp et al. 2005, 2011). Kühl et al. (1995) found that zooxanthellae photosynthesis in the light resulted in a build-up of O_2 in the photosynthetic tissue of up to 250 % saturation and a tissue pH of up to 8.6 (i.e. 0.7 pH units above the pH value of the overlying seawater). In darkness the O_2 within the coral tissue was depleted by respiration to near anoxic (<2 % air saturation) conditions, with tissue pH of 7.3–7.4. O_2 and pH profiles demonstrated the presence of a 200–300 μ thick BL that separated the coral tissue from the overlying flowing seawater. Two recent models invoke boundary layer controls on coral calcification. One (Kaandorp et al. 2005, 2011)

addresses BL limitation of DIC influx and the other (Jokiel 2011a, 2011b) focuses on BL limitation of proton efflux.

Corals experience the highest water motion and thinnest BL at the distal parts of the corallum (Figs. 2.2, and 2.3). Projections of the skeleton and branch tips are covered by thin, colorless tissue which is devoid of zooxanthellae (Fig. 2.2a). These areas are more responsive to changes in water motion than adjacent areas (Jokiel 1978). Increased water flow reduces the thickness of the BL over these structures, increasing local calcification to produce the hoods, papillae, spines, verrucae and other projections that characterize many species of reef corals (Veron 2000). In turbulent water these projections grow outward and increase frictional drag and protect the polyp. In calm, low light environments they remain suppressed (Jokiel 1978).

2.1.10 Material Fluxes

Coral calcification rates based on changes in CO_2-carbonate chemistry describe net flux through the boundary layer that isolates the "black box" of the coral from the water column and do not represent processes at the site of calcification. Distinguishing between calicodermal flux, epidermal flux and gastrodermal flux within the "black box" can be informative. Epidermal flux as defined here refers to the exchange of materials between the epidermis and the external water column (Fig. 2.1b). Rate of epidermal flux is limited by the BL and is characterized by carbonic anhydrase- facilitated transport of bicarbonate HCO_3^- into the coral tissue and efflux of H^+ as described in the Proton Flux Model (Jokiel 2011a, 2011b). Calicodermal flux as defined here includes and emphasizes the exchange of material between coral calicodermal cells and the space between the calicodermis and the $CaCO_3$ accretion site of the skeleton. H^+ must be actively removed from the calcifying space by calicodermal cells if the reaction at the skeleton is to move towards $CaCO_3^{2-}$ precipitation (Eqs. 2.5, 2.6 and 2.7). The mechanism involved appears to be one or more proton pumps (Furla et al. 2000a; Cohen and McConnaughey 2003; Allemand et al. 2004). Allison et al. (2014) used skeletal boron geochemistry to study the DIC chemistry of the fluid used for coral calcification. They showed that corals concentrate DIC in the calcifying fluid at the skeleton calcification site and that bicarbonate makes up a significant amount of the DIC pool used to build the skeleton. Corals actively increase the pH of the calcification fluid to create a diffusion gradient favorable to the transport of molecular CO_2 from the overlying coral tissue into the calcification site. The increased calcification fluid pH and higher [DIC] results in a high aragonite saturation state within the calcifying fluid which is favorable to aragonite precipitation.

However, the waste H^+ being rapidly removed from the calcifying fluid must be dissipated out of the calicodermis and other tissue layers into the water column. Otherwise acidosis will develop in the tissues and block metabolism. The coelenteron fluid can exchange with sea water through the polyp mouths and into the BL. Gagnon et al. (2012) provided evidence for rapid cation exchange (but not anion exchange) between seawater and the calcifying fluid. This mechanism does not alleviate the need to move protons out of the "black box"- through the boundary layer and into the water column. The boundary layer is a physical limitation that is not under biological control.

It appears that metabolic energy is required to transport Ca^{2+} across the calicodermis into the calcifying fluid (between the calicodermis and the skeleton) at a rate sufficient to maintain normal calcification (Al-Horani et al. 2003a, 2003b). Tambutté et al. (1996) concluded that transport of Ca^{2+} across the epidermis and gastrodermis appears to be facilitated by paracellular pathways that connect the calcifying fluid adjacent to the skeleton with the sea water in the BL (Tambutté et al. 2012). The pH in the calcifying space under the calicodermis has been shown to be elevated relative to the polyp surface and to the inside of the coelenteron (Al-Horani et al. 2003a; Ries 2011; Venn et al. 2011). Ca^{2+} is transported over considerable distances within a colony with the direction of transport toward areas of maximum growth and calcification (Taylor 1977). Translocation of metabolic material within the coral has been demonstrated experimentally (Pearse and Muscatine 1971; Taylor 1977; Rinkevich and Loya 1983; Fine et al. 2002). One mechanism for such transport was described by Gladfelter (1983). Polyps of the coral *Acropora cervicornis* are connected in a complex gastrovascular system, which is lined with flagellated cells that can move the gastrovascular fluid at velocities of more than 2 cm min^{-1}. This type of circulation system serves to exchange fluids between the ZP and the ZC.

2.2 The Two-Compartment Proton Flux Model

This model (Jokiel 2011b) considers four major observations not included in earlier models of coral metabolism:

- Boundary-layers control exchange of materials at the tissue-seawater interface, which includes efflux of waste protons as well as influx of dissolved inorganic carbon.
- Zooxanthellae are lacking in rapidly calcifying areas of the coral (Goreau and Goreau 1959; Goreau 1963; Pearse and Muscatine 1971; Crossland and Barnes 1974; Lamberts 1974; Jaubert 1977; Brown et al. 1983; Kajiwara et al. 1997; Marshall and Wright 1998; Fang

et al. 2004; Al-Horani et al. 2005b; Tambutté et al. 2007; Santos et al. 2009).

- Photosynthate (CH_2O) is transported from areas containing zooxanthellae toward areas of rapid calcification that lack zooxanthellae (Pearse and Muscatine 1971; Taylor 1977). Translocation suggests that areas of photosynthesis and areas of rapid calcification are metabolically different and require different chemical environments. A coral colony contains a proximal region of zooxanthellae-rich tissues, termed the zone of rapid photosynthesis (ZP) and a second zone consisting of distal portions of the skeleton (branch tips, outer septal plates, and projecting trabeculae) covered by thin, colorless or lightly pigmented tissues and termed the zone of calcification or ZC (Jokiel 2011b).
- Primary and secondary calcification occurs in corals. Primary calcification in branch tips, septal margins, trabeculae and spines is characterized by rapid outgrowth (extension). This is followed by secondary calcification (accretion) on the sides of branches (Gladfelter 1982, 1983). Skeletal density variations result from differing rates of extension vs. accretion under different conditions of temperature, irradiance and water motion (Barnes and Lough 1993).

2.2.1 Description of the Two-Compartment Proton Flux Model

The model is described using the equations for calcification (Eqs. 2.5, 2.6 and 2.7) and photosynthesis-respiration (Eqs. 2.8, 2.9 and 2.10). The three dimensional hemispherical layered form of the coral tissues is reduced to a two dimensional diagram in Fig. 2.6a. The resulting fluxes and recycling pathways are shown in Fig. 2.6b for protons, Fig 2.6c for carbon and Fig. 2.6d for oxygen. In the ZP, interconversion between HCO_3^- and CO_2 (Eq. 2.2) occurs at an extremely rapid rate due to abundant CA. In the second compartment, or the ZC, both primary calcification and respiration occur but there is no photosynthesis. The major fluxes of H^+, HCO_3^-, O_2 and CH_2O are shown as arrows. In either compartment, as $CaCO_3$ precipitates out of solution, the H^+ must be removed if calcification is to continue. In the ZP, some of the protons produced by the secondary calcification can be used to drive photosynthesis. In the ZC, the excess H^+ is removed via direct flux across the BL. Reducing the description of metabolic reactions to only two sets of equations places the focus on proton flux and eliminates the need to complicate matters by including OH^-. Previous models invoke the use of OH^- derived from photosynthesis as a means of neutralizing the H^+ produced in calcification. However, this approach (Fig. 2.1) requires that OH^- be transported from areas of photosynthesis to the areas of rapid calcification. The focus on pathways of H^+ (Fig. 2.2b) is a very powerful and direct method of balancing material flux and describing the major metabolic processes and pathways in reef coral metabolism.

Placement of the rapidly calcifying areas adjacent to the BL facilitates rapid dissipation of H^+ into the water column from the ZC, and also allows for an efficient method of transporting excess H^+ from secondary calcification sites (ZP) into the water column (Fig 2.6b). The protons produced by secondary calcification are used in the production of photosynthate which is then translocated to the ZC. Respiration of the photosynthate produces ATP energy in the ZC and releases the H^+ into the BL. Thus, translocation of photosynthate serves as a means of transporting both protons and energy from the ZP to the ZC. Furthermore, the major source of carbon (HCO_3^-) used in calcification is derived from the metabolism of photosynthate (Fig. 2.6c), which is consistent with results reported by Furla et al. (2000a, 2000b). Protons being produced by both primary calcification and secondary calcification are concentrated in the ZC, where they can be dissipated into the adjacent water column or into the underlying ZP as needed to maintain maximum metabolic activity. Production, uptake and movement of H^+ within the coral influences localized pH within cells and tissues.

The high oxygen flux required for respiration in the ZC is readily supplied as the by-product from photosynthetic production in the underlying ZP (Fig. 2.6d). Colombo-Pallotta et al. (2010) found that high calcification rate in corals depends on hyperoxic conditions. High oxygen concentration facilitates increased mitochondrial respiration in the ZC which, in turn, generates the large amount of ATP needed to support the rapid deposition of $CaCO_3$. During daylight hours much of the oxygen produced in the ZP is consumed by the high rate of respiration in the overlying ZC. Al-Horani et al. (2003b) found that gross photosynthesis was approximately seven times higher than net photosynthesis, indicating that respiration consumes most of the O_2 produced by the zooxanthellae. The respiration rate in light was approximately 12 times higher than in the dark. The coupling of gross photosynthesis and light respiration produces intense cycling of internal carbon and O_2. Thus hyperoxia is a key feature of reef coral metabolism that is managed very well by the coral under normal conditions through a variety of mechanisms. However, high oxygen tension can lead to oxidative stress and bleaching in corals exposed to abnormally high temperature and high solar irradiance (Lesser 2011).

The skeletal material of the ZC modifies the irradiance in the ZP. Extensive scattering of photons by the skeleton enhances light absorption by symbiotic algae (Enríquez et al. 2005; Marcelino et al. 2013). Coral skeleton can absorb harmful ultraviolet radiation and fluoresce the energy into the visible portion of the spectrum (Reef et al. 2009). Rapid calcification on distal portions of the coral produces conditions in the understory that greatly enhance photosynthetic efficiency (Jokiel and Morrissey 1986). Coral skeletons are efficient at trapping, transporting and redistributing light throughout the colony (Marcelino et al. 2013), so lack of zooxanthellae in the growing tips can also be viewed as an adaptation that allows light to enter the skeleton. As light penetrates a

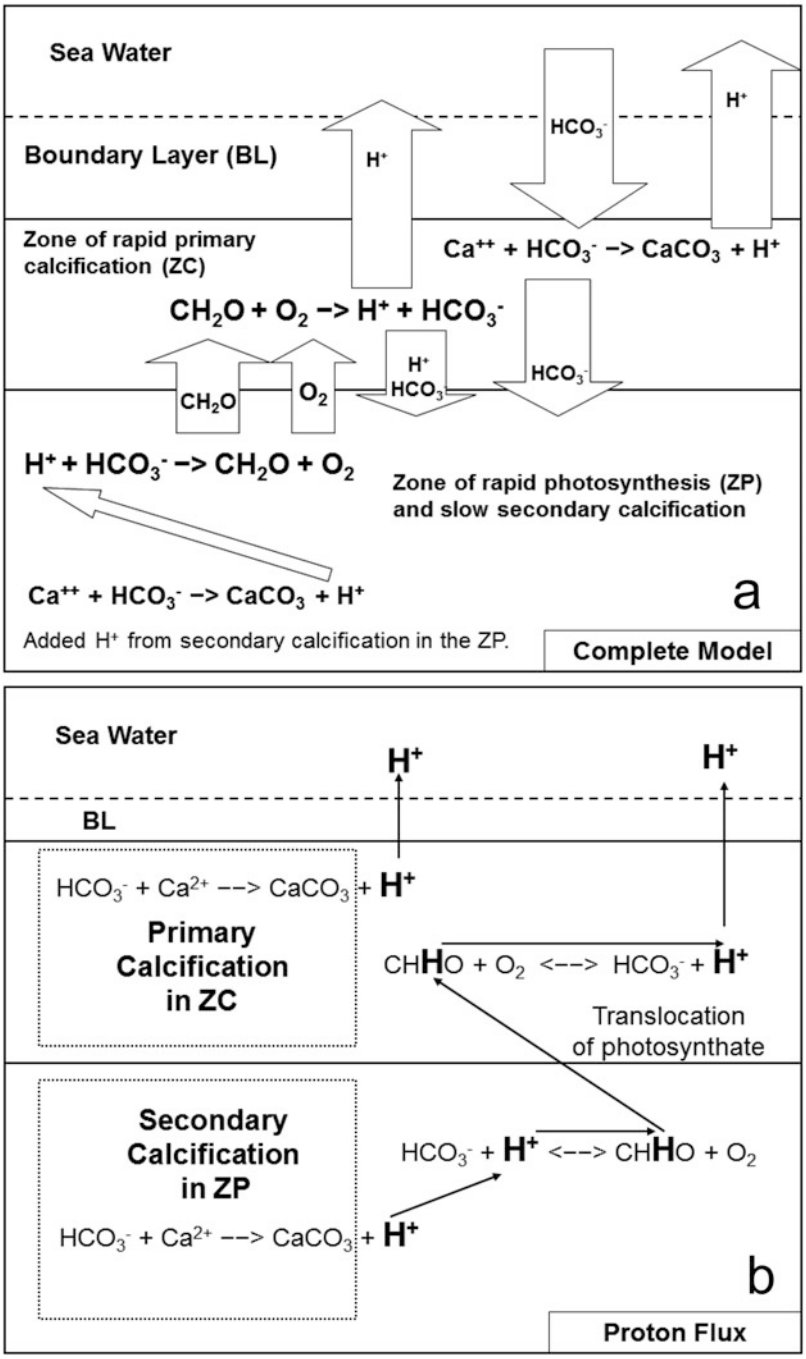

Fig. 2.6 Simplified two compartment proton flux model model: (**a**) spatial arrangement of chemical reactions, (**b**) pathways of protons, (**c**) carbon flux and (**d**) oxygen flux

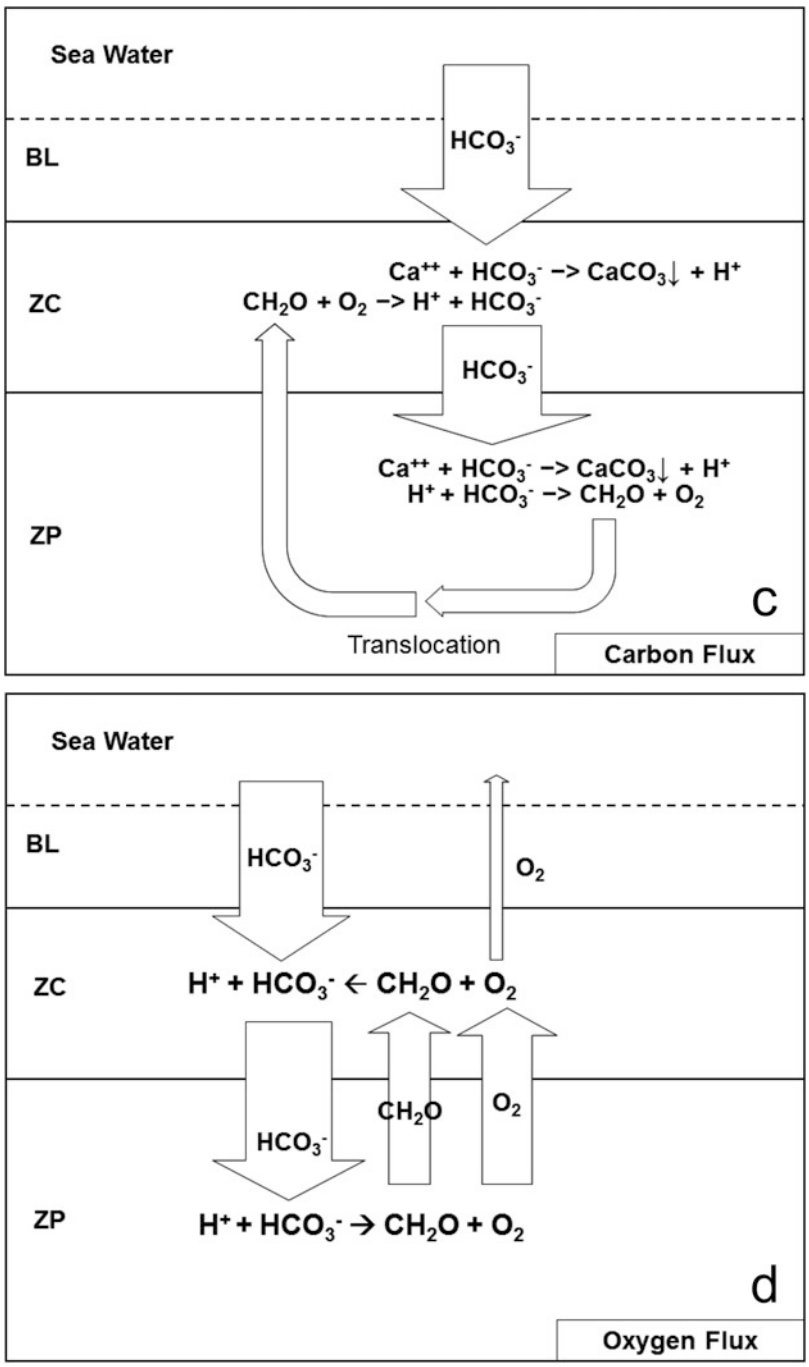

Fig. 2.6 (continued)

skeletal septum in the distal portion of a corallite it scatters and will diffuse into neighboring septa and redistribute throughout the colony. This enables millimeter-size structures to increase amplification as much as twenty-fold by trapping light within coral tissue due to multiple passes. This mechanism of redistribution enhances delivery of light to zooxanthellae and also delivers light to shaded parts of the coral colony.

2.2.2 Application of Model to Other Coral Morphologies

The generalized Proton Flux Model applies over a wide range of coral morphologies (Figs. 2.2 and 2.3) and over broad spatial scales. Branched morphology creates an outer zone of calcifying branch tips exposed to turbulent water where rapid outward growth of the skeleton occurs and

where solar irradiation is very high. Rapid photosynthesis occurs largely in the inner quiescent zone of the corallum. In branched colonies the ZC encompasses the outer tips. The morphology of perforate corals replicates the same spatial configuration but at a scale of mm rather than cm. At the upper end of the spatial scale Kajiwara et al. (1997) studied large thickets of the coral *Acropora pulchra* and compared growth of outer white-tipped branches (ZC) to growth of brown-tipped branches (ZP) located deeper in the colony. Zooxanthellae concentration in the white-tipped branches was low compared to the dark-tipped branches. The white-tipped branches showed three times the skeletal weight increase and 14 times the linear extension increase of the brown-tipped branches. The authors concluded that white-tipped branches with a lightly-calcified skeleton expand the area covered by the coral colony while brown-tipped branches develop a heavily-calcified skeleton that strengthens the colony. Fang et al. (2004) showed higher concentrations of ATP in the white tips compared to the brown stalks, providing the ready supply of the energy needed for rapid calcification. At the opposite end of the spatial scale, Al-Horani et al. (2005a, 2005b) employed microprobes and radioisotope techniques to measure the distribution of photosynthesis and calcification across polyps of the coral *Galaxea fascicularis*. The highest rates of photosynthesis occurred in the deeper parts of the calyx (ZP) that contained dense concentrations of zooxanthellae. The exert corallite septae that projected into the water column (ZC) incorporated more ^{45}Ca than the deeper portions (ZP) in both light and dark. Marshall and Wright (1998) report that there are essentially no zooxanthellae in the cell tissues covering the exert septa of *G. fascicularis* where calcium incorporation is highest. Jimenez et al. (2011) found that the BL over the surface of the corals *Platygyra sinensis* and *Leptastrea purpurea* is very thin over protruding skeletal features such as septa and calyx walls. These areas are covered with thin tissue (ZC) that lack zooxanthellae with much thicker tissues containing zooxanthellae located deeper in the calices (ZP). Therefore a wide range of morphologies from single polyps to complex colonial forms fit the general model, often in fractal patterns (Vicsek 1989) at different scales (e.g., a branching perforate coral).

Brahmi et al. (2012) studied the micro- and ultrastructural skeletal growth dynamics of the scleractinian coral *Pocillopora damicornis* and report that the coral is capable of controlling its biomineralization activity with great temporal and spatial precision. They suggested that spatial heterogeneity in coral tissue activity as described by Jokiel (2011b) should be carefully addressed in the development of better biomineralization models for scleractinian corals.

2.3 Ocean Acidification

2.3.1 Attempts to Explain How OA Reduces Coral Calcification

Much of the discussion of OA has been centered on the relationship between coral growth and Ω_{arag} and on the rate that Ω_{arag} will change over time in the surface waters of the sea. The empirical relationship between Ω_{arag} and calcification rate in tropical reef-building corals has been well established (Gattuso et al. 1999; Langdon et al. 2000; Marubini et al. 2001, 2003; Ohde and Hossain 2004; Langdon and Atkinson 2005; Schneider and Erez 2006; Jokiel et al. 2008; Cohen et al. 2009). Temperate corals have a much lower rate of metabolism and skeletal growth shows less of a decrease with decreasing Ω_{arag} (see Fig. 4 I. in Ries et al. 2009; Fig. 4 in Holcomb et al. 2010; Fig. 5 in Rodolfo-Metalpa et al. 2010).

Schneider and Erez (2006) conducted laboratory experiments designed specifically to separate the effects of Ω_{arag}, pH, $[CO_3^{2-}]$, aqueous CO_2, total alkalinity (A_T), and DIC on reef coral calcification. They concluded that calcification (both light and dark) was driven by CO_3^{2-} concentration. However, their data also show similar or higher correlations between calcification and seawater $[H^+]$, [DIC], and A_T. Likewise, Cohen and Holcomb (2009) followed this interpretation and suggested that under conditions of increasing OA corals must expend more energy to remove H^+ from the calcifying fluid between the calicodermis and the skeleton in order to raise the pH of the contained seawater and convert the increasingly plentiful HCO_3^- to CO_3^{2-}. These authors contend that the CO_3^{2-} is then moved into the calcifying fluid between the calicodermis and the skeleton and combines with Ca^{2+} to form the $CaCO_3$ crystals of the skeleton.

Jury et al. (2010) conducted experiments designed to distinguish the effects of Ω_{arag}, pH, $[CO_3^{2-}]$ and $[HCO_3^-]$ on coral calcification by conducting incubations in six regimes of highly modified seawater chemistries. Coral calcification responded strongly and consistently to variation in $[HCO_3^-]$ or DIC, but not to $[CO_3^{2-}]$, Ω_{arag} or pH. Jury et al. (2010) concluded that data from their study showed inconsistencies in the Ω_{arag} model. They suggested that coral calcification in the pH tolerant species *Madracis auretenra* is controlled by $[HCO_3^-]$, but that calcification might be controlled by the combination of seawater $[HCO_3^-]$ and pH in more pH- sensitive species. Experiments designed to test the relative importance of $[HCO_3^-]$ versus $[CO_3^{2-}]$ in coral calcification (de Putron et al. 2010) led to a conclusion opposite to that of Jury et al. (2010) in that calcification showed a better correlation with $[CO_3^{2-}]$ than with $[HCO_3^-]$.

However, calcification in these experiments also correlated with [DIC] and [H^+], consistent with the models proposed by Jury et al. (2010) and by Jokiel (2011a). Schneider and Erez (2006) showed a strong positive relationship between DIC and coral calcification at constant [H^+]. Likewise they showed a strong negative relationship between coral calcification and [H^+] at constant DIC. Comeau et al. (2012) showed that corals and crustose coralline algae uptake HCO_3^- as well as CO_3^{2-}, especially during light-enhanced calcification. Edmunds et al. (2012) studied three species of coral and found that pCO_2 and temperature independently affected calcification, but the response differed among taxa. Massive *Porites* spp. were largely unaffected by the treatments, but branching *Porites rus* grew 50 % faster at 29.3 °C compared with 25.6 °C, and 28 % slower under twice present day levels of pCO_2. Their compilation of results from previous studies revealed a high degree of variation in calcification as a function of pH, [HCO_3^-], and [CO_3^{2-}]. This synthesis supported the hypothesis that coral genera respond in dissimilar ways to pH, [HCO_3^-], and [CO_3^{2-}].

Jokiel (2013) used data on calcification rates of coral and crustose coralline algae from Comeau et al. (2012) to test the Proton Flux Model of calcification. There was a significant correlation between calcification and the ratio of DIC to proton concentration ([DIC] : [H^+] ratio). The ratio is tightly correlated with [CO_3^{2-}] and with Ω_{arag}. Jokiel (2013) noted that correlation does not prove cause and effect, and argued that Ω_{arag} and [CO_3^{2-}] have no basic physiological meaning on coral reefs other than a correlation with the [DIC] : [H^+] ratio. Comeau et al. (2013) responded by describing the type of experiments that are needed to allow further evaluation of the Proton Flux Model in relation to their model. However, they state that their interpretation of the data does not challenge the paradigm that the control of coral calcification is mediated entirely by [CO_3^{2-}]. Subsequent reports (Bach 2015; Cyronak et al. 2015; Jokiel 2015) do not support the [CO_3^{2-}] model.

2.3.2 Shortcomings of the Ω_{arag} Model (i.e., CO_3^{2-} Limitation) in Studies of Coral Calcification

Prior to our awareness of the "OA problem", the disciplines of carbonate physical chemistry and calcification physiology were largely unrelated fields (Roleda et al. 2012). The dominant role that physical chemistry played in the formative years of OA research (i.e. decreasing Ω_{arag} = decreasing [CO_3^{2-}] = decreasing coral calcification) resulted in an incomplete model of how OA will influence the physiology of calcifiers. Thus, two disparate views on calcification chemistry were advanced. The first is the classic biological view that organisms modify local carbonate chemistry of seawater and can use HCO^-or CO_2 for calcification. The second was focused primarily on a physical chemistry view implying that CO_3^{2-} is the main inorganic source of carbon used for calcification. Re-examination of the literature on the metabolic basis of calcification prior to the era of OA research (i.e. 1960–1980) supports the contention that bulk-water CO_3^{2-} is not the substrate for calcification in marine organisms (Roleda et al. 2012), and that other models are more appropriate among the various taxonomic groups.

Control of calcification by [CO_3^{2-}] is an unattractive hypothesis for several reasons. As has been pointed out (McConnaughey and Whelan 1997; Pörtner et al 2005; Wilt 2005; Hofmann and Todgham 2010), CO_3^{2-} is rarely transported across membranes, but rather indirectly passes through tissues via diffusion of CO_2 or through ion exchange transport of HCO_3^- coupled with H^+ transport. Various physiological studies have led to the conclusion that HCO_3^- appears to be the preferred form of inorganic carbon utilized by reef corals (Weis et al. 1989; Furla et al. 2000a, 2000b; Roleda et al. 2012). Bach (2015) used the basic equations that describe the physical chemistry of the sea water carbonate-carbon dioxide system to demonstrate that correlations between calcification and [CO_3^{2-}] or Ω_{arag} can be attributed to the combined influence of [HCO_3^-] and [H^+]. He went on to evaluate whether HCO_3^- or CO_3^{2-} would be the more suitable inorganic carbon substrate for calcification from a physical chemistry point of view. Three lines of analysis led him to the conclusion that HCO_3^- would be favored:

1. *Abundance*. HCO_3^- is the most abundant DIC species in seawater, so it makes sense for an organism to rely on the largest inorganic carbon pool.
2. *Homeostasis*. The hydration time of CO_2 is slow while the hydrolysis of HCO_3^- is fast. Thus CO_3^{2-} transported through the cytosol with a typical pH of 7.2 would quickly turn into HCO_3^- and bind a proton in the cytosol. The resulting HCO_3^- would be transported to the calcification site where the proton would be released back to the cytosol. Hence, the cytosolic pH would remain stable in the case of selective CO_3^{2-} uptake only when CO_3^{2-} uptake and $CaCO_3$ precipitation occur at the same rate. However, both processes probably run out of equilibrium on occasion, especially in a highly variable diurnal environment. In these cases, the utilization of CO_3^{2-} as the inorganic carbon source would constitute a substantial risk for the pH homeostasis. Excess CO_3^{2-} uptake would elevate cytosolic pH while excess $CaCO_3$ precipitation would reduce it. In contrast, a selective uptake of HCO_3^- from seawater would not perturb the cytosolic pH as much under these conditions because HCO_3^- has a relatively low potential to accept or donate H^+ at pH 7.2.

It may therefore be easier for calcifiers to keep cytosolic pH stable at 7.2 by using HCO_3^- as the substrate for calcification.

3. *Stability*. Seawater pH fluctuates substantially in a diurnal and seasonal timescale with HCO_3^- having a dominant and stable concentration over the entire pH range encountered by marine organisms, while [CO_3^{2-}] will show extreme variation. Thus HCO_3^- is a much more reliable inorganic carbon source for calcification.

2.3.3 Increasing Evidence that the Ω_{arag} Model for Coral and Coral Reefs Is Flawed

Venti et al. (2014) summarized their findings as follows: "Using short-term light and dark incubations, we show how the covariance of light and Ω_{arag} can lead to the false conclusion that calcification is more sensitive to Ω_{arag} than it really is." Comeau et al. (2014a) showed further inconsistencies in the Ω_{arag} –calcification relationship. They incubated two coral taxa (*Pocillopora damicornis* and massive *Porites*) and two calcified algae (*Porolithon onkodes* and *Halimeda macroloba*) under 400, 700 and 1000 µatm pCO_2 levels in experiments in Moorea (French Polynesia), Hawaii (USA) and Okinawa (Japan). Environmental conditions differ among the sites. Both corals and *H. macroloba* were insensitive to OA at all three locations, while the effects of OA on *P. onkodes* were location specific. In Moorea and Hawaii, calcification of *P. onkodes* was depressed by high pCO_2, but for specimens in Okinawa, there was no effect of OA. The authors concluded that a linear relationship between calcification and Ω_{arag} for corals is not universal.

Duarte et al. (2013) pointed out that metabolism in inshore waters such as coral reefs results in strong diel to seasonal fluctuations in pH, with characteristic ranges of 0.3 pH units or more on a daily basis. The extreme variability and multiple, complex metabolic controls on pH in coastal waters imply that open ocean conditions cannot be transposed directly to coastal ecosystems. Hence, they contend that ocean acidification from anthropogenic CO_2 is largely an open-ocean syndrome. This concept has been further supported by the work of Cyronak et al. (2014) who showed biogeochemical processes can influence the pCO_2 and pH of coastal ecosystems on diel and seasonal time scales, potentially modifying the long-term predicted effects of increasing atmospheric CO_2. By compiling data from the literature and removing the effects of short-term variability, they showed that the average pCO_2 of coral reefs throughout the globe has increased ~3.5 – fold faster than in the open ocean over the past 20 years. This rapid increase in coastal and reef pCO_2 confounds attempts to predict effects of OA based on oceanic Ω_{arag} (Jury et al. 2013). They constructed a simple model to demonstrate that potential drivers of elevated pCO_2 include additional local anthropogenic disturbances such as increased nutrient and organic matter inputs.

2.3.4 Future Changes in Oceanic Chemistry Due to Human Activity

Caldera and Wickett (2003) found that oceanic absorption of atmospheric CO_2 from fossil fuels may result in larger pH changes over the next several centuries than any inferred from the geological record of the past 300 million years. Pre-industrial, present and future (twice pre-industrial) concentrations of major carbonate system parameters involved in calcification are shown in Table 2.1. Ocean [Ca^{2+}] will not change significantly and is not included in the table. Note that [CO_3^{2-}] decreases while [HCO_3^-] and DIC increase with increasing OA as shown in Fig. 2.4. Carbonate ion concentration decreases from 264 µmol kg^{-1} under pre-industrial levels of atmospheric CO_2 to 170 µmol kg^{-1} under doubled CO_2 conditions, while HCO_3^- increases from 1650 µmol kg^{-1} to 1883 µmol kg^{-1}, and DIC increases from 1922 µmol kg^{-1} to 2059 µmol kg^{-1}. Thus, the majority of the seawater DIC is in the form of HCO_3^-. The majority of the

Table 2.1 Calculated change in carbonate parameters from pre-industrial to twice pre-industrial conditions

	pCO_2 atm	pH	[H^+] (nmol/kg SW)	[HCO_3^-] (µmol/kg SW)	[CO_3^{2-}] (µmol/kg SW)	DIC (µmol/kg SW)	Ω_{arag}
Pre-industrial	280	8.16	6.92	1650	264	1922	4.2
Present	386	8.07	8.51	1742	227	2121	3.6
Twice Pre-industrial	560	7.91	12.3	1883	170	2059	2.7
% Change	+100	−3	+78	+14	−36	+7	−36

Used with permission from Bulletin of Marine Science

Calculated values are based on alkalinity of 2300 µmol/kgSW with T = 25 °C and salinity = 35 ppt using the program CO2SYS (Pierrot et al. 2006)

Estimated pre-industrial saturation state of the tropical ocean in 1880 for pCO_2 is 280 µatm (Kleypas et al. 1999a, 1999b)

host intracellular DIC is also in the form of HCO_3^- (Venn et al. 2009) with very little CO_3^{2-}.

The most dramatic change in the CO_2 system in seawater will be a 78 % increase in $[H^+]$, suggesting that the effect of ocean acidification on coral calcification might directly involve $[H^+]$. According to the Proton Flux Model (Jokiel 2011a, 2011b) the net efflux of H^+ out of the coral and into the water column is influenced by the strength of the diffusion gradient between the coral and the surrounding seawater. This gradient becomes steeper with increasing OA due to increasing $[H^+]$ in the water column, with a consequent decrease in calcification rate. Fick's first law of diffusion links diffusive flux to the concentration field by stating that the flux direction is from areas of high concentration to areas of low concentration with a magnitude that is proportional to the concentration gradient. The efflux of waste protons from the corallum, through the BL and into the water column will occur at a magnitude that is proportional to the concentration gradient. According to this model, increasing the $[H^+]$ in the water column will reduce flux of protons out of the coral. The elimination of H^+ from the coral is just as important as influx or availability of DIC.

2.3.5 Future Regional Changes in Reef Carbonate Production and Dissolution Rates Due to Increasing OA

The most diverse and highly developed reefs occur in areas with very high Ω_{arag} (Kleypas et al. 1999a, 1999b) which is consistent with the hypothesis that $[CO_3^{2-}]$ drives calcification of corals and coral reefs. Thus, it has been assumed that reduction in Ω_{arag} would result in decreased growth (Langdon and Atkinson 2005; Hoegh-Guldberg et al. 2007; Pandolfi et al. 2011). The validity of this assumption was initially challenged by Jokiel (Sect. 2.3.1) who proposed that proton flux expressed as the ratio of substrate to inhibitor [DIC or HCO_3^-]/$[H^+]$ limited calcification rather than $[CO_3^{2-}]$ or Ω_{arag}. The implications of [DIC or HCO_3^-]/$[H^+]$ limited calcification rate on the global distribution of reef calcification has been described by Bach (2015), who showed the absence of a strong latitudinal gradient in $[HCO_3^-]/[H^+]$ in contrast to the strong gradients in $[CO_3^{2-}]$ and Ω_{arag}. The reason for the difference between the two is that temperature has a profound impact on $[CO_3^{2-}]$ and thus Ω_{arag}, but almost no influence on $[HCO_3^-]/[H^+]$. While Ω_{arag} and $[CO_3^{2-}]$ decrease 2–3 fold from the equator towards the poles, $[HCO_3^-]/[H^+]$ is nearly constant. Higher solubility of CO_2 at lower temperature results in an equilibrium shift away from $[CO_3^{2-}]$ towards higher $[CO_2]$ and higher $[HCO_3^-]$. Accordingly, $[CO_3^{2-}]$ declines away from centers of high coral reef development. Ω_{arag} follows the concentration of CO_3^{2-} since $[Ca^{2+}]$ is stable. The slight increase of $[HCO_3^-]$ poleward and eastward of the areas of high coral reef development is balanced by the concomitant increase in $[H^+]$, which explains the stability of $[HCO_3^-]/[H^+]$ over the latitudinal-longitudinal gradient. Thus, the carbonate chemistry conditions controlling calcification on coral reefs will be fairly constant over the globe. Also, the latitudinal pattern of Ω_{arag} and the pattern of $[HCO_3^-]/[H^+]$ are conserved through time in the course of climate change. Likewise, vertical $[CO_3^{2-}]$ and Ω_{arag} gradients in the water column decrease more severely than $[HCO_3^-]/[H^+]$ gradients largely due to the temperature decline, which is strongest in the upper few hundred meters. Lower temperatures negatively affect $[CO_3^{2-}]$ and Ω_{arag} whereas $[HCO_3^-]/[H^+]$ remains unaffected. However, Bach (2015) pointed out that reefs in peripheral areas may be the most severely affected by OA in the future because dissolution is determined by Ω_{arag}. From the carbonate production perspective, however, this is not the case. OA will be equally deleterious in all habitats where $CaCO_3$ formation is controlled by $[HCO_3^-]/[H^+]$. Thus, the relationship between dissolution and calcification undergoes change with increasing OA and increasing global temperature. Rates of secondary calcification, bioerosion, and reef dissolution are important factors in the control of structural complexity and long-term persistence of coral reefs. Silbiger and Donahue (2015) found that secondary reef calcification and dissolution in a coral rubble community responded differently to the combined effect of OA and increased temperature. Calcification had a non-linear response to the combined effect of pCO_2 and temperature: the highest calcification rate occurred slightly above ambient conditions while the lowest calcification rate occurred in the highest temperature–pCO_2 treatment. In contrast, dissolution increased linearly with increasing temperature–pCO_2 . Thus, the coral rubble community switched from net calcification to net dissolution at higher pCO_2 and increased temperature. Jury et al. (2013) reached similar conclusions using a modeling approach.

The values in Table 2.1 are for mean open ocean conditions, which vary little over a diurnal cycle compared to diurnal variations reported for various reefs throughout the world (Table 2.2). In addition to the wide variation between different geographic locations there is considerable variation over small spatial scales at a given location. For example, on a spatial scale of ~ 700 m across a single reef, different magnitudes of pH oscillations have been reported, with open water sites exhibiting less variability than back reef sites (Ohde and van Woesik 1999; Silverman et al. 2007). Processes other than OA, such as changes in nutrient loading from watersheds or change in benthic community structure, can have over-riding effects on long-term pH trends in estuaries and other shallow, nearshore marine environments (Duarte et al. 2013).

Table 2.2 Observed diurnal variation in reported pH (pH_T at 25 °C) for various coral reef habitats throughout the world compared to shallow open ocean values

Location	Habitat	Diurnal Range		Reference
		pH	Δ pH	
Eilat, Israel	Inner moat	8.10–8.30	0.20	Silverman et al. 2007
Shiraho Reef, Okinawa	Inner moat	7.80–8.40	0.60	Suzuki et al. 1995
Rukan-sho, Okinawa	Back reef	7.87–8.52	0.65	Ohde 1995
Shiraho Reef, Okinawa	Inner reef flat	7.90–8.60	0.70	Suzuki et al. 1995
Kiona Beach, O'ahu	Reef flat (sheltered)	7.92–8.13	0.21	Lantz 2011
Makapu'u, O'ahu	Reef flat (open)	7.98–8.10	0.12	Lantz 2011
Heron Island, Australia	Reef flat	8.00–8.40	0.40	Kline et al. 2012
Kāne'ohe Bay, O'ahu	Reef flat	7.90–8.20	0.30	Jokiel et al. 2008
Kāne'ohe Bay, O'ahu	Rreef flat	7.90–8.20	0.30	Martinez et al. 2012
Moloka'i, Hawai'i	Reef flat	7.80–8.40	0.40	Yates and Halley 2006
Moorea, Tahiti	Reef flat	8.02–8.12	0.10	Hofmann et al. 2011
Shiraho Reef, Okinawa	Reef crest	8.00–8.90	0.90	Suzuki et al. 1995
Palmyra, Line Islands	Reef terrace	7.85–8.10	0.25	Hofmann et al. 2011
Palmyra, Line Islands	Fore-reef	7.91–8.03	0.12	Hofmann et al. 2011
Laolao Bay, Saipan	Fore-reef (5 m)	8.16–8.28	0.12	Sean Macduff, unpub.
Laolao Bay, Saipan	Fore-reef (12 m)	8.14–8.24	0.10	Sean Macduff, unpub.
Kingman Reef, Line Is.	Open ocean	8.01–8.03	0.02	Hofmann et al. 2011
North of O'ahu, Hawai'i	Open ocean	8.08–8.12	0.04	Dore et al. 2009
Red Sea	Open ocean	8.20–8.20	0.00	Silverman et al. 2007

2.4 Biological Control or Physical Control of Calcification?

Ries et al. (2010) used the assumption that CO_3^{2-} controls calcification in corals and plotted calcification against Ω_{arag}. They found a curvilinear response which was interpreted to mean that corals exerted strong biological control of the bio-mineralization process. The Two Compartment Proton Flux Model states that coral calcification is limited by the physical process of diffusion across the BL. The Ries et al. (2010) coral calcification data are plotted against $[H^+]$ in Fig. 2.7. If physical control (diffusion of H^+ across the BL) or uptake of $[CO_3^{2-}]$ was the only factor governing calcification, then the relationship between calcification and $[H^+]$ would be linear according to Fick's first law of diffusion, which postulates that the flux of a material goes from regions of high concentration to regions of low concentration with a magnitude that is proportional to the concentration gradient. Rather, the relationship is curvilinear (Fig. 2.7) as we would expect because of the many enzyme-mediated processes involved in photosynthesis, calcification and material transport within the corallum (Fig. 2.6). Therefore a combination of linear and non-linear biological and physical processes including factors such as genetic makeup, biochemical state, temperature, irradiance, nutrient availability and water motion all affect calcification rate. Understanding large-scale spatial variability in coral calcification rates found in nature today, even in a single species, is a complex task (Kuffner et al. 2013), but hopefully establishing baseline datasets will help delineate the most important environmental drivers.

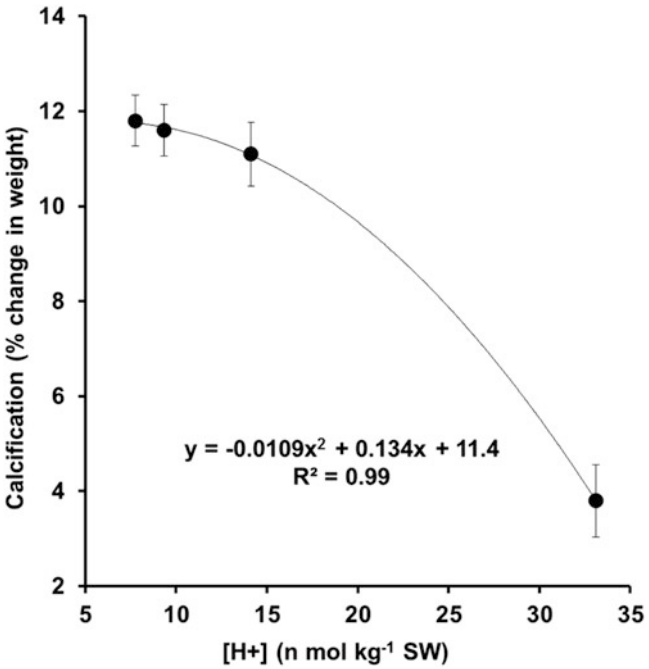

Fig. 2.7 Calcification (as % change over 60 days) plotted against $[H^+]$ rather than Ω_{arag} in the coral *Oculina arbuscula* using Ω_{arag} vs calcification data from Ries et al. (2010)

2.5 Interaction Between Environmental and Biological Factors

2.5.1 Interaction Between OA and Coral-Growth Rate

Marubini et al. (2003) measured calcification in four species of tropical reef corals (*Acropora verweyi*, *Galaxea fascicularis*, *Pavona cactus* and *Turbinaria reniformis*) under 'normal' (280 μmol kg^{-1}) and 'low' (140 μmol kg^{-1}) carbonate-ion concentrations. They report that the calcification rate was affected uniformly across all species tested (13–18 % reduction). An experiment involving the temperate coral *Oculina arbuscula* (Ries et al. 2009) was conducted under similar conditions and provides a useful comparison. Marubini et al. (2003) concluded that a decrease in [CO_3^{2-}] results in a significant reduction in calcification rate for all species tested while Ries et al. (2010) concluded calcification was only minimally impaired in the temperate coral. Plotting these reported calcification rates against [H^+] provides an alternate way of examining the data and provides additional insights (Fig. 2.8, left panel). There was a seven-fold difference in species calcification rate over the range of [H^+] used in the treatments. The corals with higher calcification rate (y-intercept in Fig. 2.8) showed greater calcification reductions (change in slope from −0.81 to −0.11 over the range of equations) in response to increased [H^+]. These data are re-plotted in the right panel of Fig. 2.8 to show change in calcification rate for corals grown under normal conditions (pH = 8.06, [H^+] = 8.7 nmol kg^{-1} SW) compared to acidified conditions (pH = 7.75, [H^+] = 17.7 nmol kg^{-1} SW). According to the Proton Flux Model the more rapidly growing tropical corals must dissipate greater quantities of protons through the BL against an increasingly steep [H^+] gradient and will show a stronger reduction in growth. The data suggest that fast-calcifying species are more vulnerable to OA. Comeau et al. (2014b) found that fast calcifiers were more sensitive to ocean acidification than slow calcifiers. The strong linear trend in the graph of metabolic rate (as initial calcification rate) versus change in calcification rate (Fig. 2.8) is consistent with diffusion limitation of material transport at the tissue-water interface.

2.5.2 Temperature and OA

Temperature controls rates of reaction at the site of calcification, in the tissues of the coral and in the water column outside the coral. The combined effects of temperature and OA are influenced by physical chemistry as well as by biochemistry.

Physical Chemistry A model of coral growth based on enhanced kinetics of calcification at higher temperature has been developed (McCulloch et al. 2012). This model

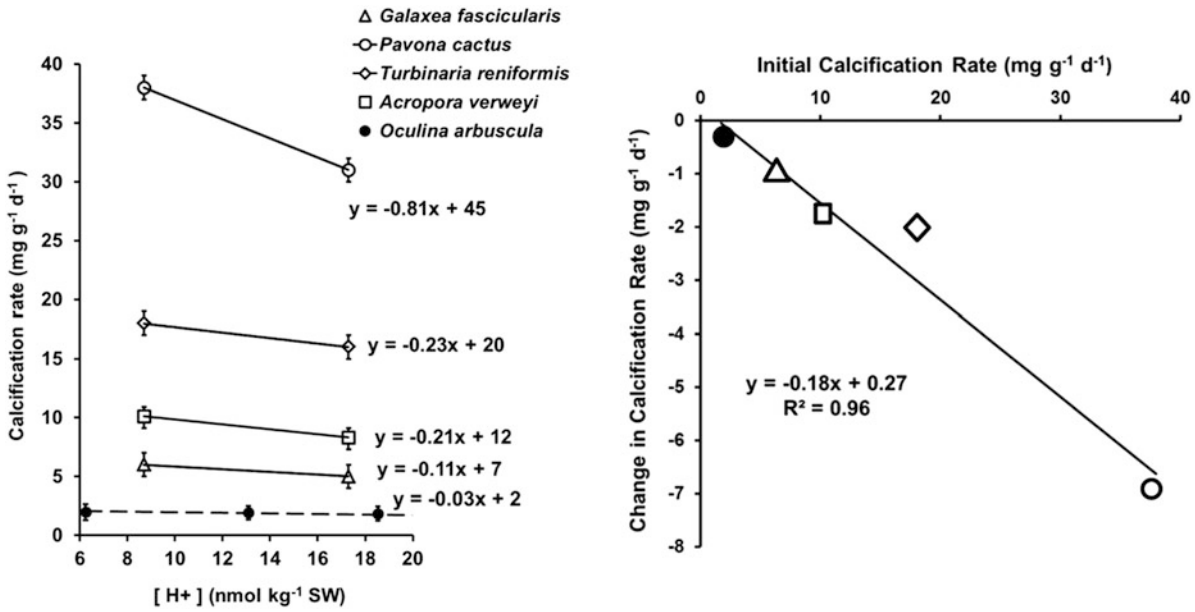

Fig. 2.8 *Left* panel shows calcification rate vs. [H^+] for four species of tropical corals (data from Marubini et al. 2003 as *open symbols*) and for the temperate coral *Oculina arbuscula* (data from Ries et al. 2010 as *solid circles*) with *error bars* as ± SE as re-analyzed by Jokiel (2011a). In the *right* panel the data were re-plotted to show change in calcification rate for corals grown under normal conditions (pH = 8.06) compared to corals grown under acidified conditions (pH = 7.75). The regression is significant with p = 0.004 (Figure from Jokiel (2011a) used with permission from Bulletin of Marine Science)

describes the effect of increased temperature on abiotic processes in the calcifying fluid located in the space between calicodermis and the skeleton and does not consider limiting processes within the coral tissue, processes at the tissue-seawater interface and changes in the boundary layer. The authors concluded that the increase in calcification due to global warming will outweigh the negative effects of declining carbonate ion concentration based solely on physical chemistry considerations in the calcifying fluid. Obviously this conclusion does not fit the preponderance of data showing decrease of coral growth with increasing OA. This model is reminiscent of the earlier model of McNeil et al. (2004) that was based on the assumption that calcification increases linearly with increasing temperature above the present day temperature range. The McNeil model predicted an increase in net coral reef calcification rate of 35 % by the year 2100, a conclusion that runs counter to nearly all experimental observations, which suggest a 15–30 % decrease under these conditions. The McNeil model failed to account for the biological calcification response to temperature (Kleypas et al. 2005). Growth response to temperature is not linear, but declines sharply above peak summer temperature with bleaching and eventual death of corals under future temperature scenarios. McCulloch et al. (2012) ultimately noted that extensive biological experimental and observational data do not support their model, and concluded that the fate of corals will ultimately depend on biochemical adaptation to rapidly changing conditions.

Increasing OA will increase [DIC] in the water column which will enhance influx of the inorganic carbon needed for calcification and photosynthesis. On the other hand, the concomitant increase in $[H^+]$ will reduce efflux of this waste product and thereby slow calcification. By this argument the ratio of [DIC] to $[H^+]$ will correlate with calcification rate. Temperature influences the [DIC] and $[H^+]$ through abiotic carbonate kinetics of seawater (Fig. 2.9). The change in the ratio should have a direct relationship to calcification rate. For example, the shift in the ratio from pre-industrial (280 µatm, 28 °C) to twice pre- industrial (560 µatm, 30 °C) is shown in Fig. 2.9 as a dashed arrow. This is a 33 % reduction in the ratio, which is consistent with the reduction observed in coral calcification under these conditions (Gattuso et al. 1999). As can be seen from the figure, the impact of temperature on the ratio is much less than that of pCO_2.

Biological Response Some corals show a strong biological response to temperature-OA interactions. Reynaud et al. (2003) grew small colonies of the reef coral *Stylophora pistillata* in a matrix of two temperature treatments (25 °C vs. 28 °C) and two pCO_2 treatments (460 µatm vs. 750 µatm) and report no statistical difference between pCO_2 treatments at 25 °C. However, there was a large decline in calcification

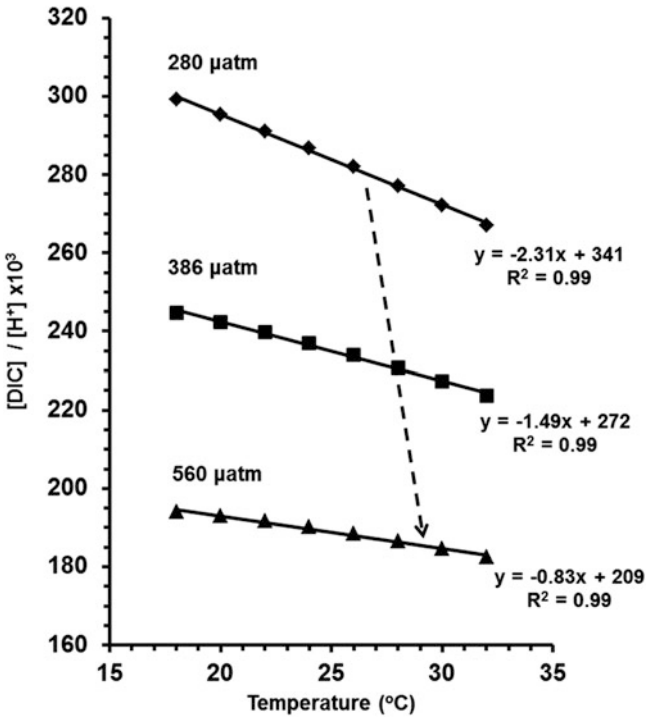

Fig. 2.9 Plot of the ratio of the calcification reactant DIC to the calcification waste product H^+ in the water column relative to temperature under pre-industrial concentrations (280 µatm), 2011 concentrations (386 µatm) and possible future (560 µatm) concentrations of pCO_2 as presented by Jokiel (2011a) (Data used with permission from Bulletin of Marine Science. The *dashed* line shows the 33 % decrease in the ratio from pre-industrial conditions at 280 µatm at 28 °C to twice pre-industrial pCO_2 with an associated greenhouse effect increase of 2 °C)

(approximately 50 %) at 28 °C under acidified conditions. Anlauf et al. (2011) studied the effects of a 1 °C increase in temperature and a 0.20–0.25 unit decrease in pH on the growth of primary polyps in the coral *Porites panamensis*. The growth of polyps was reduced marginally by acidic seawater but the combined effect of higher temperature and lowered pH caused a significant growth reduction of approximately 30 %. A similar 30 % decline at higher temperature – elevated pCO_2 was shown by Edmunds et al. (2012) for the rapidly growing branched coral *Porites rus*, but a slower growing massive *Porites* sp. did not show the effect. The temperature – pCO_2 interaction has been observed in other calcifying reef organisms. Martin and Gattuso (2009) observed the same effect on the coralline alga *Lithophyllum cabiochae*. Algae were maintained in aquaria for one year at ambient or elevated temperature (+3 °C) and at ambient pCO_2 (~400 µatm) or elevated pCO_2 (~700 µatm). During summer the net calcification of the algae decreased by 50 % when both temperature and pCO_2 were elevated while no effect was found under elevated temperature or elevated pCO_2 alone.

A biochemical mechanism can be proposed to explain the temperature-pCO_2 synergism. Coles and Jokiel (1977) showed that coral photosynthesis and respiration increase with increasing temperature, but respiration increases more rapidly. Consequently the ratio of photosynthesis to respiration decreases with increasing temperature to a value of unity near the upper thermal limit, and a mutually beneficial symbiosis cannot be maintained above that level. As temperature increases, the resulting high rates of photosynthesis and respiration require much higher exchange of materials through the boundary layer. Thus corals show greater demand to uptake inorganic carbon and a greater need to dissipate waste H^+ at higher temperature. Perhaps this explains why coral skeletal growth shows a positive correlation with increasing temperature, but only up to an "optimal temperature" (Jokiel and Coles 1977) and then declines rapidly to lethal conditions.

2.5.3 Water Motion and Irradiance

Models of Coral Growth Kaandorp et al. (2005, 2011) used simulation experiments and isotope analyses of coral skeletons to test the hypothesis that water motion and localized external BL gradients of DIC determine gradients of calcification that directly control the morphogenesis of branching, phototrophic corals. Their model is entirely driven by a diffusion-limited BL process and can generate coral growth patterns and morphologies that are virtually indistinguishable from three dimensional images of the actual colonies. This model provides strong support for the contention that water motion increases calcification by breaking down diffusion barriers in the BL. They concluded that inorganic carbon supply on the reactant side of Eqs. 2.5, 2.6 and 2.7 represents the limiting factor for calcification rate. The Kaandorp et al. (2005, 2011) model will show an erroneous increase in coral growth as OA increases, because DIC increases with increasing OA. This problem would be resolved if the model incorporated the influence of H^+ flux; i.e., the model would produce a similar morphological output, but with reduction rather than an increase in coral growth under increasing acidified conditions.

Changes in Growth Form with Increasing Depth From a topological point of view we can treat the myriad coral growth forms (Fig. 2.2) as simple hemispheres, with the hemispherical ZC encapsulating the ZP (Fig. 2.3). The model as presented in Fig. 2.6 represents a cross section at a given point on the hemispherical corallum. Coral reef environments show strong vertical and horizontal gradients of both water motion and irradiance, so these factors are not uniform over the surface of a colony and can influence colony growth form as shown in Fig. 2.10. The colonies of many massive and branching coral species become more flattened and plate-like with increasing depth (e.g., Roos 1967; Graus and Macintyre 1976; Jaubert 1977) in response to submarine irradiance distribution (direction and intensity). Growth along an axis diminishes with decreasing irradiance and with decreasing water motion.

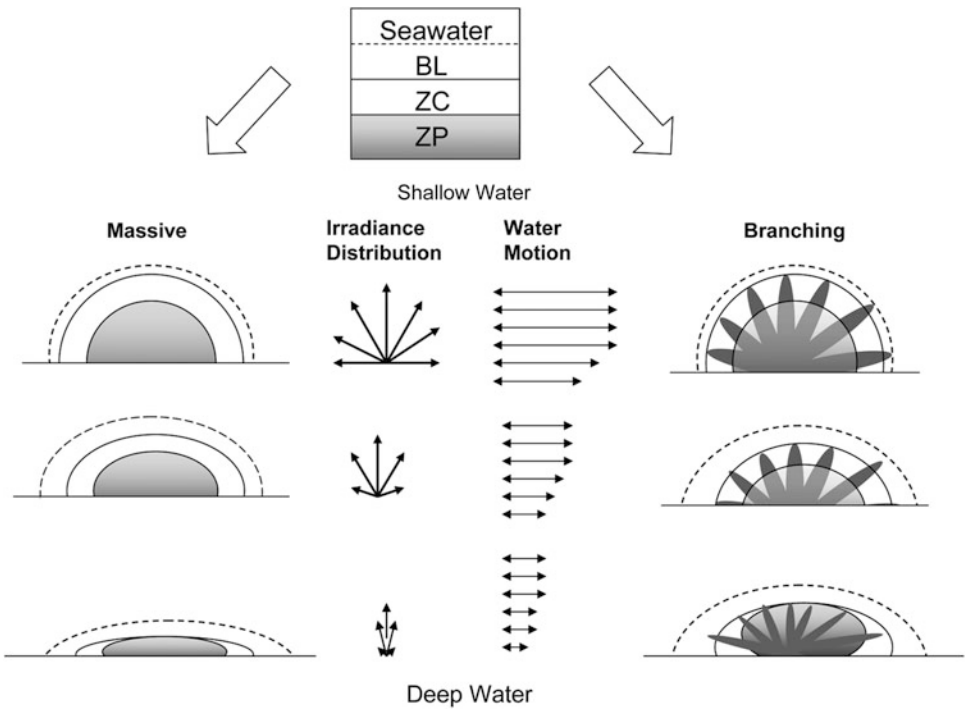

Fig. 2.10 The relationship between the zone of primary calcification (*ZC*), zone of primary photosynthesis (*ZP*) and the boundary layer (*BL*) showing the relative changes in different growth axes due to gradients in the irradiance-water motion field with increasing depth (Figure from Jokiel (2011b) used with permission from Journal of Experimental Marine Biology and Ecology)

2.6 Coral Nutrition

2.6.1 Inorganic Nutrients

Corals grown at elevated levels of inorganic nutrients (nitrogen and phosphorous) increase photosynthetic rate while simultaneously decreasing calcification rate (Hallock and Schlager 1986; Stambler et al. 1991). Corals grown under increased levels of pCO_2 also show a decline in calcification (Gattuso et al. 1999; Schneider and Erez 2006). Corals cultured under a combined high inorganic nutrient – high pCO_2 treatment continue to grow, but do not grow as rapidly as corals growing under ambient conditions (Marubini and Atkinson 1999; Renegar and Riegl 2005). Atkinson et al. (1995) described seawater conditions at the Waikiki Aquarium where corals were growing in high-nutrient (PO_4 ~ 0.6 μM; NO_3 ~ 5 μM; NH_4 ~ 2 μM), high pCO_2 (400–880 μatm) water drawn from a saltwater well. These observations led the authors to conclude that corals can flourish under high nutrient, high pCO_2 conditions, although they did not conduct any comparisons with corals grown at low pCO_2 and low nutrient. This anomalous conclusion persisted until aquarists at the Waikiki Aquarium discovered that adding a flow of low nutrient, low pCO_2 oceanic sea water to the coral display tank greatly improved coral growth compared to corals held in flowing well water (Richard Klobuchar, personal communication, 17 May 2011). Therefore, the situation at the aquarium now appears to be in agreement with results of the various controlled experiments conducted to date (e.g., Marubini and Atkinson 1999; Renegar and Riegl 2005), with the aquarium corals growing at a lower rate under conditions of high nutrient and high pCO_2. However, controlled experiments comparing growth in sea water versus well water at the Waikiki Aquarium are needed.

2.6.2 Organic Nutrient Heterotrophy

It has been suggested that coral sensitivity to OA may depend on energetic status (Cohen and Holcomb 2009) which has recently been shown experimentally (Chauvin et al. 2011; Edmunds 2011). It follows that increasing the nutritional status or energy stores of the coral could potentially ameliorate OA effects on calcification if the coral is able to use these resources to increase ion transport. The ability to do this, however, may be species-specific. For instance, some corals are able to recover faster from bleaching when allowed to feed on plankton, whereas other species are unable to take advantage of the opportunity (Grottoli et al. 2006). These ideas are not in conflict with the Proton Flux Model, since the coral's increased energy supply to proton pumps could result in raising pH in the calcifying space. This in turn would increase the gradient in $[H^+]$.

2.6.3 Organic vs Inorganic Nutrients and Coral Calcification

The success of reef corals in shallow tropical seas stems from the symbiotic association between endocellular zooxanthellae and the host (Muscatine and Porter 1977). This association allows corals and coral reef communities to thrive in spite of the low concentrations of nitrogen (N) and phosphorus (P) in the oligotrophic waters. However, a contradiction was presented by Kinsey and Davies (1979) who showed that increasing the concentration of inorganic N and/or inorganic P reduces, rather than increases, coral growth. In contrast, corals supplied with an increased supply of organic N and organic P in the form of zooplankton increase rather than decrease their skeletal growth rate. Ferrier-Pagès et al. (2003) performed laboratory experiments designed to assess the effect of feeding on the tissue and skeletal growth in the coral *Stylophora pistillata*. Fed colonies exhibited significantly higher levels of protein and chlorophyll per unit surface area than starved colonies. Feeding had a strong effect on tissue growth, increasing it by two to eight times. Calcification rates were also 30 % higher in fed than in starved corals. Thus N and P provided to the coral in the inorganic form results in decreased calcification while increased N and P provided from organic sources result in increased calcification rate.

This paradox can be resolved by incorporating the model of Dubinsky and Jokiel (1994) into the Proton Flux Model. According to the Dubinsky-Jokiel model the zooxanthellae produce CH_2O in great excess of their basic metabolic needs which is translocated to the ZC (Fig. 2.6). However, this energy-rich photosynthate has been described as "junk food" because it lacks the N and P needed to support tissue growth (Falkowski et al. 1984). Under normal conditions the zooxanthellae gain access to inorganic N and P as metabolic waste products from their host in return for fixed carbon. The symbiosis retains and recycles N and P, which in the absence of the algae would have been excreted into the sea and lost. The animal fraction of the symbiosis can obtain organic N and P by feeding on zooplankton, but cannot utilize inorganic N and P directly. In contrast, the zooxanthellae assimilate dissolved inorganic N and P compounds, but cannot assimilate zooplankton. Under normal reef conditions the supply of plankton and inorganic plant nutrients is very limited.

Thus zooxanthellae are normally under nutrient-starved conditions, so given additional inorganic N and P they

quickly uptake these substances and put their energy into new plant cell growth. Less photosynthate is translocated from the ZP to the ZC with a consequent decrease in skeletal growth. On the other hand, increased supply of organic N and P in the form of zooplankton gives the advantage to the animal portion of the symbiosis. As the animal digests the zooplankton, it can use the organic N and P for increased cell growth and can also benefit from the energy value of the zooplankton food. The increased energy can be utilized to increase calcification as well as increase animal cell growth. Flow of photosynthate from the ZP is not reduced and skeletal growth in the ZC continues, enhanced by energy derived from the digestion of the zooplankton. The fed coral will produce additional metabolic waste N and P for the zooxanthellae and the plant biomass will eventually increase along with increases in the animal biomass, but at a rate that does not give the advantage to the plant fraction of the symbiosis. Thus, according to the combined model the mechanism responsible for reduced calcification under increased inorganic nutrient concentration is related to diminished fixed-carbon flux from the ZP to the ZC. The cause of reduced growth under increased pCO_2 is reduction of proton efflux out of the tissues and into the water column due to increased $[H^+]$ in the water column. However, the two are additive when inorganic nutrient level and pCO_2 are increased simultaneously (Renegar and Riegl 2005).

2.7 Acclimatization and Adaptation

One of the great unknowns in predicting the effects of ocean acidification on corals and coral reef communities in the future is the ability of coral species to acclimatize and/or adapt to future conditions (Gattuso et al. 1999). There is little evidence thus far that corals can acclimatize to ocean acidification. During the course of a nine-month long mesocosm experiment, corals did not show any decrease in response to the OA treatment (Jokiel et al. 2008). Similarly, nubbins of the coral *Stylophora pisitillata* showed the same sensitivity to OA after either 24 h or 1 year of exposure to reduced pH (Venn et al. 2013). The potential for adaptation, on the other hand, seems more promising (Pandolfi et al. 2011). Coral species and populations have shown differential responses to repeated bleaching events (Guest et al. 2012), offering some hope that enough genetic variability exists in at least some coral populations to allow adaptation to chronic environmental stressors. Evidence for local and regional adaptation also exists, with species showing resilience to naturally occurring extremes in seawater carbonate chemistry (Fagan and Mackenzie 2007; Fabricius et al. 2011) and temperature regimes (Coles 1988; Harriott and Banks 2002).

2.8 Resolving Unexplained Paradoxes with New Insights

Understanding of the importance of proton flux (Jokiel 2011a) and clarification of the spatial relationship between the BL, ZC and ZP (Jokiel 2011b) has resolved a number of apparent contradictions in the coral calcification literature as described below.

2.8.1 Paradox of Decreasing Coral Growth Rate in the Face of Increasing HCO_3^- and Increasing DIC

Marubini et al. (2008) found that doubling the $[HCO_3^-]$ resulted in a coral calcification increase of approximately 27 % at all levels of $[H^+]$ tested. Herfort et al. (2008) also found that coral calcification increased rapidly in response to added HCO_3^-. Since OA increases $[HCO_3^-]$ (Fig. 2.4) we might expect increasing skeletal growth due to higher pCO_2. However, Gattuso et al. (1999) compiled existing information and estimated that coral $CaCO_3$ production decreased by 10 % between 1880 and 1990. They projected an additional 9–30 % (mid estimate: 22 %) reduction from 1990 to 2100 due to OA for a total of 32 % reduction between pre-industrial and twice pre-industrial pCO_2 concentrations. More recent estimates (Marubini et al. 2001; Anthony et al. 2008; Jokiel et al. 2008) support this generalization. The calculated increase in $[HCO_3^-]$ that can be attributed to change from pre-industrial to twice pre-industrial is 14 % (Table 2.1). Using the estimate of Marubini et al. (2008) that a doubling of $[HCO_3^-]$ will result in a 27 % increase in calcification, the expected change in coral growth due to projected increased $[HCO_3^-]$ would only be on the order of +3.8 % compared to the predicted change of -32 % due to increased $[H^+]$. Thus any benefit to skeletal growth due to higher future $[HCO_3^-]$ will be overwhelmed by the order of magnitude greater negative impact due to increased $[H^+]$.

2.8.2 Paradox of Rich Coral Reefs Growing Under Low Ω_{arag} Conditions

Palau Rock Islands Shamberger et al. (2014) reported the existence of highly diverse, coral-dominated reef communities in the Rock Islands of Palau under chronically low pH and low Ω_{arag}. They noted that identification of the biological and environmental factors that enable coral communities to persist under these conditions could provide important insights into the future of coral reefs under anthropogenic acidification. Jokiel (2015) re-analyzed their data

from the perspective of the Proton Flux Model and provided the following explanation. The Rock Islands are located in the south lagoon of Palau between Koror and Peleliu. This area is an uplifted ancient coral reef that forms a complex carbonate labyrinth of shallow channels and lagoons containing 250–300 small islands. These uninhabited islands are actually carbonate outcrops. Some of the islands display a mushroom shape with a narrow base created by rapid dissolution and bioerosion by sponges and bivalves and intense grazing by chitons, urchins and fish in the intertidal (Lowenstam 1974; Glynn 1997). The extreme bioerosion and carbonate dissolution in the area coupled with very low rates of seawater exchange produces atypical conditions that provide an important insight into CO_2-carbonate system dynamics.

Understanding the hydrodynamics of the ocean in the vicinity of Palau is critical to our understanding of the processes involved. Golbuu et al. (2012) showed that water circulation in and around the Palau archipelago is very different from circulation around an isolated island or reef, because the mean-water circulation is steered away from and around the archipelago. This deflection generates slower mean currents inside the archipelago compared to accelerated currents surrounding the archipelago. Water exchange is further diminished in shallow waters (depth < 20 m) by the non-linear friction-driven interaction between the tidal currents and the prevailing regional currents. The highest water retention is apparent in the southern lagoon in the Rock Islands area where extensive shallow reef formations occur. The Shamberger et al. (2014) sites at 7–9 km from open ocean waters were located in the shallow flow-restricted bays of the Rock Islands, while sites at 1–3 km were located in the areas of accelerated currents outside of the archipelago that experience rapid flushing with oceanic waters.

The investigators did not make measurements during nighttime when respiration greatly increases pCO_2. Dissolution of carbonates increases A_T (Wisshak et al. 2013). Therefore, additional A_T produced during the night was available to the calcifying organisms during the day due to long residence time of sea water in the lagoon. High rainfall and tidal variation result in submarine groundwater discharge (SGD), which serves as another source of A_T to the calcifying organisms. Rainfall is high and varies between 200 and 450 mm month^{-1} due to Palau's location on the edge of the Western Pacific Warm Pool and the year-long influence of the Intertropical Convergence Zone (Australian Bureau of Meteorology and CSIRO 2011). Cyronak et al. (2013a) measured increased A_T flux due to SGD at Muri Lagoon, Cook Islands, with the daily flux rate of up to 1080 mmol m^{-2} day^{-1}. Dissolution of the complex non-living carbonates supplemented with additional A_T from SGD in the low-flushing reefs of the Rock Islands over the 24 h period would provide considerable A_T buffering of the protons being generated by calcification.

G_{net} was not measured in the study, but a high rate of calcification was implied from the dense standing crop of corals and other calcifying organisms. G_{net} includes dissolution, which occurs at a high rate in such carbonate formations. P_{net} was not measured either, but presumably was very high due to high biomass of corals and other photosynthetic organisms. G_{net} is driven by P_{net}, and not by Ω_{arag} (Jokiel et al. 2014a). Ω_{arag} is actually a dependent variable on G_{net}. Ω_{arag} lags behind G_{net} by several hours during the diurnal cycle (Shamberger et al. 2011; McMahon et al. 2013; Jokiel et al. 2014a). Flux data are lacking, but fortunately the concentration data were taken along a horizontal environmental gradient, which permits calculating flux rates. A crude description of the dynamic benthic processes involved in coral calcification at this site can be made with the available data for $[A_T]$, [DIC] and $[H^+]$. This analysis requires that we accept the assumptions implicit in the experimental design that horizontal mixing is uniform throughout the area of study and that $[A_T]$, [DIC] and $[H^+]$ are not greatly modified by pelagic processes in relation to benthic processes. The environmental gradient between the lagoon and open ocean is shown for $[A_T]$ (Fig. 2.11a), [DIC] (Fig. 2.11b) and $[H^+]$ (Fig. 2.11c). The strongest gradient ($p < 0.001$, Fig. 2.11c) is for net flux of protons out of the lagoon. Net flux of A_T into the lagoon also shows a strong gradient ($p < 0.001$, Fig. 2.11a). Net DIC flux into the lagoon did not show a statistically significant correlation ($p = 0.089$, Fig. 2.11b). This pattern is consistent with detailed observations made by Jokiel et al. (2014a) in mesocosm studies. Dissipation of the protons generated by calcification is a major factor limiting coral growth. Flushing of the Rock Islands with oceanic waters removes H^+ and brings in water with higher $[A_T]$. Water motion can further diminish boundary layers and enhance H^+ and A_T exchange with the benthos (Cyronak et al. 2013b). DIC is abundant in sea water and is not as important as proton flux (Jokiel et al. 2014a) in relation to calcification as reflected in Fig. 2.11b, which shows a weaker relationship than $[A_T]$ or $[H^+]$ with distance from the open ocean.

The situation in the Rock Islands is defined by extremely high rates of carbonate dissolution and restricted water flow. Figure S4 of the Shamberger et al. (2014) report shows a rich coral community at the Rock Islands lacking in macroalgae and turf algae, probably due to intense grazing pressure and low inorganic nutrient supply. A larger macroalgae component would have increased pH during daylight hours without altering A_T. The higher pH in such situations shifts the equilibria toward increased $[CO_3^{2-}]$ and therefore higher Ω_{arag}. In this system, as in other systems, Ω_{arag} simply describes the portion of DIC that is being expressed as CO_3^{2-} under prevailing pH conditions. Such pH conditions can be rapidly modified by algal photosynthesis without changing A_T and thus Ω_{arag} is not very useful as a universal metric related to coral calcification. There is a local correlation

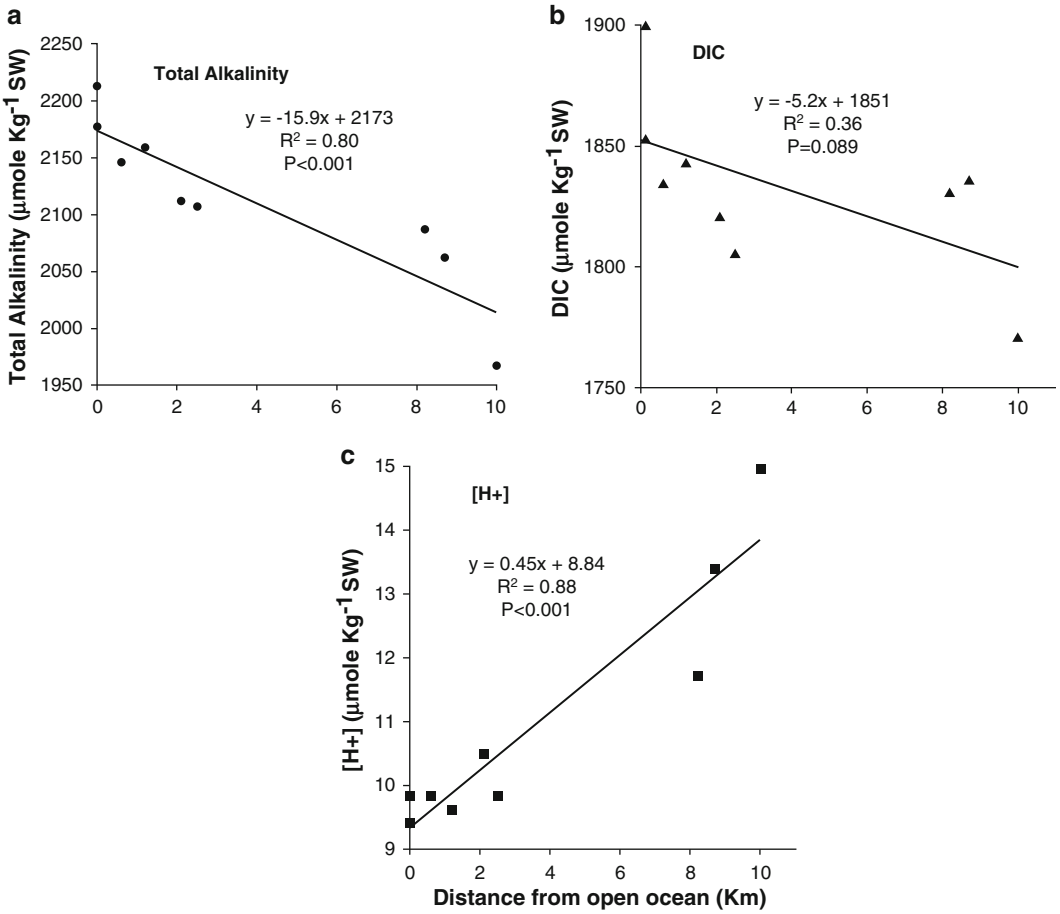

Fig. 2.11 Change in concentration from open ocean to coral lagoon using data from Shamberger et al. (2014) for: (**a**) Total Alkalinity, (**b**) Dissolved Inorganic Carbon, and (**c**) Proton Concentration (Figure from Jokiel (2015) used with permission)

between Ω_{arag} and G_{net}, but Ω_{arag} is a dependent variable on several factors including P_{net} and local dissolution rate of carbonates (e.g., Murillo et al. 2014). The relationship of G_{net} to Ω_{arag} holds within a given system, but varies between systems due to differences in P_{net}, which drives G_{net} (Jokiel 2015). Systems with a higher portion of P_{net} being provided by non-calcifying photosynthetic organisms will have a different relationship to Ω_{arag} than a system dominated by calcifying photosynthetic organisms.

The findings of Murillo et al. (2014) provide additional insight into the situation in the Rock Islands. They conducted flume studies and found that corals isolated from other reef components (carbonate sediment and algae) calcified at a 2:1 ratio of A_T flux to Ca^{2+} flux ($\Delta A_T:\Delta Ca^{2+} = 2.0$). The same corals incubated in a community that contained carbonate sediment and macroalgae calcified at a lower ratio ($\Delta A_T:\Delta Ca^{2+} = 1.6$), which indicates the presence of additional sources of alkalinity (i.e. buffering) from carbonate sediments. Carbonate sediments incubated in isolation from the other components buffered the water column, maintaining higher and more stable levels of pH while increasing A_T and DIC.

The A_T of seawater increases with carbonate dissolution in areas such as the Rock Islands that are dominated by carbonate rock and sediment. Corals growing in the presence of such rapidly dissolving carbonates are supplemented with a local source of A_T and live in an environment that is more favorable to calcification compared to environments that lack carbonate deposits. Even so, concentration of A_T on the reefs of the Rock Islands is much lower than offshore (Fig. 2.11a) due to intense calcification which lowers [A_T] by two moles for every mole of $CaCO_3$ precipitated. However, A_T concentration does not tell us anything about A_T flux or its relation to net calcification-dissolution flux (G_{net}). Understanding the dynamics of calcification requires measurement of flux rates. All of the data provided in the Rock Islands study consisted of concentration measurements (pH, [A_T], [DIC], [CO_3^{2-}]). Jokiel et al. (2014a) demonstrated the pitfalls of this approach and pointed out the need to measure flux rates (H^+ flux, DIC flux, A_T flux, and G_{net}) along with net flux of carbon due to photosynthesis-respiration (P_{net}).

In sum, the combination of biological and environmental factors that enable the reef communities in the Rock Islands to

persist at chronically low pH and low Ω_{arag} can be identified. First, the extremely high rate of carbonate dissolution increases the A_T available for neutralizing protons. Second, highly restricted hydrodynamic flow maintains the conditions that buffer calcification. Unfortunately, observations under the highly atypical hydrodynamic and geologic conditions at the Rock Islands provide little hope that the global future of coral reefs under anthropogenic acidification can be offset on a broad scale by increased dissolution (Andersson et al. 2003), but perhaps environments such as these can provide refugia on a highly localized scale.

Kāne'ohe Bay, Hawai'i Kāne'ohe Bay, Hawai'i contains well developed coral reef communities that have shown remarkable resilience to various environmental stressors (Hunter and Evans 1995). These rich reefs have developed under high pCO_2 levels. The elevated pCO_2 is due to metabolism of terrigenous organic material transported into the bay by streams. Fagan and Mackenzie (2007) found that pCO_2 was approximately 500 µatm on average in the northern bay while central and southern bay waters had an average pCO_2 of 460 µatm with the entire bay and nearshore reef experiencing levels well above atmospheric pCO_2 (Shamberger et al. 2011). Such levels of pCO_2 are believed to be highly deleterious to coral growth (summarized by Hoegh-Guldberg et al. 2007). One estimate is that when atmospheric partial pressure of CO_2 reaches 560 µatm all coral reefs will cease to grow and start to dissolve (Silverman et al. 2009). So how do we account for the paradox of rich coral reefs of Kāne'ohe Bay growing at levels of pCO_2 that should eliminate them?

The Proton Flux Model provides an explanation. Previous estimates of coral response to ocean acidification have been based on Ω_{arag}. The parameters Ω_{arag} and $[H^+]$ do not always correlate reliably with each other in shallow inshore systems due to the intense metabolic activity of inshore reef communities, input of terrigenous materials, high rates of carbonate dissolution and long residence time of sea water. In a mixed inshore coral-algae community the $[H^+]$ can be very low during daylight hours due to high rates of photosynthesis and low rates of water exchange, while during the night the $[H^+]$ increases dramatically due to respiration of the reef communities. Night $[H^+]$ is of less importance to corals because they do not calcify rapidly in darkness, but it is important during daytime LEC. Use of pH rather than $[H^+]$ can be deceptive. For example, the 0.4 ΔpH range reported for the Moloka'i reef flat in Table 2.2 represents a 5.1 % change in pH, but a 151 % change in $[H^+]$. This strong diurnal signal on shallow coral reefs attenuates with distance offshore and is quite small in oceanic waters. Both Ω_{arag} and $[H^+]$ vary over the diurnal cycle on inshore reefs but are not tightly coupled (Shamberger et al. 2011). Therefore, Kāne'ohe Bay barrier reef daily calcification rates were found to be the same or higher than rates measured on other coral reefs despite the comparatively low Ω_{arag} levels.

2.8.3 Paradox of Rapid LEC in Areas of The Coral Colony That Do Not Contain Photosynthetic Zooxanthellae

This paradox has gone unexplained for half a century. Goreau (1959) noted that "Although the zooxanthellae seem to play an important role in determining calcification rates of reef-building corals, certain, as yet unknown, physiological factors operate to control the basic mineralization process in a manner which bears no obvious relationship to the number of algae present in a given species". More recently, Tambutté et al. (2007) conducted more detailed studies and report that the tissues which calcify at the highest rates do not possess zooxanthellae. The paradox has been resolved by the Two Compartment Proton Flux Model through the realization that calcification and photosynthesis compete for available inorganic carbon and must be spatially separated within the coral (Jokiel 2011b). Reef corals have resolved this conflict by evolving a morphology that places the calcifying sites (ZC) distal to the photosynthetic sites (ZP).

2.9 Alteration of Seawater Chemistry by Corals Over the Diurnal Cycle

Extreme diurnal alteration of pH occurs on shallow coral reefs (Table 2.2). Jokiel et al. (2014a) conducted mesocosm experiments that precisely measured the changes in bulk sea water chemistry and material flux that accompany these pH oscillations over a diurnal cycle. The experiment was conducted in the flow-through mesocosm system at the Hawaii Institute of Marine Biology, Kāne'ohe Bay, O'ahu, Hawai'i. The mesocosm system has been described in detail (Jokiel et al. 2008; Andersson et al. 2009; Jokiel et al. 2014b). Major findings of the Jokiel et al. (2014a) investigation are summarized below.

Calcification over the 24 h period (Fig. 2.12) shows the diurnal pattern related to irradiance, light-enhanced calcification and dark calcification. Values for G_{net} are high due to the large biomass of live coral, high solar irradiance in the shallow mesocosms and absence of sediment or dead carbonate skeleton which could weaken and confound the coral calcification signal through carbonate dissolution. Light saturation of calcification did not occur up to the maximum irradiance which exceeded 1500 µmole photons m^{-2} s^{-1}. This value is many times higher than that supplied by the artificial light typically used in most laboratory studies of coral calcification. There is a drop in calcification to zero around midnight with a dark calcification rate peak at approximately 03:00 h.

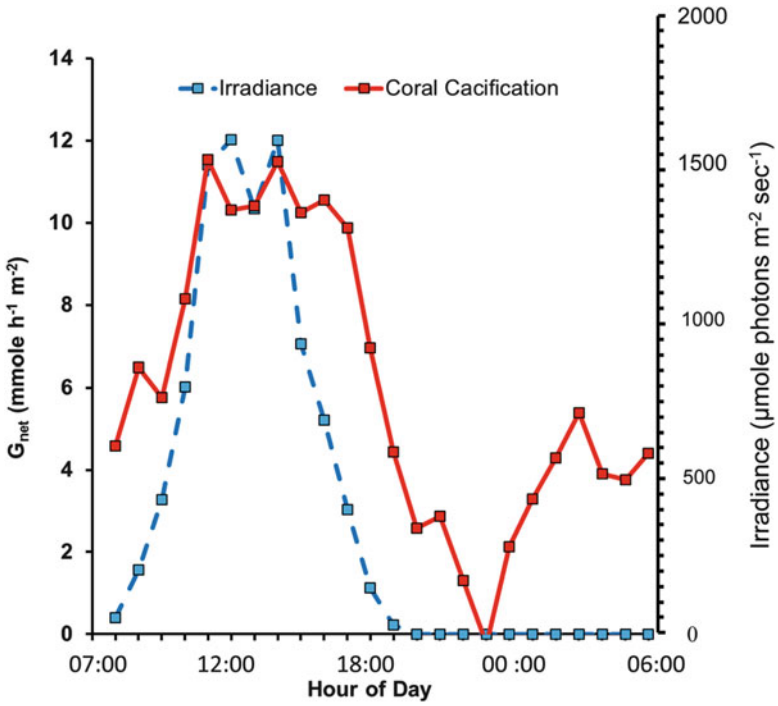

Fig. 2.12 Diurnal net calcification rate (G_{net}) and irradiance for a mesocosm containing corals (Figure from Jokiel et al. (2014a) used with permission)

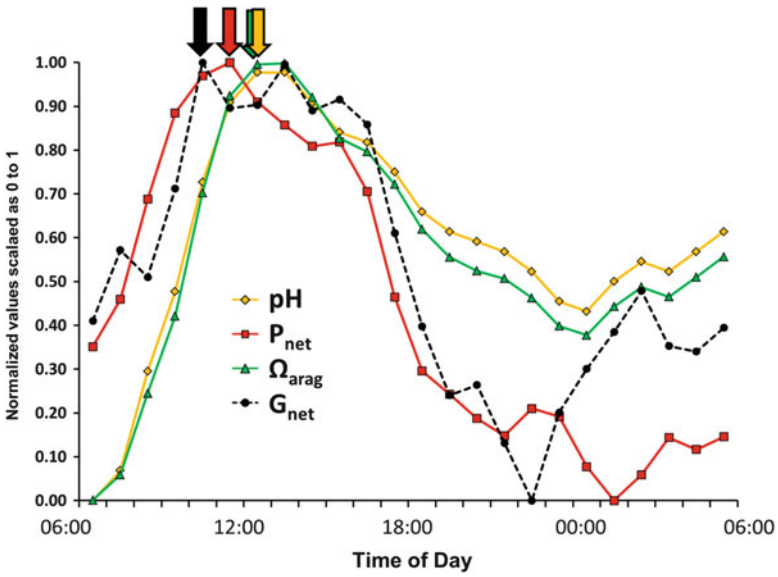

Fig. 2.13 pH, Ω_{arag}, P_{net} and G_{net} values versus time of day with all values normalized to a 0–1 scale. Arrows point to relative maxima for each parameter (Figure and data from Jokiel et al. (2014a) used with permission)

2.9.1 Phase Shifts

Figure 2.13 shows that peak pH and Ω_{arag} lag behind G_{net} throughout the daily cycle by two or more hours. The figure also shows that peak G_{net} follows P_{net} during daylight photosynthetic hours with a reversal during the nighttime hours. Shamberger et al. (2011) previously reported that Ω_{arag} lags behind G_{net} on the reefs of Kāneʻohe Bay. McMahon et al. (2013) reported that peak G_{net} rates occurred 2–3 h before the Ω_{arag} maximum on the Great Barrier Reef. Thus Ω_{arag} (along with closely correlated [CO_3^{2-}], pH and [DIC]:[H^+] ratio) cannot be the primary driver of coral calcification over a diurnal cycle. The use of Ω_{arag} to calculate future changes in G_{net} on a global scale must consider future changes in the other processes that have a great influence on G_{net} on smaller spatial and temporal scales. Figures 2.12 and 2.13 show that diurnal irradiance drives P_{net}, which in turn drives G_{net}. P_{net} and G_{net} alter pH (Eqs. 2.5, 2.6, 2.7, 2.8, 2.9 and 2.10), which controls [CO_3^{2-}] and Ω_{arag} in addition to the other variables based on concentration such as the ratio of [DIC] to [H^+].

2.9.2 Night Calcification

Laboratory studies show that coral calcification continues in darkness, but at a lower rate than observed in light enhanced calcification (Schneider and Erez 2006). Night calcification rates have generally been assumed to be low and constant at night, although this assumption has largely gone untested. Figures 2.12 and 2.13 show decreasing dark calcification following sunset, reaching zero near midnight followed by an increasing rate of dark calcification and an increase in respiration that rises to a peak at 03:00, which is well before dawn. This pattern has occurred consistently in our mesocosm experiments, with the same pattern observed in 30 separate mesocosm runs with different communities under various conditions as well as in flume studies (Murillo et al. 2014). Barnes and Crossland (1980) used time-lapse photography to measure diurnal growth in the staghorn coral *Acropora acuminata* and found that night-time extension rate was similar to or greater than day-time extension. They suggested that, "symbiotic association permits rapid growth because the coral can invest in flimsy scaffolding at night with the certainty that bricks and mortar will be available in the morning". Wooldridge (2013) has proposed a new model for "dark" coral calcification, whereby O_2-limitation of aerobic respiration during the night initiates a homeostatic host response that forms the skeletal organic matrix. The matrix formed at night subsequently allows rapid growth of the aragonite fibers during the "light-enhanced" period of calcification, when abundant energy derived from photosynthesis is available. Perhaps the midnight calcification minimum observed in Figs. 2.12 and 2.13 at 00:00 reflects this period of organic matrix formation that precedes the 03:00 night calcification peak.

Diurnal changes in pH, DO and plankton feeding also have an effect on diurnal calcification in light and darkness. Wijgerde et al. (2012) measured the short-term effects of zooplankton feeding on light and dark calcification rates of the scleractinian coral *Galaxea fascicularis* at oxygen saturation levels ranging from 13 to 280 %. Significant main and interactive effects of oxygen, heterotrophy and light on calcification rates were found. Light and dark calcification rates of unfed corals were affected by hypoxia and hyperoxia. Light calcification rates of fed corals showed highest calcification rates at 150 % saturation. In contrast, dark calcification rates of fed corals were close to zero under all oxygen saturations. The authors concluded that oxygen exerts a strong control over light and dark calcification rates of corals, and proposed that *in situ* calcification rates are highly dynamic. Nevertheless, the inhibitory effect of heterotrophy on dark calcification appeared to be oxygen-independent. They hypothesized that dark calcification is impaired during zooplankton feeding by decrease in pH and aragonite saturation state of the calcifying fluid adjacent to the skeleton resulting from the increased respiration rates.

2.9.3 Diurnal Changes in Concentration of A_T, pH, Ω_{arag} and DO

The variables of A_T, pH, Ω_{arag} DIC, and DO are concentrations while P_{net} and G_{net} are flux rates. Caution must be taken when comparing concentrations to flux rates because flux rate can be high when concentration is high or low, or flux rate can be low when concentration is high or low. Figure 2.13 shows patterns that are difficult to interpret because the figure mixes flux rates with concentrations. Much can be learned by plotting DIC flux and H^+ flux rather than [DIC], [H^+] or pH in relation to P_{net} and G_{net}. DIC flux and H^+ flux are plotted with P_{net} and G_{net} in Fig. 2.14. This figure illustrates the dynamic geochemical and physiological relationships involved in coral metabolism.

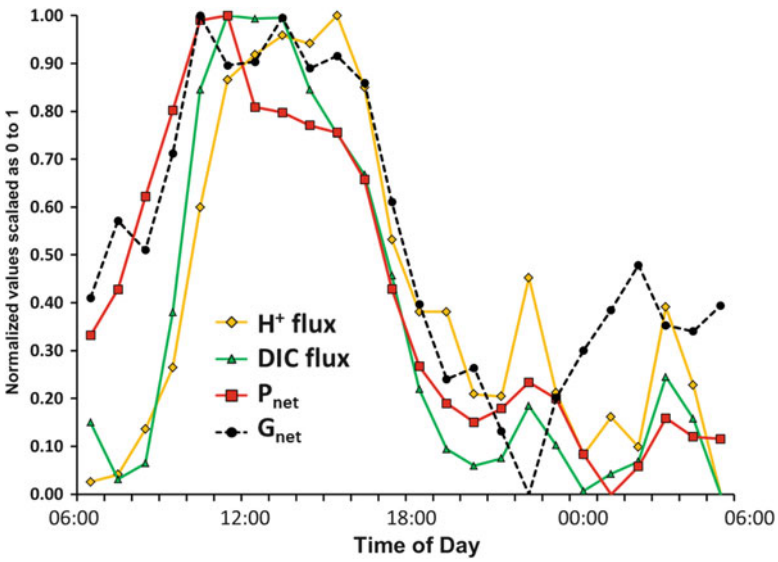

Fig. 2.14 Plot of normalized data for P_{net}, G_{net}, inverse DIC flux and H^+ flux with all values normalized to a 0 to 1 scale (Figure from Jokiel et al. (2014a) used with permission)

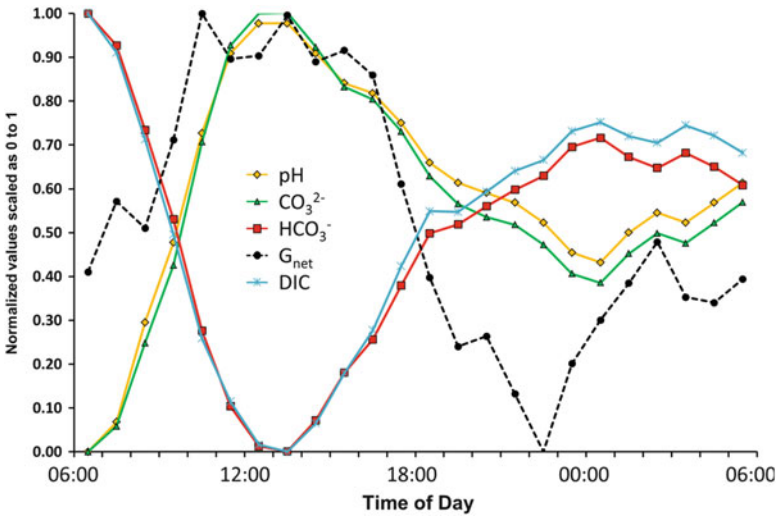

Fig. 2.15 The flux rate of calcification-dissolution (G_{net}) plotted against the concentrations of important variables in the CO_2-carbonate system with all values normalized to a 0–1 scale (Figure from Jokiel et al. (2014a) used with permission)

DIC flux (uptake) in the rapidly calcifying mesocosms increases with increasing P_{net} from 06:00 until mid-day peak P_{net} and then decreases rapidly as P_{net} decreases with decreasing irradiance. Furla et al. (2000a) demonstrated the presence of a DIC pool within coral tissues. The size of this pool was dependent on the lighting conditions, since it increased 39-fold after 3 h of illumination. If we apply this observation to the data shown in Fig. 2.14, it appears that the DIC pool had increased by mid-day, so rate of DIC uptake dropped rapidly as irradiance and photosynthesis declined. However, note that the high dissipation rates of H^+ continued for 2–3 h following the peak rates of P_{net} and G_{net} as the corals rid the backlog of H^+ generated by rapid calcification. Thus the lag of pH behind the peak flux rates of P_{net} and G_{net} represents a disequilibrium resulting from the lag in proton efflux from the corals. The correlation between Ω_{arag} and G_{net} is simply the response of the CO_2-carbonate system to pH as $[H^+]$ shifts the equilibria and redistributes the $[CO_3^{2-}]$ relative to the other DIC components of $[HCO_3^-]$ and $[CO_2]$ (Eqs. 2.4, 2.5, 2.6, 2.7, 2.8, 2.9 and 2.10). Therefore Ω_{arag} closely tracks pH whereas G_{net} tracks P_{net}. Changes in Ω_{arag} are a consequence of changes in both P_{net} and G_{net}. Hence the Ω_{arag} peak and the pH peak lag behind the P_{net} and G_{net} peak (Fig. 2.13) due to lag in proton efflux. This observation demonstrates the importance of understanding the difference between H^+ concentration and H^+ flux. During the night the H^+ flux rate is very responsive to changes in G_{net} due to changes in respiration.

2.10 Back to the Basics

The preceding sections show the importance of using flux rates rather than concentrations when describing a dynamic metabolic system such as a coral or coral reef. Most of the previous research in this area has focused on the relationship between G_{net}, $[CO_3^{2-}]$ (or its surrogate Ω_{arag}), $[HCO_3^-]$, and $[H^+]$ expressed as pH. Plotting these variables in exemplary Figure 2.15 is very informative. A coral must uptake inorganic carbon in order to maintain high rates of photosynthesis and calcification. As a result [DIC] will decrease no matter which carbonate species (HCO_3^-, CO_3^{2-} or CO_2) is taken up by the coral (Eqs. 2.5, 2.6, 2.7, 2.8, 2.9 and 2.10). Thus we see a decline in [DIC] at high rates of G_{net}. $[HCO_3^-]$, which has been identified as the preferred substrate for photosynthesis and calcification (Weis et al. 1989; Goiran et al. 1996; Furla et al. 2000b; Jury et al. 2010; Roleda et al. 2012), drops rapidly as calcification rate increases while closely tracking [DIC] during daylight hours (Fig. 2.15). In contrast, $[CO_3^{2-}]$ lags behind G_{net} and closely tracks pH during the day as shown for Ω_{arag} in Fig. 2.13. If $[CO_3^{2-}]$ (or its surrogate Ω_{arag}) drives calcification, then how do we explain the lag behind G_{net}? And if $[CO_3^{2-}]$ is limiting, how do we explain the fact that $[CO_3^{2-}]$ is increasing rather than decreasing as the coral calcifies rapidly and takes up inorganic carbon? In fact $[CO_3^{2-}]$ increases simply because of the increase in pH caused by rapid photosynthesis that shifts the equilibrium between $[HCO_3^-]$ and $[CO_3^{2-}]$ (Eqs. 2.5, 2.6, 2.7, 2.8, 2.9 and 2.10, Fig. 2.4). Thus, P_{net} is the driver of changes in G_{net} and $[CO_3^{2-}]$. A basic physiological interpretation of the patterns shown in Fig. 2.15 is that daytime coral metabolism rapidly removes DIC (primarily in the form of HCO_3) while photosynthesis provides the energy that drives G_{net}. Higher pH resulting from rapid photosynthesis pushes the equilibria toward higher $[CO_3^{2-}]$. This scenario results in a correlation between G_{net} and Ω_{arag}, with both Ω_{arag} and G_{net} as dependent variables on P_{net} along with pH and changes in A_T due to local dissolution. During the night $[HCO_3^-]$, [DIC], $[CO_3^{2-}]$ and pH mirror changes in G_{net}. However, $[HCO_3^-]$ diverges from [DIC], and $[CO_3^{2-}]$ diverges from pH in darkness. The night divergence can be attributed to respiration causing a decrease in pH. The decreasing pH shifts the equilibria so that $[CO_3^{2-}]$ is converted to $[HCO_3^-]$, thereby changing the offset between the points.

2.11 Conclusions

The physical chemist's concept of Ω_{arag} is of critical importance to our understanding of global distribution and changes in the carbonate chemistry of the sea. The vertical and horizontal distribution of Ω_{arag} in the past, present and future will continue to be the subject of extensive research, and the concept of Ω_{arag} as a fundamental driver of abiotic processes, such as the chemical dissolution of carbonates, is indisputable. However, some scientists involved in OA studies have previously adopted Ω_{arag} as the most important independent variable related to coral calcification based on empirical correlation, but without evidence for causation. According to the proton flux hypothesis, coral physiology is responding to $[H^+]$, which shows a correlation with Ω_{arag}. The preoccupation with supply of materials required for calcification (limiting nutrient analogy of N vs. P) with a focus on two interchangeable forms of inorganic carbon (CO_3^{2-} and HCO_3^-) rather than on elimination of waste H^+ prevented a complete understanding of physiological processes. Results must be viewed in the context of reactants and products (Eqs. 2.5, 2.6 and 2.7). Equations describing control of calcification by the ratio of substrate concentration (DIC) to proton concentration (H^+) were derived from a physiological perspective in Sect. 2.1.8. Bach (2015) rearranged the terms in the physical chemistry equations describing the sea water carbonate-carbon dioxide system and demonstrated that calcification is a function of the [DIC] : $[H^+]$ ratio.

Linear regression using Ω_{arag} as the independent variable is a poor descriptor of G_{net} on coral reefs. Much of the existing data on coral calcification was developed in static or low turnover incubation experiments under typical laboratory low-irradiance, artificial-light sources on a 12-h light, 12-h dark cycle (Jokiel et al. 2014b). This regime results in an unrealistic simulation of the actual diurnal cycles that occur on coral reefs. The standard protocol has been to compare linear regressions between or among laboratory treatments. Linear regression provides a very limited description of the actual relationship between the key factors controlling organic and inorganic processes on coral reefs, which are more adequately described by data presentations such as that in Figs. 2.13, 2.14, and 2.15. The linear regression approach does not fully embrace natural diurnal calcification patterns and phase lags because these processes are non-linear (Jokiel et al. 2014a). The linear regression approach can lead to the assumption that Ω_{arag} is the independent variable driving the calcification reaction. Use of Ω_{arag} as an independent variable to compare spatial and temporal variation in G_{net} is known to create difficulties (Shamberger et al. 2011; Falter et al. 2012).

Well-developed reefs occur within a narrow geographic range characterized by open ocean $\Omega_{arag} > 3.3$ (Kleypas et al. 1999a, 1999b), suggesting that high coral Ω_{arag} along with warm shallow waters and high irradiance promotes reef development. Further it has been suggested that reef communities have limited capacity to adapt to lower levels of Ω_{arag} that will occur with future levels of anthropogenic ocean acidification (OA). Recent reports suggest that healthy coral reefs could cease to exist within this time frame as OA continues and oceanic Ω_{arag} decreases (Hoegh-Guldberg et al. 2007; Silverman et al. 2009). However, there are inconsistencies in the relationship (slope and x-intercept) between G_{net} as a function of Ω_{arag} on various reefs throughout the world (Shamberger et al. 2011, 2014; Jokiel 2015). Evenhuis et al. (2015) developed a model of coral reef calcification that embraces the major assumptions that are widely accepted in modeling global coral reef calcification. Jokiel (2015) documented the problems associated with each of the following widely used assumptions: (1) oceanic conditions of Ω_{arag} control (or are at least highly correlated with) G_{net} on coral reefs; (2) calcification rate is driven by bulk water $[CO_3^{2-}]$ expressed as Ω_{arag}; (3) changes in coral calcification rate can be used to estimate future changes in coral reef calcification rate; (4) the impact of OA is additive and not synergistic with other environmental factors such as increased temperature; and (5) predicted Ω_{arag} based on modeled open ocean conditions can be applied to coral reefs. The problems inherent in using these assumptions and the uncertainties and contradictions that result are described in Jokiel (2015) and show the need to re-evaluate basic assumptions.

The physical chemistry concept of Ω_{arag} has no basic physiological meaning in describing G_{net} other than a correlation with the [DIC]:$[H^+]$ ratio (Jokiel 2013; Bach 2015) as well as with other factors such as pH. There is no consistent relationship between Ω_{arag} and G_{net} when comparing reefs throughout the world (Shamberger et al. 2011). Coral reefs are systems in constant disequilibrium with the water column. We must take care not to be led astray in our thinking about the variables that actually drive and control coral and coral reef metabolism and bulk water chemistry. The correlation between G_{net} and other factors is a result of P_{net} driving both G_{net} and Ω_{arag} (McMahon et al. 2013). The observed phenomenon of diurnal hysteresis and diurnal phase lag show the importance of measuring flux rates and emphasizes the challenge in predicting the future effects of OA on coral reefs. The method of using linear extrapolations of Ω_{arag} to determine threshold levels that will shift coral reefs from net calcifying systems to net dissolving states has been questioned (McMahon et al. 2013). Perhaps predicted changes in Ω_{arag} in the open ocean can be used to calculate changes on reefs if we assume that the baseline on the reefs will change in concert with ocean values and that all other processes such as P_{net} and carbonate dissolution will not be influenced by OA. An explanation for the many paradoxes of coral calcification discussed herein has been presented as the "Two Compartment Proton Flux Model of Coral Metabolism" (Jokiel 2011b). This model is focused on localized gradients that influence coral metabolism with a focus on proton flux, carbon pools and translocation of fixed carbon. A major feature of the model is the presence of boundary layers which control local pH gradients and inorganic carbon speciation in addition to proton flux.

2.12 Future Research Directions

The paradigm that G_{net} is controlled by aragonite saturation state Ω_{arag} of bulk seawater on coral reefs is widely embraced in modeling impact of future climate change on coral reefs but is not correct as discussed above. Additional experiments and observations are needed to further examine and resolve entrenched scientific contradictions concerning coral and coral reef carbon metabolism in the face of climate change. Studies are needed on the response of corals and coral reefs to the actual carbonate chemistry of the sea water in contact with the organisms and substrate, rather than relative to changes in the offshore water chemistry. Finely controlled mesocosm investigations focused on measurement of material flux will further test various aspects of the proposed Proton Flux Model. Such experimentation will define the importance of global warming and ocean acidification on G_{net} and P_{net} in a wide range of major coral reef community components under various environmental conditions. A more complete understanding of how boundary layers influence material flux of protons as well as other metabolically important materials is needed. Measurements of changes in the diffusion boundary layer (DBL), momentum boundary layer (MBL) and benthic boundary layer (BBL) as discussed in Sect. 2.1.9 are potentially transformative in the re-evaluation of existing paradigms concerning coral and coral reef metabolism. Such data is vital to the understanding of carbonate dynamics and the ecology of present day reefs and ancient coral reef ecosystems.

The time lag between G_{net} and Ω_{arag} reported previously in field studies (Shamberger et al. 2011; Cyronak et al. 2013b; McMahon et al. 2013) provides evidence that diffusion and advection of materials between the coral and the water column involves time delays. One reason is that corals convert inorganic carbon to organic carbon, translocate the organic carbon to distal calcification sites, store organic carbon as lipid, and can eventually convert stored organic carbon back to inorganic carbon (Jokiel 2011b), creating numerous possible phase lags for metabolic materials. The second reason for the time lag is that rapidly calcifying systems have difficulty dissipating waste protons as shown by continued rapid proton efflux for hours after peak calcification (Fig. 2.14). What other mechanisms can account for the phase lag? Thick boundary layers (BL) resulting from low water motion can slow the exchange of metabolic materials between the coral and the water column. The results of Cyronak et al. (2013b) revealed that stirring had a net stimulatory effect on A_T flux and on the diurnal cycle of hysteresis. Increased attention to the often ignored variable of water-motion regime in experiments could provide insight into results thought previously to be paradoxical. Comeau et al. (2014c) tested effects of water flow on coral reef communities maintained in outdoor flumes under ambient pCO_2 and high pCO_2 (1300 µatm). Net calcification of coral communities, which included sediment communities, was affected by both flow and pCO_2. Calcification correlated positively with flow under both pCO_2 treatments. The effect of flow was less evident for sediments where dissolution exceeded precipitation of calcium carbonate under all flow speeds at high pCO_2. For corals and calcifying algae there was a strong flow effect, particularly at high pCO_2 where positive net calcification was maintained at night in the high flow treatment. These results demonstrate the importance of water flow in modulating the coral reef community response to OA and highlight the need to consider this parameter when assessing the effects of OA on coral reefs.

Studies of reef metabolism on shallow reef flats beginning with the classic work of Odum and Odum (1955) at Enewetak Reef flat were followed by others (Shamberger et al. 2011; Falter et al. 2012) at other locations. All of these studies were based on measurements of diurnal changes in chemistry of sea water within the BBL (see Sect. 2.1.9). Substantial boundary layers also occur over reefs in deeper water. For example, Price et al. (2012) took diurnal metabolic measurements within the BBL for a range of sites from exposed coastal situations to lagoons. They found that ambient variability in pH was substantial and oscillated over a diurnal cycle with diel fluctuations in pH exceeding 0.2. Daily pH maxima were identified as an important control on calcification. Net accretion among sites was positively related to the magnitude and duration of pH above the climatological seasonal low, despite myriad other ecological (e.g., local supply, species interactions, etc.) and physical oceanographic (e.g., temperature, current magnitude and direction, wave strength, latitudinal gradients, etc.) drivers. In general, accretion rates were higher at sites that experienced a greater number of hours at high pH values each day. Where daily pH within the BBL failed to exceed pelagic climatological seasonal lows, net accretion was slower and fleshy, non-calcifying benthic organisms dominated space. Thus, key aspects of coral reef ecosystem structure and function are clearly related to natural diurnal variability in pH, which is driven primarily by photosynthesis and respiration as P_{net}.

We conclude that future progress in understanding of calcification in corals as well as coral reefs will result from a better description of boundary layer processes and from studies of irradiance – water chemistry interactions that occur over a diurnal cycle (e.g., Jokiel et al. 2014a). In addition, studies of interactions among temperature, irradiance, pH and changes in the carbonate-CO_2 seawater system will be very productive.

Acknowledgements This work was supported in part by NOAA Grant "Research in Support of the NWHI Coral Reef Ecosystem Reserve", the EPA Star Grant Program, the Pacific Island Climate Change Cooperative (PICCC), the USGS Cooperative Agreement G13AC00130, and the George Melendez Wright Climate Change Fellowship Program. IBK's involvement was supported by the USGS Coastal and Marine Geology Program. Any use of trade names herein was for descriptive purposes only and does not imply endorsement by the U.S. Government.

Appendix

Appendix Table 2.1 Data reported for A_T, Ca^{2+}, CO_3^{2-}, HCO_3^-, Ω_{arag}, pH and G during each of the experimental trials (Langdon et al. 2000) and calculations for [DIC], $[H^+]$ and the [DIC]:$[H^+]$ ratio

Date		pCO_2	A_T		H^+	Ca^{2+}	CO_3^{2-}	HCO_3^-	CO_2	DIC			G
Start	End	µatm	µeq kg^{-1}	pH	nmol kg^{-1}	mmol kg^{-1}	µmol kg^{-1}	µmol kg^{-1}	µmol kg^{-1}	µmol kg^{-1}	DIC:H^+ × 10^{-3}	Ω_{arag}	mmol $CaCO_3$ m^{-2} day^{-1}
16-Mar-95	21-Mar-95	1394	3384	7.88	131.8	9.27	174.5	2981.3	19.2	3175	24.1	2.43	32.7
21-Mar-95	23-Jun-95	890	2517	7.97	107.2	9.14	146.0	2160.3	11.1	2317	21.6	2.01	8.7
23-Jun-95	11-Jul-95	571	1743	7.97	107.2	8.66	104.1	1471.0	7.7	1583	14.8	1.35	−2.6
11-Jul-95	24-Jul-95	777	1877	7.88	131.8	8.77	93.3	1638.1	10.7	1742	13.2	1.23	−8
25-Jul-95	1-Aug-95	713	2101	7.94	114.8	8.78	118.4	1797.0	10.1	1925	16.8	1.56	14.8
1-Aug-95	19-Aug-95	1160	2120	7.78	166.0	8.83	87.9	1920.5	15.9	2024	12.2	1.17	−3.6
9-Apr-96	17-Apr-95	416	1748	8.09	81.3	8.98	131.7	1404.6	5.4	1542	19.0	1.78	21.1
7-Aug-96	25-Sep-96	688	1834	7.92	120.2	9.34	101.0	1573.9	9.3	1684	14.0	1.42	2.9
4-Mar-97	5-Apr-97	555	1861	8.01	97.7	9.15	121.2	1549.1	7.3	1678	17.2	1.67	16.1
5-Apr-97	5-May-97	443	1633	8.05	89.1	9.02	113.7	1392.8	5.7	1512	17.0	1.54	2.8
5-May-97	6-Jun-97	337	1510	8.11	77.6	8.89	120.2	1184.1	4.4	1309	16.9	1.61	0.8
7-Jun-97	30-Jun-97	458	1941	8.09	81.3	8.80	151.6	1554.2	6.0	1712	21.1	2.01	6.1
3-Jun-97	17-Jul-97	739	2906	8.04	91.2	8.62	209.1	2412.0	10.5	2632	28.9	2.71	27.3
17-Jul-97	9-Sep-97	842	2523	7.96	109.6	8.55	154.8	2136.6	11.4	2303	21.0	1.99	17.9
19-Sep-97	26-Sep-97	773	3249	8.10	79.4	8.60	258.5	2655.5	9.8	2924	36.8	3.34	78.6
26-Sep-97	8-Oct-97	811	3004	8.05	89.1	8.47	218.4	2496.8	10.5	2726	30.6	2.78	45.2
9-Oct-97	12-Oct-97	623	3548	8.20	63.1	8.03	345.1	2772.3	8.0	3125	49.5	4.17	117.2
12-Oct-97	16-Oct-97	710	3347	8.14	72.4	7.82	288.2	2684.9	9.0	2982	41.2	3.39	77.6
23-Oct-97	13-Nov-97	790	2913	8.05	89.1	7.61	212.4	2421.5	10.2	2644	29.7	2.43	24.8
21-Nov-97	26-Nov-97	566	3468	8.23	58.9	7.69	357.5	2651.1	7.1	3016	51.2	4.13	111.9
26-Nov-97	1-Dec-97	717	3287	8.13	74.1	7.60	280.8	2670.5	9.1	2960	39.9	3.21	25.2
1-Dec-97	18-Dec-97	729	3154	8.10	79.4	7.62	258.4	2596.6	9.5	2865	36.1	2.84	19.4
2-Jan-98	12-Jan-98	832	2942	8.03	93.3	7.64	203.8	2473.4	10.9	2688	28.8	2.34	17.5
14-Jan-98	20-Jan-98	526	3644	8.28	52.5	7.55	405.3	2770.8	6.4	3183	60.6	4.6	85.9
20-Jan-98	29-Jan-98	611	3310	8.17	67.6	6.96	297.5	2594.6	8.1	2900	42.9	3.11	50.1
5-Feb-98	19-Feb-98	733	2983	8.08	83.2	6.86	229.1	2449.4	9.6	2688	32.3	2.36	10.6
26-Feb-98	10-Mar-98	548	2728	8.06	87.1	6.84	236.7	2162.9	9.3	2409	27.7	2.44	40
11-Mar-98	15-Mar-98	414	3565	8.23	58.9	6.89	422.1	2615.4	7.3	3045	51.7	4.38	124.7
15-Mar-98	26-Mar-98	548	3278	8.22	60.3	6.90	326.1	2548.1	6.9	2881	47.8	3.39	52
26-Mar-98	16-Apr-98	471	2919	8.08	83.2	6.93	285.7	2269.1	9.4	2564	30.8	2.97	28
16-Apr-98	7-May-98	401	2650	8.09	81.3	6.86	266.6	2016.7	8.2	2292	28.2	2.75	16.3
7-May-98	28-May-98	366	2479	8.08	83.2	6.87	253.4	1867.2	7.9	2129	25.6	2.62	11.1
28-May-98	25-Jun-98	364	2364	8.05	89.1	6.95	231.8	1572.5	8.3	1813	20.3	2.42	5.2
10-Jul-98	22-Jul-98	383	2284	8.02	95.5	9.27	223.3	1737.6	8.7	1970	20.6	3.11	15.7
22-Jul-98	11-Aug-98	397	2194	8.03	93.3	9.49	190.8	1708.1	8.1	1907	20.4	2.72	8.7
11-Aug-98	26-Aug-98	368	2110	8.03	93.3	9.45	187.4	1634.7	7.8	1830	19.6	2.67	7.1
26-Aug-98	3-Sep-98	366	2065	8.11	77.6	8.87	195.0	1578.8	6.0	1780	22.9	2.6	3.8
10-Sep-98	22-Sep-98	457	3227	8.05	89.1	9.03	366.6	2405.3	11.3	2783	31.2	4.66	95
22-Sep-98	1-Oct-98	495	2893	7.96	109.6	8.44	287.8	2242.8	13.1	2544	23.2	3.66	30
1-Oct-98	22-Oct-98	580	2694	7.96	109.6	8.01	236.1	2157.3	12.2	2406	21.9	2.99	19
22-Oct-98	12-Nov-98	821	2561	7.81	154.9	8.29	163.4	2179.5	17.7	2361	15.2	2.04	7.4
2-Feb-99	30-Mar-99	192	2463	8.30	50.1	9.15	375.0	1549.0	4.0	1928	38.5	5.16	114

References

Al-Horani FA, Al-Moghrabi SM, De Beer D (2003a) Microsensor study of photosynthesis and calcification in the scleractinian coral, *Galaxea fascicularis*: active internal carbon cycle. J Exp Mar Biol Ecol 288:1–15 [doi:10.1016/S0022-0981(02)00578-6]

Al-Horani FA, Al-Moghrabi SM, De Beer D (2003b) The mechanism of calcification and its relation to photosynthesis and respiration in the scleractinian coral *Galaxea fascicularis*. Mar Biol 142:419–426 [doi:10.1007/s00227-002-0981-8]

Al-Horani FA, Al-Rousan SA, Manasrah RS, Rasheed MY (2005a) Coral calcification : Use of radioactive isotopes and metabolic inhibitors to study the interactions with photosynthesis and respiration. Chem and Ecol 21(5): 325–335 [doi: 10.1080/02757540500258724]

Al-Horani FA, Ferdelman T, Al-Moghrabi SM, De Beer D (2005b) Spatial distribution of calcification and photosynthesis in the scleractinian coral *Galaxea fascicularis*. Coral Reefs 24:173–180 [doi:10.1007/s00338-004-0461-3]

Allemand D, Ferrier-Pagès C, Furla P, Houlbrèque F, Puverel S, Reynaud S, Tambutté E, Tambutté S, Zaccola D (2004) Biomineralisation in reef-building corals: from molecular mechanisms to environmental control. Comptes Rendus Palevol 3:453–467. [doi:10.1016/j.crpv.2004.07.011]

Allemand D, Furla P, Bénazet-Tambutté S (1998) Mechanisms of carbon acquisition for endosymbiont photosynthesis in Anthozoa. Can J Bot 76:925–941 [doi: 10.1139/b98-086]

Allemand D, Tambutté E, Zoccola D, Tambutté S (2011) Coral calcification, cells to reefs. In: Dubinsky Z, Stambler N (eds), Coral reefs: an ecosystem in transition. New York; Springer Press pp 119–150

Allison N, Cohen I, Finch AA, Erez J, Tudhope AW (2014) Corals concentrate dissolved inorganic carbon to facilitate calcification. Nature Communications 5:5741[doi: 10.1038/ncomms6741]

Allison N, Tudhope AW, Fallick AE (1996) Factors influencing the stable carbon and oxygen isotopic composition of *Porites lutea* coral skeletons from Phuket, South Thailand. Coral Reefs 15:43–57 [10.1007/BF01626076]

Andersson AJ, Kuffner IB, Mackenzie FT, Jokiel PL, Rodgers KS, Tan A (2009) Net loss of $CaCO_3$ from coral reef communities due to human induced seawater acidification. Biogeosci 6, 1811–1823 [doi: 10.5194/bg-6-1811-2009]

Andersson AJ, Mackenzie FT, Ver LM (2003) Solution of shallow-water carbonates: An insignificant buffer against rising atmospheric CO_2. Geology 31:513–516 [doi: 10.1130/0091-7613(2003)031<0513:SOSCAI>2.0.CO;2]

Anlauf H, D'Croz L, O'Dea A (2011) A corrosive concoction: The combined effects of ocean warming and acidification on the early growth of a stony coral are multiplicative. J Exp Mar Biol Ecol 397:13–20 [doi:10.1016/j.jembe.2010.11.009]

Anthony KR, Kline DI, Diaz-Pulido G, Dove S, Hoegh-Guldberg O (2008) Ocean acidification causes bleaching and productivity loss in coral reef builders. Proc Natl Acad Sci 105:17442–17446 [doi: 10.1073/pnas.0804478105]

Atkinson MJ, Carlson B, Crow GL (1995) Coral growth in high-nutrient, low-pH seawater: a case study of corals cultured at the Waikiki Aquarium, Honolulu, Hawaii. Coral Reefs 14:215–223 [10.1007/BF00334344]

Australian Bureau of Meteorology and CSIRO (2011) Climate change in the Pacific: Scientific assessment and new research. Volume 1: Regional Overview (ISBN: 9781921826733 (pbk.) ISBN: 9781921826740 (ebook))

Bach LT (2015) Reconsidering the role of carbonate ion concentration in calcification by marine organisms. Biogeosci Discuss 12:6689–6722. [doi:10.5194/bgd-12-6689-2015]

Barnes DJ, Crossland CJ (1980) Diurnal and seasonal variations in the growth of a staghorn coral measured by time-lapse photography. Limnol Oceanog 35(6): 1113–1117 [doi: 10.4319/lo.1980.25.6.1113]

Barnes DJ, Lough JM (1993) On the nature and causes of density banding in massive coral skeletons. J Exp Mar Biol Ecol 167: 91–108 [doi:10.1016/0022-0981(93)90186-R]

Brahmi C, Kopp C, Domart-Coulon I, Stolarski J, Meibom A (2012) Skeletal growth dynamics linked to trace-element composition in the scleractinian coral *Pocillopora damicornis*. Geochimica et Cosmochimica Acta 99:146–158

Brown BE, Hewit R, Le Tissier MAA (1983) The nature and construction of skeletal spines in *Pocillopora damicornis* (Linnaeus). Coral Reefs 2:81–89 [10.1007/BF02395278]

Caldera K, Wickett ME (2003) Anthropogenic carbon and ocean pH. Nature 425:365 [doi:10.1038/425365a]

Carpenter KE, Abrar M, Aeby GR, Aronson B, Banks S, Bruckner A, Chiriboga A, Cortes J, Delbeek JC, DeVantier L, Edgar GJ, Edwards AJ, Fenner D, Guzmán HM, Hoeksema BW, Hodgson G, Johan O, Licuanan WY, Livingstone SR, Lovell ER, Moore JA, Obura DO, Ochavillo D, Polidoro BA, Precht WF, Quibilan MC, Reboton C, Richards ZT, Rogers AD, Sanciangco J, Sheppard A, Sheppard C, Smith J, Stuart S, Turak E, Veron JEN, Wallace C, Weil E, Wood E (2008) One-third of reef-building corals face elevated extinction risk from climate change and local impacts. Science 321:560–563 [doi: 10.1126/science.1159196]

Chauvin A, Denis V, Cuet P (2011) Is the response of coral calcification to seawater acidification related to nutrient loading? Coral Reefs 30:911–923 [10.1007/s00338-011-0786-7]

Chave KE (1984) Physics and chemistry of biomineralization. Ann Rev Earth Planet Sci 12: 293–305 [doi: 10.1146/annurev.ea.12.050184.001453]

Cohen AL, Holcomb M (2009) Why corals care about ocean acidification. Oceanography 22:118–127 [doi.org/10.5670/oceanog.2009.102]

Cohen AL, McConnaughey TA (2003) Geochemical perspectives on coral mineralization. In: Dove PM, Weiner S, deYoreo JJ (eds) Biomineralization. reviews in mineralogy and geochemistry vol 54, The Mineralogical Society of America, Washington DC, pp 151–187 [doi:10.2113/0540151]

Cohen AL, McCorkle DC, de Putron S, Gaetani GA, Rose KA (2009) Morphological and compositional changes in the skeletons of new coral recruits reared in acidified seawater: Insights into the biomineralization response to ocean acidification. Geochem Geophys Geosyst 10:Q07005 [doi:10.1029/2009GC002411]

Coles SL (1988) Limitations on reef coral development in the Arabian Gulf: temperature or algal competition? Proc 6th Int Coral Reef Symp 3:211–216

Coles SL, Jokiel PL (1977) Effects of temperature on photosynthesis and respiration rates of reef corals. Mar Biol 43:209–216 [doi:10.1007/BF00402313]

Colombo-Pallotta MF, Rodríguez-Román A, Iglesias-Prieto R (2010) Calcification in bleached and unbleached *Montastraea faveolata*: evaluating the role of oxygen and glycerol. Coral Reefs 29:899–907 [doi:10.1007/s00338-010-0638-x]

Comeau S, Carpenter RC, Nojiri Y, Putnam HM, Sakai K, Edmunds PJ. (2014a) Pacific-wide contrast highlights resistance of reef calcifiers to ocean acidification. Proc R Soc B 281: 20141339. [doi:10.1098/rspb.2014.1339]

Comeau S, Carpenter RC, Edmunds PJ (2012) Coral reef calcifiers buffer their response to ocean acidification using both bicarbonate and carbonate. Proc R Soc B 280:20122374 [doi:10.1098/rspb.2012.2374]

Comeau S, Carpenter RC, Edmunds PJ (2013) Response to coral reef calcification: carbonate, bicarbonate and proton flux under conditions of increasing ocean acidification. Proc R Soc B 280:20131153. [doi:10.1098/rspb.2013.1153]

Comeau S, Edmunds PJ, Lantz CA, Carpenter RC (2014c) Water flow modulates the response of coral reef communities to ocean acidification. Sci Reports 4:6681 [doi:10.1038/srep06681]

Comeau S, Edmunds PJ, Spindel NB, Carpenter RC (2014b) Fast coral reef calcifiers are more sensitive to ocean acidification in short-term laboratory incubations. Limnol Oceanogr 59:1081–1091

Connolly SR, Lopez-Yglesias MA, Anthony KRN (2012) Food availability promotes rapid recovery from thermal stress in a scleractinian coral. Coral Reefs 31:951–960. [doi: 10.1007/s00338-012-0925-9]

Crossland CJ, Barnes DJ (1974) The role of metabolic nitrogen in coral calcification. Mar Biol 28:325–332

Cyronak T, Santos IR, Erler DV, Eyre BD (2013a) Groundwater and porewater as major sources of alkalinity to a fringing coral reef lagoon (Muri Lagoon, Cook Islands), Biogeosci 10:2467–2480 [doi:10.5194/bg-10-2467-2013]

Cyronak T, Santos IR, McMahon A, Eyre BD (2013b) Carbon cycling hysteresis in permeable carbonate sands over a diel cycle: Implications for ocean acidification. Limnol Oceanogr 58 (1):131–143 [doi:10.4319/lo.2013.58.1.0131]

Cyronak T, Schulz KG, Santos IR, Eyre BD (2014) Enhanced acidification of global coral reefs driven by regional biogeochemical feedbacks. Geophys Res Lett 41(15): 5538–5546 [doi:10.1002/2014GL060849]

Cyronak T, Schulz KG, Jokiel PL (2015) The Omega myth: what really drives lower calcification rates in an acidifying ocean. ICES J Mar Sci [doi:10.1093/icesjms/fsv075]

de Putron SJ, McCorkle DC, Cohen AL, Dillon AB (2010) The impact of seawater saturation state and bicarbonate ion concentration on calcification by new recruits of two Atlantic corals. Coral Reefs. 30 (2):321–328 [doi:10.1007/s00338-010-0697-z]

Dore JE, Lukas R, Sadler DW, Church MJ, Karl DM (2009) Physical and biogeochemical modulation of ocean acidification in the central North Pacific. Proc Natl Acad Sci USA 106:12235–12240 [doi: 10.1073/pnas.0906044106]

Duarte CM, Hendriks IE, Moore TS, Olsen YS, Steckbauer A, Ramajo L, Carstensen J, Trotter JA, McCulloch M (2013) Is ocean acidification an open-ocean syndrome? Understanding anthropogenic impacts on seawater pH. Estuaries and Coasts 36:221–236 [doi:10.1007/s12237-013-9594-3]

Dubinsky Z, Jokiel PL (1994) Ratio of energy and nutrient fluxes regulates symbiosis between zooxanthellae and corals. Pac Sci 48:313–324

Edmunds PJ (2011) Zooplanktivory ameliorates the effects of ocean acidification on the reef coral *Porites* spp. Limnol Oceanogr 56:2402–2410 [doi:10.4319/lo.2011.56.6.2402]

Edmunds PJ, Brown D, Moriarty V (2012) Interactive effects of ocean acidification and temperature on two scleractinian corals from Moorea, French Polynesia. Global Change Biology. 18:2173–2183 [doi: 10.1111/j.1365-2486.2012.02695.x]

Enns T (1967) Facilitation by carbonic anhydrase of carbon dioxide transport. Science 155:44–47 [doi:10.1126/science.155.3758.44]

Enríquez S, Méndez ER, Iglesias-Prieto R (2005) Multiple scattering on coral skeletons enhances light absorption by symbiotic algae. Limnol Oceanogr 50:1025–1032 [doi: 10.1364/AO.49.005032]

Erez J, Reynaud S, Silverman J, Schneider K, Allemand D (2011) Coral calcification under ocean acidification and global change. In: Dubinsky Z, Stambler N (eds) Coral reefs: an ecosystem in transition. New York, Springer Press, pp 151–176

Evenhuis C, Lenton A, Cantin NE, Lough JM (2015) Modelling coral calcification accounting for the impacts of coral bleaching and ocean acidification. Biogeosci 12:2607–2630 [doi:10.5194/bg-12-2607-2015]

Fabricius KE, Langdon C, Uthicke S, Humphrey C, Noonan S, De'Ath G, Okazaki R, Muehllehner N, Glas MS, Lough JM (2011) Losers and winners in coral reefs acclimatized to elevated carbon dioxide concentrations. Nature Climate Change 1:165–169 [doi:10.1038/nclimate1122]

Fagan KE, Mackenzie FT (2007) Air–sea CO_2 exchange in a subtropical estuarine-coral reef system, Kaneohe Bay, Oahu, Hawaii. Mar Chem 106:174–191 [doi:10.1016/j.marchem.2007.01.016]

Falkowski PG, Dubinsky Z, Muscatine L, Porter J (1984) Light and the bioenergetics of a symbiotic coral. BioScience 34:705–709 [doi:10.2307/1309663]

Falter JL, Lowe RJ, Atkinson MJ, Cuet P (2012) Seasonal coupling and de-coupling of net calcification rates from coral reef metabolism and carbonate chemistry at Ningaloo Reef, Western Australia. J Geophys Res 117:C05003 [doi:10.1029/2011JC007268]

Fang L-s, Chen Y-wJ, Chen C-s (2004) Why does the white tip of stony coral grow so fast without zooxanthellae? Mar Biol 103:359–363 [doi:10.1007/BF00397270]

Feely RA, Doney C, Cooley S (2009) Ocean acidification. Oceanography 22:36–47

Ferrier-Pagès C, Witting, J, Tambtutté E, Sebens KP (2003) Effect of natural zooplankton feeding on the tissue and skeletal growth of the scleractinian coral *Stylophora pistillata*. Coral Reefs 22:229–240 [doi:10.1007/s00338-003-0312-7]

Fine M, Oren U, Loya Y (2002) Bleaching effect on regeneration and resource translocation in the coral *Oculina patagonica*. Mar Ecol Prog Ser 234:119–125 [doi:10.3354/meps234119]

Furla P, Galgani I, Durand I, Allemand D (2000b) Sources and mechanisms of inorganic transport for coral calcification and photosynthesis. J Exp Mar Biol Ecol 203:3445–3457

Furla P, Orsenigo MN, Allemand D (2000a) Involvement of H^+-ATPase and carbonic anhydrase in inorganic carbon absorption for endosymbiont photosynthesis. Am J Physiol 278: R870–R881

Gagnon AC, Adkins JF, Erez J (2012) Seawater transport during coral biomineralization. Earth and Planetary Science Letters 329–330:150–161 [doi:10.1016/j.epsl.2012.03.005]

Galloway SB, Work TM, Bochsler VS, Harley RA, Kramarsky-Winters E, McLaughlin SM, Meteyer CU, Morado JF, Nicholson JH, Parnell PG, Peters EC, Reynolds T, Rotstein DS, Sileo L, Woodley CM (2007) Coral disease and health workshop: Coral histopathology II. NOAA Technical Memorandum NOS NCCOS 56 and NOAA Technical Memorandum CRCP 4. National Oceanic and Atmospheric Administration, Silver Spring, MD 84 pp

Gattuso JP, Allemand D, Frankignoulle M (1999) Photosynthesis and calcification at cellular, organismal and community levels in coral reefs: A review on interactions and control by carbonate chemistry. Am Zool 39:160–183 [doi: 10.1093/icb/39.1.160]

Gladfelter EH (1982) Skeletal development in *Acropora cervicornis*: I. Patterns of calcium carbonate accretion in the axial corallite. Coral Reefs 1:45–51 [doi:10.1007/BF00286539]

Gladfelter EH (1983) Circulation of fluids in the gastrovascular system of the reef coral *Acropora cervicornis*. Biol Bull 165:619–636

Glynn PW (1997) Bioerosion and coral reef growth: a dynamic balance. In: Birkeland C (ed.) Life and death of coral reefs. New York: Chapman and Hall. 68–95

Goiran C, Almoghrabi S, Allemand D, Jaubert J (1996) Inorganic carbon uptake for photosynthesis by the symbiotic coral/dinoflagellate association. 1. Photosynthetic performances of symbionts and dependence on sea water bicarbonate. J Exp Mar Biol Ecol 199:207–225 [doi: 10.1016/0022-0981(95)00201-4]

Golbuu Y, Wolanski E, Idechong JW, Victor S, Isechal AL, Oldiais NW, Idip Jr D, Richmond RH, van Woesik R (2012) Predicting Coral Recruitment in Palau's Complex Reef Archipelago. PLoS ONE 7(11):e50998. [doi:10.1371/journal.pone.0050998]

Goreau TF (1959) The physiology of skeleton formation in corals. I. A method for measuring the rate of calcium deposition by corals under different light conditions. Biol Bull 116:59–75

Goreau TF (1963) Calcium carbonate deposition by coralline algae and corals in relation to their roles as reef-builders. Ann NY Acad Sci 109:127–167 [doi: 10.1111/j.1749-6632.1963.tb13465.x]

Goreau TF, Goreau NI (1959) The physiology of skeleton formation in corals. II. Calcium deposition by hermatypic corals under various conditions in the reef. Biol Bull 117:239–250

Goreau TJ (1977) Coral skeletal chemistry: physiological and environmental regulation of stable isotopes and trace metals in *Montastrea annularis*. Proc R Soc B 196:291–315 [doi: 10.1098/rspb.1977.0042]

Graham D, Smillie RM (1976) Carbonate dehydratase in marine organisms of the Great Barrier Reef. Aust J Plant Physiol 3:113–119 [doi: 10.1071/PP9760113]

Graus RR, Macintyre IG (1976) Light control of growth form in colonial reef corals: computer simulation. Science 193:895–897 [doi: 10.1126/science.193.4256.895]

Grottoli AG, Rodrigues LJ, Palardy JE (2006) Heterotrophic plasticity and resilience in bleached corals. Nature 440:1186–1189 [doi:10.1038/nature04565]

Guest JR, Baird AH, Maynard JA, Muttaqin E, Edwards AJ, Campbell SJ, Yewdall K, Affendi YA, Chou LM (2012) Contrasting patterns of coral bleaching susceptibility in 2010 suggest an adaptive response to thermal stress. PLoS ONE 7(3): e33353 [doi:10.1371/journal.pone.0033353]

Hallock P, Schlager W (1986) Nutrient excess and the demise of coral reefs and carbonate platforms. Palaios 7:389–398 [doi:10.2307/3514476]

Harriott VJ, Banks SA (2002) Latitudinal variation in coral communities in eastern Australia: a qualitative biophysical model of factors regulating coral reefs. Coral Reefs 21:83–94 [doi: 10.1007/s00338-001-0201-x]

Herfort L, Thake B, Taubner I (2008) Bicarbonate stimulation of calcification and photosynthesis in two hermatypic corals. J Phycol 44:91–98 [10.1111/j.1529-8817.2007.00445.x]

Hoegh-Guldberg O, Mumby PJ, Hooten AJ, Steneck RS, Greenfield P, Gomez E, Harvell CD, Sale PF, Edwards AJ, Caldeira K, Knowlton N, Eakin CM, Iglesias-Prieto R, Muthiga N, Bradbury RH, Dubi A, Hatziolos ME (2007) Coral reefs under rapid climate change and ocean acidification. Science 318:1737–1742 [doi: 10.1126/science.1152509]

Hofmann GE, Smith JE, Johnson KS, Send U, Levin LA, Micheli F, Paytan A, Price NN, Peterson B, Takeshita Y, Matson PG, Crook ED, Kroeker KJ, Gambi MC, Rivest EB, Frieder CA, Yu PC, Martz TR (2011) High-frequency dynamics of ocean pH: A multi-ecosystem comparison. PLoS ONE 6(12): e28983 [doi:10.1371/journal.pone.0028983]

Hofmann GE, Todgham AE (2010) Living in the now: physiological mechanisms to tolerate a rapidly changing environment. Annu Rev Physiol 72:127–45 [doi: 10.1146/annurev-physiol-021909-135900]

Holcomb MC, McCorkle DC, Cohen AL (2010) Long-term effects of nutrient and CO_2 enrichment on the temperate coral *Astrangia poculata* (Ellis and Solander, 1786). J Exp Mar Biol Ecol 386:27–33 [doi:10.1016/j.jembe.2010.02.007]

Hönisch B, Ridgwel A, Schmidt DN, Thomas E, Gibbs SJ, Sluijs A, Zeebe R, Kump, L, Martindale RC, Greene SE, KiesslingW, Ries J, Zachos JC, Royer DL, Barker S, Marchitto TM Jr, Moyer R, Pelejero C, Ziveri P, Foster GL, Williams B (2012) The geological record of ocean acidification. Science 335:1058–1063 [doi: 10.1126/science.1208277]

Hunter CL, Evans CW (1995) Coral reefs in Kaneohe Bay, Hawaii: two centuries of western influence and two decades of data. Bull Mar Sci 57:501–515

IPCC (2001) Climate Change 2001: The scientific basis. The contribution of Working Group I to the Third Assessment Report of the Intergovernmental Panel on Climate Change. Houghton JT, Ding Y, Griggs DJ et al. (eds) Cambridge University Press, New York pp 1–881

IPCC (2007) Technical Summary. Climate Change 2007: The physical science basis. Contribution of Working Group I to the Fourth Assessment Report of the Intergovernmental Panel on Climate Change. Solomon S, Qin D, Manning M, Chen Z, Marquis M, Averyt KB, Tignor M, Miller HL (eds). Cambridge University Press, New York pp 19–91

Jaubert J (1977) Light metabolism and growth forms of the hermatypic scleractinian coral *Synaraea convexa* (Verrill) in the lagoon of Moorea (French Polynesia). Proc 3rd Int Coral Reef Symp 1:483–488

Jimenez IM, Kühl M, Larkum AWD, Ralph PJ (2011) Effects of flow and colony morphology on the thermal boundary layer of corals. J R Soc Interface 8:1785–1795 [doi:10.1098/rsif.2011.0144]

Jokiel PL (1978) Effects of water motion on reef corals. J Exp Mar Biol Ecol 35:87–97

Jokiel PL (2011a) Ocean acidification and control of reef coral calcification by boundary layer limitation of proton flux. Bull Mar Sci 87:639–657 [doi.org/10.5343/bms.2010.1107]

Jokiel PL (2011b) The reef coral two compartment proton flux model: A new approach relating tissue-level physiological processes to gross corallum morphology. J Exp Mar Biol Ecol 409:1–12 [doi:10.1016/j.jembe.2011.10.008]

Jokiel PL (2013) Coral reef calcification: carbonate, bicarbonate and proton flux under conditions of increasing ocean acidification. Proc R Soc B 20130031 [doi:10.1098/rspb.2013.0031]

Jokiel PL (2015) Predicting the impact of ocean acidification on coral reefs: evaluating the assumptions involved. ICES J Mar Sci [doi: 10.1093/icesjma/fsv091]

Jokiel PL, Bahr KD, Rodgers KS (2014b) Low-cost, high-flow mesocosm system for simulating ocean acidification with CO_2 gas. Limnol Oceanogr Methods 12:313–322 [doi:10.4319/lom.2014.12.313]

Jokiel PL, Coles SL (1977) Effects of temperature on the mortality and growth of Hawaiian reef corals. Mar Biol 43:201–208

Jokiel PL, Jury CP, Rodgers KS (2014a) Coral-algae metabolism and diurnal changes in the CO_2-carbonate system of bulk sea water. PeerJ 2:e378 [doi:10.7717/peerj.378]

Jokiel PL, Morrissey JI (1986) Influence of size on primary production in the reef coral *Pocillopora damicornis* and the tropical macroalga *Acanthophora spicifera*. Mar Biol 91:15–26 [doi:10.1007/BF00397566]

Jokiel PL, Rodgers KS, Kuffner IB, Andersson AJ, Cox EF, Mackenzie FT (2008) Ocean acidification and calcifying reef organisms: a mesocosm investigation. Coral Reefs 27:473–483 [doi:10.1007/s00338-008-0380-9]

Jury CP, Thomas FI, Atkinson MJ, Toonen RJ (2013) Buffer capacity, ecosystem feedbacks, and seawater chemistry under global change. Water 5:1303–1325

Jury CP, Whitehead RF, Szmant A (2010) Effects of variations in carbonate chemistry on the calcification rates of *Madracis auretenra* (= *Madracis mirabilis* sensu Wells, 1973): bicarbonate concentrations best predict calcification rates. Global Change Biol 16:1632–1644 [doi:10.1111/j.1365-2486.2009.02057.x]

Kaandorp JA, Sloot PMA, Merks RMH, Bak RPM, Vermeij MJA, Maier C (2005) Morphogenesis of the branching reef coral *Madracis mirabilis*. Proc R Soc B 272:127–133 [doi:10.1098/rspb.2004.2934]

Kaandorp, JA, Filatov M, Chindapol N (2011) Simulating and quantifying the environmental influence on coral colony growth form. In: Dubinsky Z, Stambler N (eds) Coral reefs: an ecosystem in transition. New York; Springer Press, pp 177–185

Kajiwara K, Yokoch H, Nagai A, Ueno S (1997) Growth patterns of white-tipped and brown-tipped branches of the reef building coral, *Acropora pulchra* from Amitori Bay, Iriomote Island. Bull Inst Ocean Res Dev, Tokai Univ 18: 1–10

Kawaguti S, Sakumoto D (1948) The effects of light on the calcium deposition of corals. Bull Oceanogr Inst Taiwan 4:65–70

Kinsey DW (1978) Alkalinity changes and coral reef calcification. Limnol Oceanog 23(5):989–991 [doi: 10.4319/lo.1978.23.5.0989]

Kinsey DW, Davies PJ (1979) Effect of elevated nitrogen and phosphorus on coral reef growth. Limnol Oceanogr 24:935–940 [10.4319/lo.1979.24.5.0935]

Kleypas JA, Buddemeier RW, Archer D, Gattuso JP, Langdon C, Opdyke BN (1999b) Geochemical consequences of increased atmospheric carbon dioxide on coral reefs. Science 284:118–120 [doi:10.1126/science.284.5411.118]

Kleypas JA, Buddemeier RW, Eakin CM, Gattuso J-P, Guinotte J, Hoegh-Guldberg O, Iglesias-Prieto R, Jokiel PL, Langdon C, Skirving W, Strong AE (2005) Comment on "Coral reef calcification and climate change: The effect of ocean warming," Geophys. Res. Lett., 32, L08601 [doi:10.1029/2004GL022329]

Kleypas JA, Feely RA, Fabry VJ, Langdon C, Sabine CI, Robbins LL (2006) Impacts of Ocean Acidification on Coral Reefs and Other Marine Calcifiers: A Guide for Future Research, report of a workshop held 18–20 April 2005, St. Petersburg, Fl, sponsored by NSF, NOAA and US Geological Survey. 88 pp

Kleypas JA, McManus JW, Meñez LAB (1999a) Environmental limits to coral reef development: where do we draw the line? Amer Zool 39 (1): 146–159. [doi: 10.1093/icb/39.1.146]

Kline DI, Teneva L, Schneider K, Miard T, Chai A, Marker M, Headley K, Opdyke B, Nash M, Valetich M, Caves JK, Russell BD, Connell SD, Kirkwood BJ, Brewer P, Peltzer E, Silverman J, Caldeira K, Dunbar RB, Koseff JR, Monismith SG, Mitchell BG, Dove S, Hoegh-Guldberg O. (2012) A short-term in situ CO_2 enrichment experiment on Heron Island (GBR). Sci Rep 2:413 [doi:10.1038/srep00413]

Kuffner IB, Hickey TD, Morrison JM (2013) Calcification rates of the massive coral *Siderastrea siderea* and crustose coralline algae along the Florida Keys (USA) outer-reef tract. Coral Reefs 32:987–997 [doi:10.1007/s00338-013-1047-8]

Kühl, M, Cohen Y, Dalsgaard T, Jørgensen BB, Revsbech NP (1995) Microenvironment and photosynthesis of zooxanthellae in scleractinian corals studied with microsensors for O_2, pH and light. Mar Ecol Prog Ser 117:159–172

Lamberts AE (1974) Measurement of alizarin deposited by coral. Proc 2nd Int Coral Reef Symp 2:241–244

Langdon C, Atkinson MJ (2005) Effect of elevated pCO_2 on photosynthesis and calcification of corals and interactions with seasonal change in temperature/irradiance and nutrient enrichment. J Geophys Res [doi:110 C09S07/10.1029/2004JC002576]

Langdon C, Takahashi T, Sweeney C, Chipman D, Goddard J, Marubini F, Aceves H, Barnett H. (2000) Effect of calcium carbonate saturation state on the calcification rate of an experimental coral reef. Global Biogeochem Cycles 14:639–654 [doi: 10.1029/1999GB001195]

Lantz C (2011) Spatiotemporal analysis of the carbonate system on a coral reef, Oahu, Hawaii. MS Thesis. Hawaii Pacific University, Honolulu. 103 pp

Lesser MP (2011) Coral bleaching: causes and mechanisms. In: Dubinsky Z, Stambler N (eds). Coral reefs: an ecosystem in transition. New York, Springer Press. pp 405–419

Lesser MP, Weis VM, Patterson, MR, Jokiel PL (1994) Effects of morphology and water motion on carbon delivery and productivity in the reef coral, *Pocillopora damicornis* (Linnaeus) – diffusion barriers, inorganic carbon limitation, and biochemical plasticity. J Exp Mar Biol Ecol 178:153–179

Lowenstam HS (1974) Impact of life on chemical and physical processes. In: Goldberg ED (ed.), The Sea, vol. 5, Marine chemistry, pp 725–796. Wiley, New York

Marcelino LA, Westneat MW, Stoyneva V, Henss J, Rogers JD, Radosevich A, Turzhitsky V, Siple M, Fang A, Swain TD, Fung J, Backman V (2013) Modulation of light-enhancement to symbiotic algae by light-scattering in corals and evolutionary trends in bleaching. PLoS ONE 8(4): e61492 [doi: 10.1371/journal.pone.0061492]

Marshall AT, Wright A (1998) Coral calcification: autoradiography of a scleractinian coral *Galaxea fascicularis* after incubation in ^{45}Ca and ^{14}C. Coral Reefs 17:37–47 [doi: 10.1007/s003380050092

Martin S, Gattuso J-P (2009) Response of Mediterranean coralline algae to ocean acidification and elevated temperature. Global Change Biol 15:2089–2100 [doi: 10.1111/j.1365-2486.2009.01874.x]

Martinez JA, Smith CM, Richmond RH (2012) Algal mats degrade coral reef physical habitat quality. Estuar Coast Shelf Sci 99:42–49 [doi:10.1016/j.ecss.2011.12.022]

Marubini F, Atkinson MJ (1999) Effects of lowered pH and elevated nitrate on coral calcification. Mar Ecol Prog Ser 188:117–121 [doi:10.3354/meps188117]

Marubini F, Barnett H, Langdon C, Atkinson MJ (2001) Dependence of calcification on light and carbonate ion concentration for the hermatypic coral *Porites compressa*. Mar Ecol Prog Ser 220:153–162

Marubini F, Ferrier-Pages C, Furla P, Allemand D (2008) Coral calcification responds to seawater acidification: a working hypothesis towards a physiological mechanism. Coral Reefs 27:491–499 [doi:10.1007/s00338-008-0375-6]

Marubini F, Ferrier-Pages C, Cuif J (2003) Suppression of skeletal growth in scleractinian corals by decreasing ambient carbonate-ion concentration: a cross-family comparison. Proc R Soc B 270:179–184 [doi:10.1098/rspb.2002.2212]

Mass T, Genin A, Shavit U, Grinstein M, Tchernov D (2010) Flow enhances photosynthesis in marine benthic autotrophs by increasing the efflux of oxygen from the organism to the water. Proc Natl Acad Sci USA 107:2527–2531[doi: 10.1073/pnas.0912348107]

McConnaughey TA, Whelan JF (1997) Calcification generates protons for nutrient and bicarbonate uptake. Earth Sci Rev 42:95–117

McCulloch M, Falter J, Trotter J, Montagna P (2012) Coral resilience to ocean acidification and global warming through pH up-regulation. Nature Climate Change [doi:10.1038/nclimate1473]

McMahon A. Santos IR, Cyronak T, Eyre BD (2013) Hysteresis between coral reef calcification and the seawater aragonite saturation state. Geophys Res Lett 40:4675–4679 [doi:10.1002/grl.50802]

McNeil BI, Matear RJ, Barnes DJ (2004) Coral reef calcification and climate change: The effect of ocean warming, Geophys Res Lett 31, L22309 [doi:10.1029/2004GL021541]

Moya A, Tambutté S, Bertucci A, Tambutté E, Lotto S, Vullo D, Supuran CT, Allemand D, Zoccola D (2008) Carbonic anhydrase in the scleractinian coral *Stylophora pistillata*: characterization, location and role in biomineralization. J Biol Chem 283:25475–25484 [doi: 10.1074/jbc.M804726200]

Murillo LJ, Jokiel PL, Atkinson MJ (2014) Alkalinity to calcium flux ratios for corals and coral reef communities: variances between isolated and community conditions. PeerJ 2:e249 [doi:10.7717/peerj.24]

Muscatine, L (1973) Nutrition in corals. In; Jones OA, Endean R (eds) Biology and geology of coral reefs, 2:271–324. New York: Academic Press

Muscatine L (1990) The role of symbiotic algae in carbon and energy flux in coral reefs. pp 75–87 In: Dubinsky Z (ed) Coral reefs. Elsevier Science Publishers BV, Amsterdam.

Muscatine L, Falkowski PG, Porter J, Dubinsky Z (1984) Fate of photosynthetically fixed carbon in light and shade adapted corals. Proc R Soc Lond B Biol Sci 222:181–202 [doi: 10.1098/rspb.1984.0058]

Muscatine L, Porter J (1977) Reef corals: mutualistic symbioses adapted to nutrient-poor environments. BioScience 27: 454–460 [doi: 10.2307/1297526]

Odum HT, Odum EP (1955) Trophic structure and productivity of a windward coral reef community on Eniwetok Atoll. Ecol Monogr 25:291–320

Ohde S (1995) Calcium carbonate production and carbon dioxide flux on a coral reef, Okinawa. In: Sakai EH, Nozaki Y (eds) Biogeochemical processes and ocean flux in the Western Pacific. Terra Scientific Pub Co, Tokyo

Ohde S, Hossain MMM (2004) Effect of $CaCO_3$ (aragonite) saturation state of seawater on calcification of *Porites* coral. Geochem J 38:613–621

Ohde S, van Woesik R (1999) Carbon dioxide flux and metabolic processes of a coral reef, Okinawa. Bull Mar Sci 65: 559–576

Orr JC, Fabry VJ, Aumont O, Bopp L, Doney SC, Feely RA, Gnanadesikan A, Gruber N, Ishida A, Joos F, Key RM, Lindsay K, Maier-Reimer E, Matear R, Monfray P, Mouchet A, Najjar RG, Plattner G-K, Rodgers KB, Sabine CL, Sarmiento JL, Schlitzer R, Slater RD, Totterdell IJ, Weirig M-F, Yamanaka Y, Yool A (2005) Anthropogenic ocean acidification over the twenty first century and its impact on calcifying organisms. Nature 437:681–686 [doi:10.1038/nature04095]

Pandolfi JM, Connolly RM, Marshall DJ, Cohen AL (2011) Projecting coral reef futures under global warming and ocean acidification. Science 333:418–422 [doi: 10.1126/science.1204794]

Pearse V, Muscatine L (1971) Role of symbiotic algae (zooxanthellae) in coral calcification. Bio Bull (Woods Hole) 141: 350–363.

Pierrot D, Lewis E, Wallace DWR (2006) MS Excel Program Developed for CO_2 System Calculations. ORNL/CDIAC-105. Carbon Dioxide Information Analysis Center, Oak Ridge National Laboratory, US Dept of Energy, Oak Ridge, Tennessee

Pörtner HO, Langenbuch M, Michaelidis B (2005) Synergistic effects of temperature extremes, hypoxia, and increases in CO_2 on marine animals: from Earth history to global change. J Geophys Res 110: C09S10 [doi:10.1029/2004JC002561]

Price NN, Martz TR, Brainard RE, Smith JE (2012) Diel variability in seawater pH relates to calcification and benthic community structure on coral reefs. PLoS ONE 7(8):e43843 [doi:10.1371/journal.pone.0043843]

Reef R, Kaniewska P, Hoegh-Guldberg O (2009) Coral skeletons defend against ultraviolet radiation. PLoS ONE 4(11): e7995 [doi:10.1371/journal.pone.0007995]

Renegar DA, Riegl BM (2005) Effect of nutrient enrichment and elevated CO_2 partial pressure on growth rate of Atlantic scleractinian coral *Acropora cervicornis*. Mar Ecol Prog Ser 293:69–76

Reynaud S, Leclercq N, Romaine-Lioud S, Ferrier-Pages C, Jaubert J, Gattuso J-P (2003) Interacting effects of CO_2 partial pressure and temperature on photosynthesis and calcification in a scleractinian coral. Global Change Biol 9:1660–1668 [doi: 10.1046/j.1365-2486.2003.00678.x]

Ries JB (2011) A physicochemical framework for interpreting the biological calcification response to CO_2-induced ocean acidification. Geochim Cosmochim Acta 75:4053–4064 [doi:10.1016/j.gca.2011.04.025]

Ries JB, Cohen AL, McCorkle DC (2009) Marine calcifiers exhibit mixed responses to CO_2-induced ocean acidification. Geology. 37:1131–1134 [doi: 10.1130/G30210A.1]

Ries JB, Cohen AL, McCorkle DC (2010) A nonlinear calcification response to CO_2-induced ocean acidification by the coral *Oculina arbuscula*. Coral Reefs 29:661–674 [doi: 10.1007/s00338-010-0632-3]

Rinkevich B, Loya Y (1983) Short term fate of photosynthetic products in a hermatypic coral. J Exp Mar Biol Ecol 73:175–184 [doi:10.1016/j.gca.2011.04.025]

Rodolfo-Metalpa R, Martin S, Ferrier-Pages C, Gattuso J-P (2010) Response of the temperate coral *Cladocora caespitosa* to mid- and long-term exposure to pCO_2 and temperature levels projected for the year 2100 AD. Biogeosci 7:289–300

Roleda M, Boyd P, Hurd C (2012) Before ocean acidification: calcifier chemistry lessons. J Phycol 48:840–843 [doi: 10.1111/j.1529-8817.2012.01195.x]

Roos P (1967) Growth and occurrence of the reef coral *Porites astreoides* (Lamarck) on relation to submarine radiance distribution. Dissertation, Drukkerij Elinkwijk, Utrecht, Norway

Royal Society (2005) Ocean acidification due to increasing atmospheric carbon dioxide. Policy document 12/05. ISBN 0 85403 617 2 Download available at www.royalsoc.ac.uk

Santos SR, Toyoshima J, Kin zie III RA (2009) Spatial and temporal dynamics of symbiotic dinoflagellates (*Symbiodinium*: Dinophyta) in the perforate coral *Montipora capitata*. Galaxea, Journal of Coral Reef Studies 11:139–147 [doi:10.3755/galaxea.11.139]

Schneider K, Erez J (2006) The effect of carbonate chemistry on calcification and photosynthesis in the hermatypic coral *Acropora eurystoma*. Limnol Oceanogr 51:1284–1293 [doi:10.4319/lo.2006.51.3.1284

Shamberger KEF, Feely RA, Sabine CL, Atkinson MJ, DeCarlo EH, Mackenzie FT, Drupp PS, Butterfield DA (2011) Calcification and organic production on a Hawaiian coral reef. Marine Chem 127:64–75 [doi:10.1016/j.marchem.2011.08.003]

Shamberger, KEF, Cohen AL, Golbuu Y, McCorkle DC, Lentz SJ, Barkley HC (2014) Diverse coral communities in naturally acidified waters of a Western Pacific Reef. Geophys Res Lett 41 [doi:10.1002/2013GL058489]

Shapiro O, Fernandez VI, Garren M, Guasto JS, Debaillon-Vesque FP, Kramarsky-Winter E, Vardi A, Stocker R. (2014) Vortical ciliary flows actively enhance mass transport in reef corals. Proc Nat Acad Sci 111 (37): 13391–13396 [doi: 10.1073/pnas.1323094111]

Shashar N, Cohen Y, Loya Y (1993) Extreme diel fluctuations of oxygen in diffusive boundary layers surrounding stony corals. Biol Bull 185:455–461[doi: 10.2307/1542485]

Shashar N, Kinane S, Jokiel PL, Patterson MR (1996) Hydromechanical boundary layers over a coral reef. J Exp Mar Biol Ecol 199:17–28 [doi:10.1016/0022-0981(95)00156-5]

Silbiger NJ, Donahue MJ (2015) Secondary calcification and dissolution respond differently to future ocean conditions. Biogeosci 12:567–578 [doi:10.5194/bg-12-567-2015]

Silverman J, Lazar B, Cao L, Caldeira K, Erez J (2009), Coral reefs may start dissolving when atmospheric CO_2 doubles. Geophys Res Lett 36, L05606 [doi:10.1029/2008GL036282]

Silverman J, Lazar B, Erez J (2007) Community metabolism of a coral reef exposed to naturally varying dissolved inorganic nutrient loads. Biogeochem [doi 10.1007/s10533-007-9075-5]

Simkiss K (1964) Phosphates as crystal poisons of calcification. Biol Rev 39:487–504 [doi: 10.1111/j.1469-185X.1964.tb01166.x]

Smith SV, Buddemeier RW (1992) Global change and coral reef ecosystems. Ann Rev Ecol Syst 23:89–118

Smith SV, Key GS (1975) Carbon dioxide and metabolism in marine environments. Limnol Oceanogr 20:493–495 [doi: 10.4319/lo.1975.20.3.0493]

Smith SV, Kinsey DW, 1978. Calcification and organic carbon metabolism as indicated by carbon dioxide. In: Stoddart, DR, Johannes RE (eds) Coral reefs: research methods, pp 469–484

Stambler N, Popper N, Dubinsky Z, Stimson J (1991) Effects of nutrient enrichment and water motion on the coral *Pocillopora damicornis*. Pac Sci 45:299–307

Suzuki A, Nakamori T, Kayanne H (1995) The mechanism of production enhancement in coral reef carbonate systems: model and empirical results. Sediment Geol 99:259–280 [doi: 10.1016/0037-0738(95)00048-D]

Tambutté É, Allemand D, Mueller E, Jaubert J (1996) A compartmental approach to the mechanism of calcification in hermatypic corals. J Exp Biol 199:1029–1041

Tambutté É, Allemand D, Zoccola D, Meibom A, Lotto S, Caminiti N, Tambutté S (2007) Observations of the tissue-skeleton interface in the scleractinian coral *Stylophora pistillata*. Coral Reefs 26:517–529 [doi: 10.1007/s00338-007-0263-5]

Tambutté É, Tambutté S, Segonds N, Zoccola D, Venn A, Erez J, Allemand D (2012) Calcein labelling and electrophysiology: insights on coral tissue permeability and calcification. R Lond B 279:19–27 [doi:10.1098/rspb.2011.0733]

Taylor DL (1977) Intra-clonal transport of organic compounds and calcium in some Atlantic reef corals. Proc 3rd Int Coral Reef Symp pp 431–436

Thomsen J, Haynert K, Wegner KM, Melzner F (2015) Impact of seawater carbonate chemistry on the calcification of marine bivalves. Biogeosci Discuss 12:1543–1571 [doi: 10.5194/bgd-12-1543-2015]

Tourniaire F, Pulos S (1985) Proportional reasoning: A review of the literature. Educ Stud Math 16(2):181–204 [doi: 10.1007/BF02400937]

Vandermeulen JH, Davis ND, Muscatine L (1972) The effects of inhibitors of photosynthesis on zooxanthellae in corals and other marine invertebrates. Mar Biol 16:185–191 [doi:10.1007/BF00346940]

Venn AA, Tambutté É, Holcomb M, Allemand D, Tambutté S (2011) Live tissue imaging shows reef corals elevate pH under their calcifying tissue relative to seawater. PLoS ONE 6(5) e20013 [doi: 10.1371/journal.pone.0020013]

Venn AA, Tambutté É, Holcomb M, Laurent J, Allemand D, Tambutté S (2013) Impact of seawater acidification on pH at the tissue-skeleton interface and calcification in reef corals. Proc Natl Acad Sci 110(5):1634–1639 [doi/10.1073/pnas.1216153110]

Venn AA, Tambutté É, Lotto S, Zoccola D, Allemand D, Tambutté S (2009) Intracellular pH in Symbiotic Cnidarians. Proc Natl Acad Sci USA 106:16574–16579 [doi: 10.1073/pnas.0902894106]

Venti A, Andersson A, Langdon C (2014) Multiple driving factors explain spatial and temporal variability in coral calcification rates on the Bermuda platform. Coral Reefs 33(4):979–997 [doi:10.1007/s00338-014-1191-9]

Veron JEN (2000) Corals of the world. Vol. 1–3. Aust Inst Mar Sci, Townsville MC, Qld, Australia

Veron JEN (2008) Mass extinctions and ocean acidification: biological constraints on geological dilemmas. Coral Reefs 27:459–472 [doi:10.1007/s00338-008-0381-8]

Vicsek T (1989) Fractal growth phenomena. World Scientific, London.

Weis VM, Smith GJ, Muscatine L (1989) A "CO_2 supply" mechanism in zooxanthellate cnidarians: role of carbonic anhydrase. Mar Biol 100:195–202 [doi: 10.1007/BF00391958]

Wijgerde T, Jurriaans S, Hoofd M, Verreth JAJ, Osinga R (2012) Oxygen and heterotrophy affect calcification of the scleractinian coral *Galaxea fascicularis*. PLoS ONE 7(12): e52702. [doi:10.1371/journal.pone.0052702]

Wilt FH (2005) Developmental biology meets materials science: morphogenesis of biomineralized structures. Dev Biol 280:15–25 [doi:10.1016/j.ydbio.2005.01.019]

Wisshak M, Schönberg CHL, Form A, Freiwald A (2013) Effects of ocean acidification and global warming on reef bioerosion—lessons from a clionaid sponge. Aquat Biol 19:111–127 [doi: 10.3354/ab00527]

Wooldridge S (2013) A new conceptual model of coral biomineralisation: hypoxia as the physiological driver of skeletal extension. Biogeosci 10:2867–2884 [doi:10.5194/bg-10-2867-2013]

Yates KK, Halley RB (2006) Carbonate concentration and pCO_2 thresholds for calcification and dissolution on the Molokai reef flat, Hawaii. Biogeosci 3:357–369 [doi:10.5194/bg-3-357-2006]

Yonge CM (1968) Living corals. Proc R Soc Lond B 169:329–344

Zoccola D, Tambutté É, Sénégas-Balas F, Michiels J-F, Failla JP, Jaubert J, Allemand D (1999) Cloning of a calcium channel α1 subunit from the reef-building coral, *Stylophora pistillata*. Gene 227(2):157–167 [doi:10.1016/S0378-1119(98)00602-7]